DTS-34 -FA853-LR2

Computing the Absorption of Sound by the Atmosphere and its Applicability to Aircraft Noise Certification

Office of Environment and Energy
Washington, D.C. 20591

Edward J. Rickley

EJR Engineering
10 Lorenzo Circle
Methuen, MA 01844

Gregg G. Fleming

John A. Volpe National Transportation Systems Center
Acoustics Facility
Cambridge, MA 02142-1093

Letter Report
August 1998

U.S. Department of Transportation

Federal Aviation Administration

1. INTRODUCTION

The United States Department of Transportation, John A. Volpe National Transportation Systems Center (Volpe Center), Acoustics Facility, in support of the Federal Aviation Administration's Office of Environment and Energy (AEE), has recently completed a study of a new method for computing atmospheric absorption. This letter report presents the results of the study. Section 1 presents an introduction to the topic of atmospheric absorption as it relates to aircraft noise certification, along with the objective of the study. Section 2 discusses the evaluation procedure. Section 3 discusses the results of the evaluation. Sections 4 and 5 present conclusions and recommendations, respectively.

1.1 Background

Aircraft noise certification in the United States is performed under the auspices of the Federal Aviation Regulation, Part 36, "Noise Standards: Aircraft Type and Airworthiness Certification" (FAR 36)[1]. FAR 36 requires that aircraft position data, performance data and noise data be corrected to the following, homogeneous, reference atmospheric conditions for noise certification:

- Sea level pressure of 2116 psf (76 cm of mercury);
- Ambient temperature of 77 degrees Fahrenheit (25 degrees Celsius);
- Relative Humidity of 70 percent; and
- Zero wind.

An integral component of the FAR 36 correction process for noise data is the computation of sound absorption over the propagation path. FAR 36 requires that atmospheric absorption as a function of propagation path distance be computed for each one-third octave-band from 50 Hz to 10 kHz using the method described in the Society of Automotive Engineers Aerospace Recommended Practice 866A, "Standard Values of Atmospheric Absorption as a Function of Temperature and Humidity" (SAE ARP 866A)[2]. Herein this method is referred to as the "SAE method".

Currently the computation of atmospheric absorption for aircraft noise certification is performed using a two step, **reciprocal** process. First, absorption is computed for each one-third octave-band based on the temperature and humidity and the propagation distance at the time of the certification test (test-day absorption). Second, absorption is computed for each one-third octave-band based on the temperature and humidity, and the reference propagation distance (reference-day absorption). The as-measured noise data is then corrected to reference-day atmospheric conditions by algebraically adding the test-day absorption, and then subtracting the reference-day absorption taking into account differences in spherical spreading losses as well as other physical effects. The process is **reciprocal** in the sense that a user can take the reference-day results and work backward to calculate the original test-day data.

This correction process is performed on a one-third octave-band basis, and the individual bands are latter combined into required noise descriptors, typically either the sound exposure level (SEL), denoted by the symbol $L_{AE,}$ or the effective perceived noise level (EPNL), denoted by the symbol L_{EPN}. The net result is a sound level corrected to a reference distance as specified, and a reference-

day temperature and humidity of 70 degrees Fahrenheit (25 degrees Celsius) and 77 percent relative humidity (%RH), respectively. The SAE Method only considers the effects of temperature and relative humidity when computing atmospheric absorption, unlike the newer methods evaluated herein and discussed below, which also take into account the effects of ambient atmospheric pressure.

Two recently published standards, the updated American National Standard, "Method for Calculation of the Absorption of Sound by the Atmosphere", ANSI S1.26-1995 (ANSI S1.26) and the International Standard, "Acoustics - Attenuation of sound during propagation outdoors - Part 1: Calculation of the absorption of sound by the atmosphere", ISO 9613-1, present theoretically-founded and experimentally-validated empirical algorithms for computing atmospheric absorption.[3,4] As mentioned above, a unique characteristic of the ANSI and ISO algorithms, as compared to the algorithms of the SAE method, is that the ANSI and ISO algorithms take into account the effects of atmospheric pressure on sound absorption, in addition to the effects of temperature and relative humidity.

The ANSI and ISO equations for computing sound attenuation rates as a function of propagation distance are algebraically identical to one another, and specify computation as a function of temperature, relative humidity and atmospheric pressure for *a single discrete frequency or pure-tone*. However, FAR 36 requires that noise data be analyzed in one-third-octave bands. Recognizing this fact the authors of these two standards included methods for adapting the pure-tone algorithms for use in a fractional-octave-band analysis, e.g., a one-third octave-band or full octave-band analysis. Similarly, the SAE Method is an empirical attempt of adapting its pure-tone equations for use in a fractional octave-band analysis. Specifically, it states that for one-third-octave mid-band frequencies at or below 4 kHz, the sound attenuation rates should be computed at the nominal mid-band frequencies; and for higher frequencies, the lower-band edge-frequency should be used.

Annex D of both the ANSI and ISO standard present a relatively complex but technically sound method of adapting the pure-tone algorithms for use in a fractional octave-band analysis. Herein this method is referred to as the "spectrum integration method". The spectrum integration method requires a knowledge of both the narrow-band characteristics of the sound source and the frequency response characteristics of the one-third octave-band filters used in the analysis.

Annex E of the ANSI standard presents, in addition, a more empirical method of adapting the pure-tone algorithms to one-third octave bands. Herein this method is referred to as the "Approximate Method". The Approximate Method does not require knowledge of the narrow-band characteristics of the sound source. It uses a fairly simplistic equation to approximate one-third-octave band-level attenuation, based on the frequency response characteristics of a third-order Butterworth filter. The ISO standard does not present a method analogous to the Approximate Method of ANSI, Annex E.

This letter report presents a comparison of the SAE Method (which is currently used for aircraft noise certification) with five one-third octave-band adaptations of the ANSI/ISO pure-tone equations. For convenience, the methods will be identified as follows in the text:

SAE Method: the *SAE method* as described in SAE ARP 866A.

Method 1: the *Spectrum Integration Method* as described in Annex D of both the ANSI S1.26 and ISO 9613-1 standards.

Method 2: the *Approximate Method* as described in Annex E of the ANSI standard.

Method 3: the *Mid-Band Frequency Method* utilizing the ANSI/ISO pure-tone equations with computations at one-third octave mid-band frequencies from 50 Hz to 10 kHz.

Method 4: the *SAE Edge-Frequency Method* utilizing the ANSI/ISO pure-tone equations with computations at the SAE ARP 866A edge-frequencies for one third octave-bands above 4000 Hz, and at one-third octave mid-band frequencies for bands 50 Hz to 4000 Hz.

Method 5: the *Empirical "Edge-Frequency" Method* utilizing the ANSI/ISO pure-tone equations with computations at lower-band "edge-frequencies" based on a 2nd order empirical equation for one-third-octave bands above 4000 Hz and at one-third octave mid-band frequencies for bands 50 Hz to 4000 Hz. The basis for the 2nd order equation is discussed in Section 2.1.5.

Of the methods, Method 1 (the Spectrum Integration method) is based upon the most recent theoretical work and is considered to be the most accurate, because it more precisely takes into account parameters such as one-third octave-band filter frequency response and filter linear operating range. In addition, it computes attenuation at many discrete, pure-tone frequencies, and combines them to obtain an effective sound absorption for a specific one-third octave-band, however, it is not a reciprocal process because filter effects are spectral shape dependant.

Methods 2 through 5, as well as the SAE Method, are reciprocal processes and simply compute sound attenuation at a single "representative" frequency in each one-third octave-band to empirically account for filter effects. In this study, comparisons of methods are presented over the range of temperature and humidity conditions allowed by FAR 36 for a typical jet-powered aircraft and a typical helicopter.

.

The following definitions from the ANSI S1.26 and ISO 9613-1 standards are repeated for clarity

of the discussions presented herein:

Case1: One-third octave-band sound pressure levels known at the source, are determined for a distant receiver.

Case2: One-third octave-band sound pressure levels known at the receiver, are determined for the source.

Case3: One-third octave-band sound pressure levels known at a receiver location are adjusted for that receiver or to a new receiver location by accounting for differences in attenuation due to atmospheric absorption resulting from a different set of meteorological conditions along the propagation path.

Note: Case 1 and 2 are used for adjustments applied to account for propagation in a single direction. Whereas Case 3 is used for two-way propagation and is normally applicable to aircraft noise certification work.

1.2 Objective

The objective of this Volpe Center study is to evaluate the five one-third octave-band adaptations of the ANSI/ISO pure-tone method for computing sound absorption and to assess the feasibility of using one of them in place of the current SAE Method for correcting aircraft noise certification data to reference atmospheric conditions as required by FAR 36. All comparisons in this report are made at standard sea level pressure of 2116 psf unless other wise noted.

Specifically, this study focuses on answering the following questions: (1) What is the expected difference in the certified noise levels of typical aircraft corrected using one of the five methods, as compared with certified levels corrected using the SAE method?; and (2) What potential complications exist for noise certification applicants should they have to implement the new method? Discussion related to these questions is presented in Section 4.

An attempt was made to address the question of the accuracy of the methods utilizing 727 aircraft noise data from a 1977 Volpe Center study. Although this data included measurements at source-to-receiver distances as small as 50 meters, the signal-to-noise ratio at larger distances were insufficient to properly assess the accuracy of the methods in the high frequency bands which are most sensitive to atmospheric absorption effects. Other methods of addressing the accuracy issue are currently being pursued.

2. EVALUATION PROCEDURE

This section describes the implementation and evaluation of the five one-third octave-band adaptations of the ANSI/ISO pure-tone equations. The methodology of SAE has been successfully used by the Volpe Center since its inception in 1975. As such, readers are referred to Reference 2 for a detailed discussion of the methodology.

2.1 Implementation of Methods

As mentioned in Section 1, the general ANSI/ISO equations for computing sound attenuation rates are algebraically identical. These equations provide a means of computing attenuation rates at a single discrete frequency, i.e., for a pure-tone. This section presents the common equations used for computing pure-tone sound attenuation, Equations [1] through [6]. The pure-tone equations are the foundation of the five methods evaluated herein.

The sound attenuation rate, $\alpha(f)$, in decibels per meter, is computed as follows:

$$\alpha(f) = 8.686 f^2 \{[1.84\times10^{-11}(p_a/p_r)^{-1}(T/T_r)^{1/2}] + (T/T_r)^{-5/2}\{0.01275[\exp(-2239.1/T)][f_{rO}/(f^2_{rO}+f^2)] + 0.1068[\exp(-3352.0/T)][f_{rN}/(f^2_{rN}+f^2)]\}\}, \quad \textbf{[1]}$$

where:

f = frequency of sound at which the sound attenuation rate is to be computed, in Hz;

p_a = ambient atmospheric pressure in kPa (either test- or reference-day pressure, as appropriate);

p_r = reference ambient atmospheric pressure 101.325 kPa;

T = ambient atmospheric temperature in degrees K (either test- or reference-day temperature, as appropriate);

T_r = reference ambient temperature 293.15 degrees K;

$$f_{ro} = p_a/p_r\{24+[(4.04\times10^4 h)(0.02+h)/(0.391+h)]\}; \text{ and} \quad \textbf{[2]}$$

$$f_{rN} = (p_a/p_r)(T/T_r)^{-1/2}\{9+280(h)\exp\{-4.170[(T/T_r)^{-1/3}-1]\}. \quad \textbf{[3]}$$

In the above equations for f_{ro} and f_{rN}, Equations [2] and [3], h is equivalent to the molar concentration of water vapor, as a percentage, and is computed as follows:

$$h = h_{rel}(p_{sat}/p_r)(p_a/p_r)^{-1}, \quad \textbf{[4]}$$

where:

h_{rel} = relative humidity in percent (either test- or reference-day relative humidity, as appropriate); and

p_{sat} = $(p_r)10^V$. **[5]**

In the above equation for p_{sat}, the exponent V is computed as follows:

$$V = 10.79586[1-(T_{01}/T)]-5.02808\log_{10}(T/T_{01})+ 1.50474x10^{-4}\{1-10^{-8.29692[(T/T01)-1]}\}+ 0.42873x10^{-3}\{-1+10^{4.76955[1-(T01/T)]}\}- 2.2195983, \quad \textbf{[6]}$$

where:

T_{01} = triple-point isotherm temperature, 273.16 degrees K.

Although, Equations [1] through [6] are common to the five methods evaluated herein, the procedure used for adapting the pure-tone attenuation rate for use in a one-third octave-band analysis is quite different and is described in the following sections, Sections 2.1.1 through 2.1.5.

2.1.1 Method 1: Spectrum Integration Method

Method 1 is a relatively complex, but technically-sound approach to adapting the pure-tone sound absorption algorithms, Equations [1] through [6], for use in a one-third octave-band analysis. Annex D of both the ANSI and ISO standard provide general guidance for implementing this method, but leave several parameters and assumptions to the discretion of the user. Figure 1 presents a computer-programmer-orientated block diagram of the specific assumptions made by the Volpe Center in implementing Method 1 for use in the current study.

The first step in the process is to use the as-measured one-third octave-band sound pressure level data to derive equivalent pressure spectrum level data at the exact mid-band frequency of each band. The pressure spectrum level data at the exact mid-band frequency, $L_S(f_{m,i})$, are computed as follows:

$$L_S(f_{m,i}) = L_{BS}(f_{m,i}) - 10\log_{10}(B_i/B_0), \quad \textbf{[7]}$$

where:

$L_{BS}(f_{m,i})$ = the as-measured sound pressure for one-third octave-band, i;

$f_{m,i}$ = the exact mid-band frequency for one-third octave-band filter i, in Hz, equals $(10^{X/10})(1000)$ for base-10 design one-third octave-band filters, or equals $(2^{X/3})(1000)$ for base-2 design one-third octave-band filters, where: x is equivalent to 0 for the 1 kHz one-third octave-band filter; x is incremented by 1 for each successive one-third octave-band filter; and, x is decremented by one for each one-third octave-band filter below the 1 kHz filter;

B_i = the exact bandwidth of one-third octave-band filter, i;
= $0.23077\ f_{m,i}$, for base-10 design filters, or
= $0.23156\ f_{m,i}$, for base-2 design filters; and

B_0 = 1 Hz, normalizing bandwidth (Note: B_0 defines the reference bandwidth of the derived, pressure spectrum level data. A bandwidth of 1 Hz was conservatively chosen for this study).

The $L_S(f_{m,i})$ values between adjacent one-third octave-bands are used to compute a corresponding slope of the pressure spectrum. The slope for the upper edge of the highest one-third octave-band is computed using the change in level between the two highest bands.

Through linear interpolation, the pressure spectrum level is then computed at discrete frequencies encompassed by each one-third octave-band using the pressure spectrum level computed at adjacent mid-band frequencies along with the corresponding slope between these adjacent bands.

More specifically, for each one-third octave-band, computation of the pressure spectrum level begins at a lower frequency, $f_{L,i}=1/10(f_{1,i})$, and continues to an upper frequency, not greater than $f_{U,i}=2f_{2,i}$, in increments of $B_i/24$, i.e., one-twenty-fourth octaves, where: B_i is defined in Equation [7], and $f_{1,i}$ and $f_{2,i}$; the lower and upper edge of one-third octave-band i, are defined as follows:

$f_{1,i}$ = $(10^{-1/20})f_{m,i}$, for base-10 design one-third octave-band filters; and
= $(2^{-1/6})f_{m,i}$, for base-2 design one-third octave-band filters;

$f_{2,i}$ = $(10^{1/20})f_{m,i}$, for base-10 design one-third octave-band filters; and
= $(2^{1/6})f_{m,i}$, for base-2 design one-third octave-band filters.

The pressure spectrum level associated with each increment of frequency is then adjusted to account for the attenuating effects of a one-third octave-band filter. This adjustment, based upon the well-known response equation for a third-order Butterworth filter, is computed as follows:

$$A(f_{k,i}) = 10\log_{10}\{1/[1+(1/B_i)^6\,(f_{k,i}/f_{m,i} - f_{m,i}/f_{k,i})^6\,]\}, \qquad \textbf{[8]}$$

where:

$f_{k,i}$ = pure tone frequency at which the pressure spectrum level is computed for one-third octave-band i, in Hz; and

$f_{m,i}$ and B_i are as defined in Equation [7]

The equation for a third-order Butterworth filter meeting the requirements of Type 1-X one-third octave-band Butterworth filter as defined by the American National Standard, "Specification for Octave-Band and Fractional-Octave-Band Analog and Digital Filters", ANSI S1.11-1986 (R1993) (ANSI S1.11)[5] was used since it is one of the more common filter designs used in today's analyzers. It was also the Filter response equation used by the authors of ANSI S1.26-1995 in the development of the Approximate Method (Method 2).

Each pressure spectrum level , corrected for filter effects, $L_S^{/}(f_{k,i})$, is converted to acoustic energy, multiplied by 1/24 the bandwidth of the corresponding one-third octave-band filter ($B_i/24$), and summed on an energy basis to produce the calculated, as-measured one-third octave-band level, LEV(i). The process of multiplying the energy-equivalent of each $L_S^{/}(f_{k,i})$ value by B_i /24 is analogous to integrating acoustic energy between subsequent f_k values using a simple trapezoidal approximation.[6]

Typically, computation of the pressure spectrum level for each one-third octave-band ends at a frequency lower than $f_{U,i}$. Specifically, computation stops when five successive increments of the energy-summed $L_S^{//}(f_{m,i})$ values result in less than a 0.01 dB change in LEV(i), or when LEV(i) is equal to the as-measured one-third octave-band level, $L_{BS}(f_{m,i})$.

The pure-tone sound absorption corresponding to test-day temperature, humidity, pressure and distance are then computed at each frequency, $f_{k,i}$, using Equations [1] through [6]. The test-day absorption is algebraically added to the corresponding pressure spectrum level, corrected for filter effects, $L_S^{/}(f_{k,i})$, to obtain the pressure spectrum level at each frequency increment, corrected back to the sound source, $L_{test}(f_{k,i})$. Each $L_{test}(f_{k,i})$ value is converted to acoustic energy, multiplied by 1/24 the bandwidth of the corresponding one-third octave-band filter ($B_i/24$), and summed on an energy basis to produce a one-third octave-band level, $LEV_{test}(i)$, corrected for test-day conditions back to the sound source. The difference between the calculated source level, $LEV_{test}(i)$, and the corresponding calculated, as-measured level, LEV(i), provided a measure of the effective one-third octave-band, test-day absorption, $^*L_{Btest}(f_{m,i})$.

The sound absorption corresponding to reference-day temperature, humidity, pressure and distance is simultaneously computed over the same frequency range at each frequency, $f_{k,i}$, using Equations [1] through [6]. The reference-day absorption is algebraically subtracted from the corresponding pressure spectrum level at the source to obtain the pressure spectrum level at each frequency increment, corrected to a reference distance, based on reference-day atmospheric conditions, $L_{ref}(f_{k,i})$. Each $L_{ref}(f_{k,i})$ value is converted to acoustic energy, multiplied by 1/24 the bandwidth of the corresponding one-third octave-band filter ($B_i/24$), and summed on an energy basis to produce a one-third octave-band level, $LEV_{ref}(i)$, corrected for reference conditions. The difference between the calculated source level, $LEV_{test}(i)$, computed above, and the calculated reference level, $LEV_{ref}(i)$, provided a measure of the effective one-third octave-band, reference-day absorption, $^*L_{Bref}(f_{m,i})$.

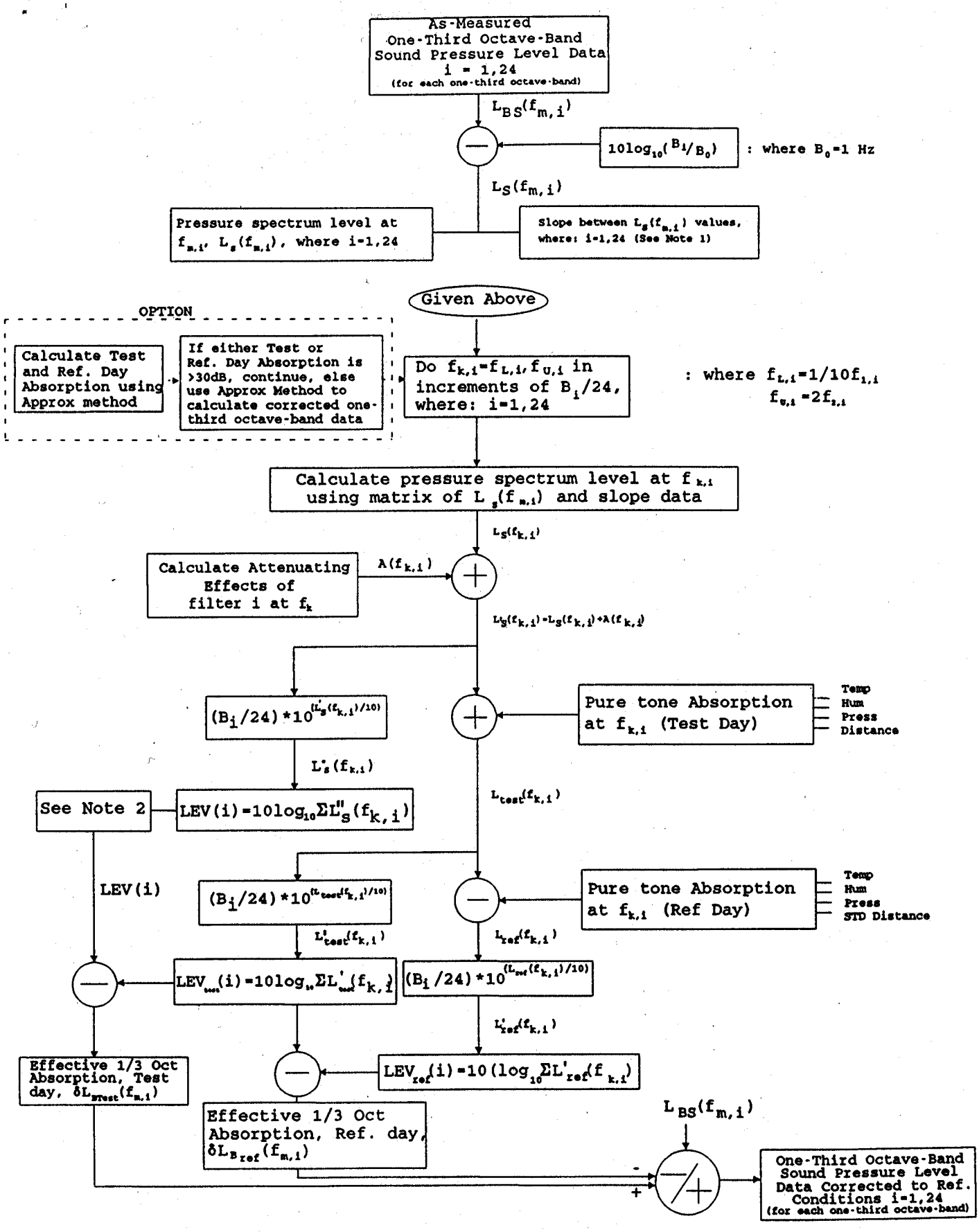

Note 1: Slope of upper edge of highest one-third octve-band is set equal to change in level between two highest bands

Note 2: Computation stops when five successive increments of the energy-summed $L_s(f_{m,i})$ values result in less than 0.01 dB change in LEV(i), or when LEV(i) is equal to the as-measured one-third octave-band level, $L_{BS}(f_{m,i})$.

Figure 1

The one-third octave-band sound levels are then corrected to reference-day conditions by algebraically adding to the measured one-third octave-band sound pressure level, L_{BS} ($f_{m,i}$), the effective one-third octave-band, test-day absorption, $^*L_{Btest}(f_{m,i})$; and subtracting the effective one-third octave-band, reference-day absorption, $^*L_{Bref}(f_{m,i})$. The corrected one-third octave-bands are weighted, as appropriate, and summed, on an acoustic energy basis, to obtain the required sound level descriptors. The result is a sound level corrected to a reference distance, and a reference-day temperature and humidity of 77° F (25° C) and 70 %RH, respectively*.

2.1.2 Method 2: Approximate Method

For Method 2, the sound absorption for any one-third octave-band over the propagation path for the specified meteorological conditions is equivalent to the product of: (1) the sound attenuation rate, computed using Equations [1] through [6], at the exact mid-band frequency of the particular one-third octave-band filter; (2) the propagation path distance; and (3) a theoretically-founded, experimentally-validated nonlinear function of the pure-tone attenuation and the normalized filter bandwidth, referred to herein as the "bandwidth adjustment function". Using Method 2, the sound absorption, $^*L_B(f_{k,i})$, for any one-third octave-band is computed as follows:

$$^*L_B(f_{k,i}) = [\alpha(f_{m,i})][s]\{1+(B_r^2/10)[1-(0.2303)[\alpha(f_{m,i})](s)]\}^{1.6}, \quad \textbf{[9]}$$

where:

$f_{k,i}$ = pure-tone frequency for one-third octave-band i, in Hz;

$\alpha(f_{m,i})$ = the sound attenuation rate computed at the exact mid-band frequency, f_m, of one-third octave-band i, using Equations [1] through [6];

$f_{m,i}$ = as defined in Equation 7;

s = the propagation path distance;

$B_r^2/10$ = 0.0053254, for base-10 design one-third octave-band filters; or
= 0.0053622, for base-2 design one-third octave-band filters; and

B_r = $(10^{1/20} - 10^{-1/20})$ for base-10 design filters; or
= $(2^{1/6} - 2^{-1/6})$ for base-2 design filters.

Note: The constant value of 0.2303 in Equation 9 is rounded from $2/[10\log_{10}(e^2)]$. The exponent of 1.6 in Equation 9 results from a best fit of empirical data.

---

*A time-saving option is shown in Figure 1 wherein the test-day and reference-day absorption could first be computed using the Approximate Method described in Section 2.1.2. If either the test-day or reference-day absorption is found to be less than 30 dB, the particular one-third octave-band sound level could then be corrected to reference conditions using the Approximate Method. Otherwise the Spectrum Integration Method would be used. The 30 dB criterion is conservatively selected as a cutoff, since Reference 3 states that "the Approximate Method may be substituted for the Spectrum Integration Method when the calculated pure-tone attenuation over the total path length is less than 50 dB at any exact mid-band frequency." This time-saving option was not implemented in the current study.

Reference 3 specifies that the above adaptation of pure-tone sound absorption provides an excellent

measure of one-third octave-band absorption for the test spectra chosen in the development of the Approximate Method, assuming that the pure-tone attenuation over the total propagation path distance is less than 50 dB at the associated exact mid-band frequency.

Equation 9, an experimentally-validated nonlinear function, is plotted in Figure 2. Note that the calculated attenuation increases, from a minimum of 0 dB, with increasing mid-band attenuation up to a mid-band attenuation of approximately 250 dB beyond which the calculated attenuation decreases with increasing mid-band attenuation. The attenuation calculated with Equation 9 was found to be in good agreement with the results of Method 1 up to approximately 50 dB mid-band attenuation (the ANSI limit). Above 50 dB the calculated attenuation diverges from Method 1 to unrealistically low values.

2.1.3 Method 3: Pure-tone Mid-Band Frequency Method

For Method 3, the pure-tone method utilizing one-third-octave mid-band frequencies from 50 Hz to 10 kHz, the sound absorption for any one-third octave-band over the propagation path for the specified meteorological conditions is equivalent to the product of: (1) the sound attenuation rate, computed using Equations [1] through [6], at the exact mid-band frequency of the particular one-third octave-band filter; and (2) the propagation path distance, as follows:

$$*L_B(f_{k,i}) = [\alpha(f_{m,i})][s], \quad \textbf{[10]}$$

where:

$f_{k,i}$ = pure-tone frequency for one-third octave-band i, in Hz;

$\alpha(f_{m,i})$ = the sound attenuation rate computed at the exact mid-band frequency for each one-third octave-band i, using Equations [1] through [6];

$f_{m,i}$ = as defined in Equation 7; and

s = the propagation path distance.

2.1.4 Method 4: Pure-tone SAE Edge-Frequency Method

For Method 4, the pure-tone method utilizing SAE edge-frequencies, the sound absorption for any one-third octave-band over the propagation path for the specified meteorological conditions is equivalent to the product of: (1) the sound attenuation rate, computed using Equations [1] through [6], at: (a) the exact mid-band frequency of the particular one-third octave-band filter up to and including 4000 Hz; and (b) the SAE lower-band edge-frequencies for filters greater than 4000 Hz; and (2) the propagation path distance, as follows:

$$*L_B(f_{k,i}) = [\alpha(f_{m,i})][s], \text{ or} \quad \textbf{[11]}$$
$$*L_B(f_{k,i}) = [\alpha(f_{edge,i})][s],$$

where:

$f_{k,i}$ = pure-tone frequency for one-third octave-band i, in Hz;

$\alpha(f_{m,i})$ = the sound attenuation rate computed at the exact mid-band frequency for each one-third octave-band up to and including 4000 Hz using Equations [1] through [6];

$\alpha(f_{edge,i})$= the sound attenuation rate computed at edge-frequencies equal to 4500, 5600, 7100, and 9000 Hz for bands greater than 4000 Hz, using Equations [1] through [6];

$f_{m,i}$ = as defined in Equation 7;

f_{edge} = 4500, 5600, 7100, and 9000 Hz; and

s = the propagation path distance.

2.1.5 Method 5: Pure-tone Empirical "Edge-Frequency" Method

For Method 5, the pure-tone method utilizing empirically derived lower-band "edge-frequencies" (i.e., a frequency close to the filters lower-band edge selected to minimize the differences in absorption as compared with those computed using the SAE method), the sound absorption for any one-third octave-band over the propagation path, for the specified meteorological conditions, is equivalent to the product of: (1) the sound attenuation rate, computed using Equations [1] through [6], at: (a) the exact mid-band frequency of the particular one-third octave-band filter up to and including 4000 Hz and: (b) empirically-derived lower-band "edge-frequencies" for filters greater than 4000 Hz; and (2) the propagation path distance.

An effort was made to obtain a smoothly changing function for the pure-tone "edge-frequencies" above 4000 Hz, while minimizing the difference in attenuation rates as compared with those computed using the SAE Method. Method 5, while minimizing any discontinuity in the existing noise certification data resulting from the replacement of the current SAE Method, would provide the added benefit of being able to account for atmospheric pressure in sound absorption calculations. As mentioned previously, the SAE Method does not provide for changes in atmospheric pressure about a sea level pressure of 2116 psf (76 cm of mercury).

A 2nd order regression equation was developed for calculating frequencies in bands above 4000 Hz. The regression was developed in such a way so as to reduce the difference in attenuation rates (as compared with those computed using the SAE Method) to less than ± 20 dB per kilometer over the FAR 36 temperature/humidity window.

Figure 3a shows the difference in attenuation rates for the 10 kHz band between the SAE Method with a 9000 Hz edge-frequency, and Method 2 with a 10 kHz mid-band frequency over the FAR 36 temperature /humidity window. Note that for some temperature/humidity combinations, differences in attenuation rates of up to 80 dB per kilometer can occur.

Figure 3b shows that the difference in attenuation rates for the 10 kHz band is reduced to less than ±20 dB when comparing the SAE Method (with a 9000 Hz edge-frequency) and Method 5 with the empirically-derived "edge-frequency" of 8286 Hz for the 10 kHz band. The difference in the attenuation rates (figures not shown) in the 8000, 6300, and 5000 Hz bands were reduced to less than +20/-10 dB, +20/-5 dB, and +20/0 dB per kilometer, respectively.

Using Method 5, the sound absorption for any one-third octave-band is computed as follows:

$$*L_B(f_{k,i}) = [\alpha(f_{m,i})][s], \text{or} \quad \textbf{[12]}$$
$$*L_B(f_{k,i}) = [\alpha(f_{emp,i})][s],$$

where:

$\alpha(f_{emp,i})$= the sound attenuation rate computed using Equations [1] through [6] at empirically-derived "edge-frequencies" ($f_{emp,i}$), using the equations defined below;

$f_{emp,i}$ = $-.0020660 + 6.0989 f_{m,i} - .23191 f_{m,i}^{2}$,
an empirically-derived formula for computing frequencies designed to minimize the difference in attenuation rates as compared with the SAE Method, within the FAR 36 temperature/humidity window for one-third octave-bands greater than 4000 Hz; and

$f_{k,i}$, $\alpha(f_{m,i})$, $f_{m,i}$, and s are as defined in Equation 11.

2.2 Comparison of Methods - Case 3

Methods 1 and 2, the Spectrum Integration and the Approximate Methods, were implemented and tested extensively against data in the literature[7,8,9]. Once satisfied with the validity of the results, relative comparisons of these two methods as well as the three additional pure-tone methods (Methods 3, 4, and 5) were performed versus the SAE Method. Case 3 (see Section 1.1) comparisons, over the range of temperature and humidity conditions allowed by FAR 36, were made using certification-quality data measured by the Volpe Center Acoustics Facility for an MD-80 jet aircraft[10] and a Schweizer 300 helicopter[11] (see representative spectra Figures 4a and 4b, respectively). Reference distances of 300 and 1000 meters were chosen for the MD-80 and 100, 300 and 1000 meters for the Schweizer 300 to encompass the extremes of distances expected to be encountered during most noise certification tests.

Noise level comparisons presented in this letter report are for the maximum Perceived Noise level descriptor, denoted by the symbol L_{PNSmx}, and the maximum A-weighted sound level descriptor, denoted by the symbol L_{ASmx}, both with slow exponential time weighting. Although L_{EPN} and L_{AE} are the descriptors of choice for aircraft noise certification in accordance with FAR 36, it was decided that the L_{PNSmx} and the L_{ASmx} descriptors were more appropriate for this comparison. This approach eliminated the possibility of the discontinuous nature of the tone-correction process, used in computing L_{EPN}, potentially masking differences between absorption methodologies. Use of the L_{PNSmx} and the L_{ASmx} descriptors is essentially equivalent to evaluating the absorption methodologies using the simplified adjustment procedure in accordance with FAR 36.

A homogeneous atmosphere was assumed in performing all Case 3 computations, i.e., temperature and humidity did not vary with altitude. Also, standard pressure was assumed, regardless of altitude.

As mentioned in Section 1, in terms of relative accuracy of the methods, the Spectrum Integration Method is considered to be the most accurate, because it more precisely takes into account parameters such as one-third octave-band filter shape and filter linear operating range. In addition, it requires the computation of attenuation at many discrete, pure-tone frequencies, and combines them to obtain the "effective" sound absorption for a specific one-third octave filter band. The other

methods evaluated simply compute sound attenuation at a single frequency for each one-third octave-band, and then attempt to account for fractional filter effects above 4000 Hz empirically.

To more precisely answer the question " What is the expected difference in the certified noise levels of typical aircraft corrected using one of these methods, as compared with certified levels corrected using the SAE Method?", the SAE Method is used as the reference method to which the other methods are compared.

Case 3 noise level difference data as a function of test-day temperature and humidity were computed and presented as a grid of values overlaid on the allowable FAR 36 test "window" Figures 5 through 12. Difference values were computed by algebraically subtracting the noise levels corrected to reference conditions using the SAE Method, from the noise levels corrected to reference conditions using in turn Method 1 ($\hat{I}1$); Method 2 ($\hat{I}2$); Method 3 ($\hat{I}3$); Method 4 ($\hat{I}4$); and Method 5 ($\hat{I}5$) (i.e. $\hat{I}x$= Method x minus SAE Method; where x= 1 through 5).

Test-day temperature and humidity were systematically varied to simulate measurements over an array of meteorological conditions allowed by FAR 36. In other words, measured noise data were not collected for this wide array of temperature and humidity conditions, but were derived. The true test-day data associated with the MD-80 was 18°C and 43 %RH for a propagation distance of 450 meters. The true test-day data associated with the Schweizer 300 was 33°C and 50 %RH for a propagation distance of 265.7 meters. Mock "test-day" spectral data for propagation distances of 300 and 1000 meters (also 100 meters for the Schweizer 300) for a matrix of temperature and humidity conditions were derived by correcting the true test-day data, using the SAE Method, to an array of mock "test-day" conditions prior to the comparison.

For example, to obtain mock "test-day" data at 10°C and 60 %RH, the true test-day data was corrected to these conditions by adding to it the SAE absorption associated with the true test day and subtracting the absorption associated with the mock test day (i.e., 10°C and 60 %RH) over the propagation distances specified (100, 300 or 1000 meters), taking into account spherical spreading as well as other physical effects, as appropriate. The mock "test-day" data were then corrected to reference-day conditions (25°C and 70 %RH), by each of the methods being evaluated as well as the SAE Method, and the L_{PNSmx} and L_{ASmx} descriptors calculated. The associated difference values as compared with the SAE Method were computed and plotted (see Figures 5 through 8 and Figures 9 through 12 for MD-80 and Schweizer 300 results, respectively).

2.3 Comparison of Methods - Case 1

Comparisons of Case 1 noise-distance curves at 25°C and 70 %RH for each of the above five methods versus the SAE Method were made using certification-quality data measured by the Volpe Center Acoustics Facility for the above referenced MD-80 jet aircraft.

Using each method in turn, the as-measured data for the MD-80 aircraft was first corrected to a near source location by adjusting for test day attenuation, including atmospheric absorption and spherical spreading. This source data were then corrected to reference conditions of 25°C and 70 %RH at a number of receiver locations from 200 to 25,000 feet (61 to 7620 meters) taking into account attenuation by atmospheric absorption and spherical spreading.

Noise level comparisons referenced to the SAE Method are shown in Figures 13 through 18. Presented, in Figures 13a through 18a are difference data for the maximum perceived noise level descriptor, L_{PNSmx}, the maximum A-weighted sound level descriptor, L_{ASmx}, and the maximum D-weighted sound level descriptor, L_{DSmx}. The L_{DSmx} descriptor was included because it has been shown to agree well with the L_{PNSmx} descriptor [13]. Figures 13b through 18b present spectral level comparisons referenced to the SAE Method for the selected one-third octave-bands of 125, 250, 500, 1k, 2k, 4k, 6.3k, 8k, and 10k Hz.

Utilizing the same technique and the as-measured data from the MD-80 aircraft as above, comparisons of Case 1 noise-distance curves were made at three additional points in the FAR 36 window, i.e. at conditions of 4°C and 70 %RH, 18°C and 43 %RH , and 33°C and 50 %RH. Noise level comparisons referenced to the SAE Method are shown in Figures 19 through 21 for Method 1 and Method 5 only.

2.4 Effects of Atmospheric Pressure - Case 1

The effects of pressure on atmospheric absorption as calculated with the pure-tone Equations [1] through [6] are presented in Figures 22 through 25. Using Method 5 and the SAE Method in turn, the previously-referenced MD-80 aircraft data were first corrected to a near source location, adjusting for both spherical spreading and test day attenuation by atmospheric absorption (at constant pressure). This source data was then corrected to a number of receiver locations from 200 to 25,000 feet (61 to 7620 meters) at the four selected reference temperature/humidity conditions (25°C and 70 %RH; 4°C and 70 %RH; 18°C and 43 %RH; 33°C and 50 %RH) taking into account atmospheric pressure changes with altitude using the standard ISO pressure lapsed rate as follows:

$$\text{Pressure} = 10^{(-5.256E-05 \times \text{alt})} \quad \text{[atmospheres] [13]}$$

where:

alt = altitude above mean sea level [meters]

Comparisons were made of noise-distance curves computed using the SAE Method, and Method 5 taking into account atmospheric pressure changes as a function of altitude. These comparisons are presented for the four selected reference temperature/relative humidity points of 25°C and 70 %RH; 4°C and 70 %RH; 18°C and 43 %RH; and 33°C and 50%RH in, Figures 22 through 25, respectively.

3. RESULTS

Section 3 discusses the results of the current study and is organized as follows:

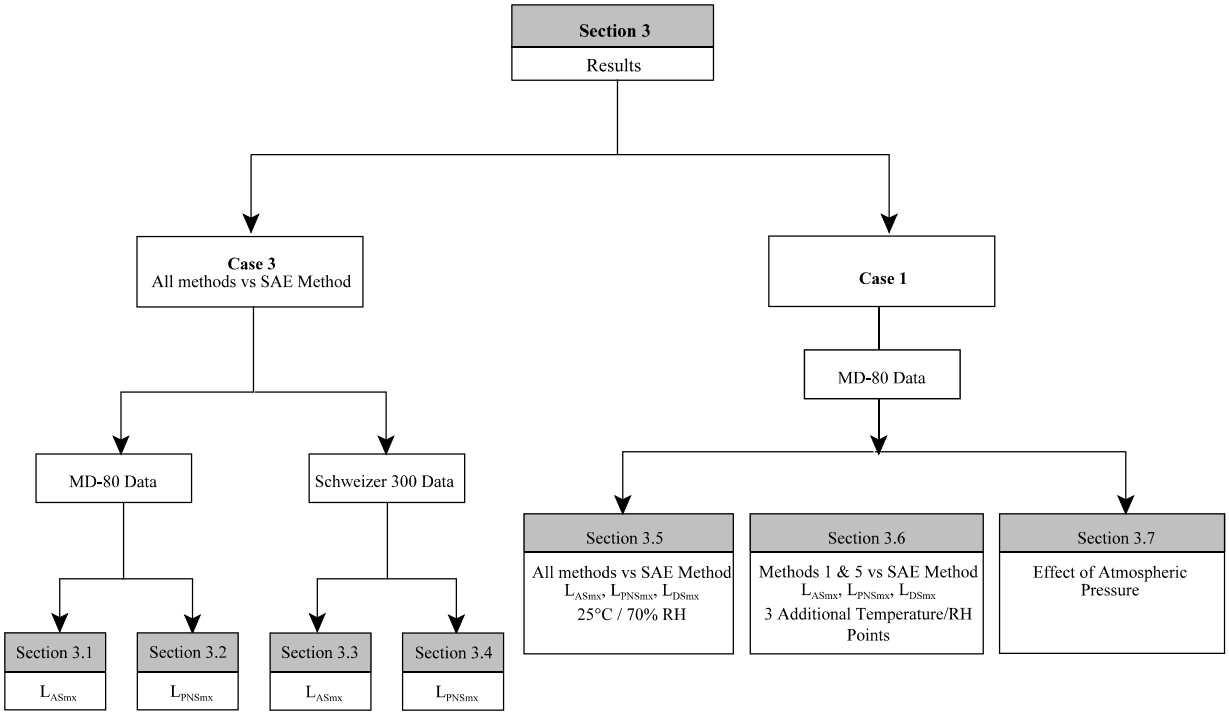

3.1 Case 3; MD-80; L_{ASmx} Difference Data

Figures 5 and 6 present, for Case 3 corrected data, a 27-point grid of L_{ASmx} difference values for the MD-80 jet aircraft as a function of test-day temperature and relative humidity at reference distances of 300 and 1000 meters, respectively. Distances of 300 and 1000 meters were selected since they generally cover the range of distances encountered during the takeoff and sideline portion of a typical fixed-wing noise certification test.

For each combination of test-day temperature and humidity, two difference values are displayed in Figures 5a and 6a for 300 and 1000 meters, respectively. The first value ($^{a}1$) represents the L_{ASmx} differences computed using Method 1 minus the SAE Method. The second value ($^{a}2$) represents the L_{ASmx} differences computed using Method 2 minus the SAE Method.

Figures 5b and 6b display, for 300 and 1000 meters respectively, three difference values. The first

value (^{a}3) represents the L_{ASmx} differences computed using Method 3 minus the SAE Method. The second value (^{a}4) represents the L_{ASmx} differences computed using Method 4 minus the SAE Method. The third value (^{a}5) represents the L_{ASmx} differences computed using Method 5 minus the SAE Method.

To determine an overall measure of the difference between methods as compared with the SAE Method, the array of difference values were algebraically averaged for each 27-point grid. The average difference value, its associated standard deviation and the maximum difference value for the MD-80 Aircraft are shown in the following table:

Reference Distance 300 meters; L_{ASmx} Data

	AVG. DIFF. (dB)	STD. DEV. (dB)	MAX. DIFF. (dB)
Method 1	0.103	0.098	0.48
Method 2	0.065	0.129	0.49
Method 3	0.120	0.132	0.33
Method 4	0.054	0.067	0.24
Method 5	0.058	0.108	0.23

Reference Distance 1000 meters; L_{ASmx} Data

	AVG. DIFF. (dB)	STD. DEV. (dB)	MAX. DIFF. (dB)
Method 1	-0.139	0.315	0.76
Method 2	-0.154	0.287	0.69
Method 3	-0.138	0.210	-0.40
Method 4	-0.184	0.252	-0.59
Method 5	-0.176	0.242	-0.54

The differences displayed are a measure of the expected change in certified A-weighted noise levels should one of the methods replace the current SAE method. A negative difference represents a decrease in certified level should the new method be adopted.

On average, as shown in the above table, all methods produce essentially the same result (at 300 meters the levels are approximately 0.1 dB greater than those computed with the current SAE Method; at 1000 meters the levels are approximately 0.2 dB less than those computed with the current SAE Method).

Note, although the average difference is negative at 1000 meters the difference transitions to positive values, in the temperature region in excess of 80°F, resulting in L_{ASmx} values greater than those computed with the current SAE Method, as much as 0.76 and 0.69 greater for Methods 1 and 2, respectively.

3.2 Case 3; MD-80; L_{PNSmx} Difference Data

Figures 7 and 8 present, for Case 3 corrected data, a 27-point grid of L_{PNSmx} difference values for the MD-80 jet aircraft as a function of test-day temperature and relative humidity at reference distances of 300 and 1000 meters, respectively. Distances of 300 and 1000 meters were selected since they generally cover the range of distances encountered during the takeoff and sideline portion of a typical fixed-wing noise certification test.

For each combination of test-day temperature and humidity, two difference values are displayed in Figures 7a and 8a for 300 and 1000 meters, respectively. The first value ($^a1$) represents the L_{PNSmx} differences computed using Method 1 minus the SAE Method. The second value ($^a2$) represents the L_{PNSmx} differences computed using Method 2 minus the SAE Method.

Figures 7b and 8b display, for 300 and 1000 meters respectively, three difference values. The first value ($^a3$) represents the L_{PNSmx} differences computed using Method 3 minus the SAE Method. The second value ($^a4$) represents the L_{PNSmx} differences computed using Method 4 minus the SAE Method. The third value ($^a5$) represents the L_{PNSmx} differences computed using Method 5 minus the SAE Method.

To determine an overall measure of the difference between methods as compared with the SAE Method, the array of difference values were algebraically averaged for each 27-point grid. The average difference value, its associated standard deviation, and the maximum difference value for the MD-80 Aircraft are shown in the following table:

Reference Distance 300 meters; L_{PNSmx} Data

	AVG. DIFF. (dB)	STD. DEV. (dB)	MAX. DIFF. (dB)
Method 1	0.354	0.284	0.76
Method 2	0.363	0.287	0.75
Method 3	0.496	0.396	1.11
Method 4	0.319	0.229	0.67
Method 5	0.333	0.245	0.73

Reference Distance 1000 meters; L_{PNSmx} Data

	AVG. DIFF. (dB)	STD. DEV. (dB)	MAX. DIFF. (dB)
Method 1	0.013	0.222	0.35
Method 2	0.125	0.185	0.38
Method 3	0.514	0.520	1.48
Method 4	0.250	0.222	0.56
Method 5	0.301	0.273	0.75

The differences displayed are a measure of the expected change in certified Perceived Noise Levels should one of the methods replace the current SAE method. A negative difference represents a decrease in certified level should the new method be adopted.

On average, as shown in the above table, Method 3 produces the largest levels, approximately 0.5 dB greater than the Perceived Noise levels produced by the SAE Method for both the 300 and 1000 meter distances. The remaining methods produce essentially the same result at both 300 and 1000 meters approximately 0.3 dB greater than the SAE Method, except for Method 1 at 1000 meters where the levels are essentially equal to those computed using the SAE Method.

Note, although the average difference is positive, the difference transitions to negative values at 300 meters in the 80°F temperature region for relative humidity values greater than 80 %RH. The transition region to negative differences at 1000 meters lies in the 80 to 95 %RH region over the 50 to 95°F temperature range.

3.3 Case 3; Schweizer 300; L_{ASmx} Difference Data

Figures 9 and 10 present, for Case 3 corrected data, a 27-point grid of L_{ASmx} difference values for the Schweizer Helicopter as a function of test-day temperature and relative humidity at reference distances of 300, and 1000 meters, respectively. Distances of 300 and 1000 meters were selected since they generally cover the range of distances encountered during a typical helicopter noise certification test. Difference values were also computed for the 100 meter distance, but these values are not displayed in the figures since they were so small. However, the statistical data for the 100 meter grid are shown in the summary table below.

For each combination of test-day temperature and humidity, two difference values are displayed in Figures 9a and 10a for 300 and 1000 meters, respectively. The first value ($^{a}1$) represents the L_{ASmx} differences computed using Method 1 minus the SAE Method. The second value ($^{a}2$) represents the L_{ASmx} differences computed using Method 2 minus the SAE Method

Figures 9b and 10b for 300 and 1000 meters, respectively, display three difference values. The first value ($^{a}3$) represents the L_{ASmx} differences computed using Method 3 minus the SAE Method. The second value ($^{a}4$) represents the L_{ASmx} differences computed using Method 4 minus the SAE Method. The third value ($^{a}5$) represents the L_{ASmx} differences computed using Method 5 minus the SAE Method.

To determine an overall measure of the difference between methods as compared with the SAE Method, the array of difference values were algebraically averaged for each 27-point grid. The average difference value, its associated standard deviation, and the maximum difference value for the Schweizer 300 Helicopter are shown in the following table:

Reference Distance 100 meters; L_{ASmx} Data

	AVG. DIFF. (dB)	STD. DEV. (dB)	MAX. DIFF. (dB)

Method 1	0.007	0.011	0.02
Method 2	0.007	0.011	0.02
Method 3	0.007	0.011	0.03
Method 4	0.007	0.011	0.02
Method 5	0.007	0.011	0.02

Reference Distance 300 meters; L_{ASmx} Data

	AVG. DIFF. (dB)	STD. DEV. (dB)	MAX. DIFF. (dB)
Method 1	-0.004	0.035	0.08
Method 2	-0.003	0.036	0.09
Method 3	-0.001	0.036	0.09
Method 4	-0.004	0.034	0.08
Method 5	-0.004	0.034	0.08

Reference Distance 1000 meters; L_{ASmx} Data

	AVG. DIFF. (dB)	STD. DEV. (dB)	MAX. DIFF. (dB)
Method 1	0.016	0.186	-0.46
Method 2	0.012	0.186	-0.46
Method 3	0.013	0.184	-0.46
Method 4	0.014	0.188	-0.46
Method 5	0.012	0.184	-0.46

The differences displayed are a measure of the expected change in certified A-weighted noise levels should one of the methods replace the current SAE method. A negative difference represents a decrease in certified level should the new method be adopted.

On average, as shown in the table, all methods produce essentially the same A-weighted noise levels as the SAE Method at 100, 300 and 1000 meters. In all cases, these difference values are extremely small, effectively negligible. In the case of the 1000-meter data the maximum differences are as large as -0.46 dB, indicating a lower level (as compared with SAE) should anyone of the new methods be adopted.

3.4 Case 3 - Schweizer 300 - L_{PNSmx} Difference Data

Figures 11 and 12 present, for Case 3 corrected data, a 27-point grid of L_{PNSmx} difference values for the Schweizer 300 Helicopter as a function of test-day temperature and relative humidity at

reference distances of 300 and 1000 meters, respectively. Distances of 300 and 1000 meters were selected since they generally cover the range of distances encountered during a typical helicopter noise certification test. Difference values were also computed for the 100 meter distance, but these values are not displayed in the figures since they were so small. However, the statistical data for the 100 meter grid are shown in the summary table below.

For each combination of test-day temperature and humidity, two difference values are displayed in Figures 11a and 12a for 300 and 1000 meters, respectively. The first value ($^{a}1$) represents the L_{PNSmx} differences computed using Method 1 minus the SAE Method. The second value ($^{a}2$) represents the L_{PNSmx} differences computed using Method 2 minus the SAE Method.

Figures 11b and 12b for 300 and 1000 meters, respectively, display three difference values. The first value ($^{a}3$) represents the L_{PNSmx} differences computed using Method 3 minus the SAE Method. The second value ($^{a}4$) represents the L_{PNSmx} differences computed using Method 4 minus the SAE Method. The third ($^{a}5$) value represents the L_{PNSmx} differences computed using Method 5 minus the SAE Method.

To determine an overall measure of the difference between methods as compared with the SAE Method, the array of difference values were algebraically averaged for each 27-point grid. The average difference value, its associated standard deviation, and the maximum difference value for the Schweizer 300 Helicopter are shown in the following table:

Reference Distance 100 meters; L_{PNSmx} Data

	AVG. DIFF. (dB)	STD. DEV. (dB)	MAX. DIFF. (dB)
Method 1	0.040	0.039	0.09
Method 2	0.052	0.047	0.12
Method 3	0.052	0.051	0.12
Method 4	0.051	0.049	0.08
Method 5	0.041	0.039	0.09

Reference Distance 300 meters; L_{PNSmx} Data

	AVG. DIFF. (dB)	STD. DEV. (dB)	MAX. DIFF. (dB)
Method 1	0.083	0.080	0.16
Method 2	0.115	0.109	0.23
Method 3	0.138	0.132	0.32
Method 4	0.091	0.086	0.19
Method 5	0.103	0.097	0.23

Reference Distance 1000 meters; L_{PNSmx} Data

	AVG. DIFF. (dB)	STD. DEV. (dB)	MAX. DIFF. (dB)
Method 1	0.048	0.172	0.32

Method 2	0.114	0.183	0.42
Method 3	0.217	0.250	0.56
Method 4	0.145	0.189	0.45
Method 5	0.171	0.211	0.48

The differences displayed are a measure of the expected change in certified Perceived Noise levels should one of the methods replace the current SAE method. A negative difference represents a decrease in certified level should the new method be adopted.

On average, as shown in the table, Method 3 at 1000 meters produces the largest levels, approximately 0.2 dB greater than the perceive noise levels produced by the SAE Method. The remaining methods each produce essentially the same average result at 100, 300 and 1000 meters, approximately 0.1 dB greater than the SAE produced levels.

Note, although the average difference is positive at both 300 meters and 1000 meters the difference transitions to negative values producing L_{PNSmx} levels less than the SAE Method in the upper right hand corner (high temperature, high humidity region) of the FAR36 window. The differences also transition to negative in the region along the left hand edge of the window for Methods 1 and 2.

3.5 Case 1; MD-80;L_{ASmx}, L_{PNSmx}, L_{DSmx} NOISE-DISTANCE Comparisons; 25°C/70%RH

Using the previously-referenced data for the MD-80 jet aircraft, comparisons were made of noise-distance curves generated at temperature/humidity conditions of 25°C and 70 %RH for each of the five methods compared herein with the SAE Method.

Comparisons are shown in Figures 13 through 17. Figures 13a through 17a present, for each method, the difference data for the maximum A-weighted sound level descriptor, L_{ASmx}, the maximum perceived noise level descriptor, L_{PNSmx}, and the maximum D-weighted sound level descriptor, L_{DSmx}. Figures 13b through 17b present comparisons of spectral noise data for selected one-third octave-bands from 125 to 10,000 Hz.

Inspection of the L_{ASmx}, L_{PNSmx}, and L_{DSmx} noise descriptor data presented in Figures 13a through 17a shows that no one method differs substantially from the others. Through 1920 meters the L_{ASmx} descriptor differs by no more than 0.2 dB regardless of the method used to generate the noise-distance curves; while the L_{PNSmx} and L_{DSmx} descriptors compare within 0.5 dB. Over the remaining distances, the three noise descriptors are within 1 dB to 3048 meters, 2 dB to 4876 meters, and 3.5 dB to 7620 meters regardless of the method. A positive difference represents an increase in certified level should the new method be adopted.

The spectral difference data of Figures 13b through 17b reveal some fairly substantial differences as a function of frequency when comparing each method with the SAE Method. Note first that all methods closely track one another in all one-third-octave bands up to and including the 1000 Hz band through a distance of 7620 meters, with differences increasing to as much as ±5 dB at 7620 meters.

Method 1, Figure 13b, shows the difference data to increase rapidly in the negative direction indicating a rapid decrease in high frequency absorption versus the SAE Method (note for example the 10 kHz band at distances greater than 610 m). This decrease in absorption noted with Method 1 is a phenomenon of the shape and linear operating range of the one-third octave-band filters assumed in this study. Specifically, it is caused by "leakage" of sound energy into the band in question through the low-frequency skirts of the filter. The result is a lower than expected "effective" absorption for the band in question. This effect is more pronounced for high frequency spectral noise data. This phenomenon was not found when an "ideal" filter shape was assumed in the study, because an "ideal" filter has skirts with an infinite-slope outside the passband and the inaccuracy of low frequency "leakage" is eliminated since there is no transmission of acoustic energy outside of the passband.

Method 2, Figure 14b, shows the Approximate Method breaking down when the pure-tone attenuation exceeds the ANSI-recommended limit of 50 dB total absorption over the propagation path. Specifically, note that the difference data increases rapidly in the negative direction indicating a decrease toward unrealistically low values of high frequency absorption (e.g., 10 kHz above 610 meters, 8 kHz above 1219 meters, 6.3 kHz above 1920 meters, and 4 kHz above 4876 meters). See the discussion of the Approximate Method in Section 2.12 for further details on the breaking down of the method.

Methods 3, 4, and 5 (Figures 15b, 16b, and 17b) produce identical results, one to the other through 7620 meters up to and including the 4000 Hz band. This is expected since the identical procedure is used for the three methods through 4000 Hz. Note the difference versus the SAE Method above 1000 Hz increases in a negative direction to a maximum of -12 dB and -25 dB in the 2000 Hz and 4000 Hz bands, respectively. The differences above 4000 Hz for the three Methods are commented on below.

Method 3, Figure 15b, shows large positive differences for one-third octave-bands greater than 4000 Hz as compared with the SAE Method. This indicates a higher rate of absorption than that computed with the SAE Method. Although the data is not presented, Method 3 was shown to produce results very close to those that would be obtained using Method 1 when modified for the case of an "ideal" one-third octave-band filter with 100 dB dynamic range.

Method 4, Figure 16b, shows that the 6.3 kHz data agrees almost exactly with the SAE method through 7620 meters while the attenuation for the two higher bands is greater (positive difference levels) than that obtained with the SAE Method.

Method 5, Figure 17b shows the closest agreement (maximum difference of 25 dB in the 10 kHz band at 7620 meters) of all the methods tested as compared with the SAE Method. This agreement is obviously somewhat expected since the frequencies chosen for computing absorption in bands above 4000 Hz were selected to minimize differences as compared with the SAE Method.

It is important to point out that both the L_{ASmx} and the L_{PNSmx} descriptors (Figures 13a through 17a) appear insensitive to the large frequency-based differences shown in Figures 13b through 17b. Inspection of corrected spectral data levels (not shown herein) showed the high-frequency levels are so small that the associated weighted descriptor is controlled almost entirely by data in the vicinity of the 500 to 1000 Hz range for distances greater than 1920 meters.

3.6 Case 1; MD-80; L_{ASmx}, L_{PNSmx}, L_{DSmx} NOISE-DISTANCE Comparisons; Three Additional Temperature/RH Points

Case 1 comparisons with the SAE Method were also made using the MD-80 data at the three additional reference points of 4°C and 70 %RH; 18°C and 43 %RH; and 33°C and 50 %RH using Method 1, the Spectral Integration Method, and Method 5, the Pure-Tone Empirical "Edge-Frequency" Method.

Presented in Figures18a through 23a for each method are difference data for the maximum A-weighted sound level descriptor, L_{ASmx}, the maximum Perceived Noise level descriptor, L_{PNSmx}, and the maximum D-weighted sound level descriptor, L_{DSmx}. Figures18b through 23b presents comparisons of spectral data for selected one-third octave-bands from 125 to 10,000 Hz.

Comparison of the difference curves for the three noise descriptors (L_{ASmx}, L_{PNSmx}, and L_{DSmx}) generated with Method 1 and Method 5 (Figure 18a with Figure 19a, Figure 20a with Figure 21a, and Figure 22a with Figure 23a) shows that for a specific temperature/humidity point both methods produce essentially the same result as compared with the SAE Method. However, as expected, the results within the same Method for unique temperature/humidity points are all noticeably different. The data for the 18°C and 43 %RH point (Figures 20a and Figure 21a) has the closest tracking versus the SAE Method over the 7620 meters (less than 0.5 dB). The 4°C and 70 %RH point displays the largest differences of the three points tested when compared with the SAE Method (less than 0.5 dB through 610 meters increasing to less than 4 dB at 7620 m).

The spectral difference data of Figures 18b through 23b reveal some fairly substantial differences as a function of frequency when comparing each method with the SAE Method. As with the 25°C and 70 %RH data discussed in Section 3.5, both methods closely track one another at these three data points in all bands up to and including the 1000 Hz band (less than ±5 dB at 7620 m), with differences versus the SAE Method increasing in the negative direction to less than 20 dB for the 2000 Hz band at 7620 meters.

Method 1, Figures 18b, 20b, and 22b, shows that for bands greater than 2000 Hz, the difference levels increase rapidly in the negative direction (smaller than expected attenuation versus the SAE Method) because of filter "leakage" effects.

Method 5 data track the SAE Method data to 7620 meters in bands greater than 2000 Hz with differences less than -35 dB at 4°C and 70 %RH (Figure 19b), and less than +30 dB at 33°C and 50 %RH (Figure 23b) at 10 kHz. At the 18°C, and 43 %RH point (Figure 21b) differences in excess of +50 dB are noted.

Here, as was the conclusions in Section 3.5, because of the long propagation distance and associated large absorption values, the highly-sensitive high frequency data has little if any effect (for both Methods 1 and 5) on the calculated noise descriptors.

3.7 Effect of Atmospheric Pressure

Case 1 comparisons with the SAE Method were made using MD-80 data and assuming a pressure lapse versus altitude introduced into the ISO Equations [1] through [6] at the four reference conditions of 25°C and 70 %RH, 4°C and 70 %RH, 18°C and 43 %RH, and at 33°C and 50 %RH using only Method 5, the Pure-Tone Method with Empirical "Edge-Frequencies".

Comparisons of noise-distance data referenced to SAE-adjusted data are shown in Figures 24 through 27. Presented for Method 5 (Figures 24a through 27a) are difference data for the maximum Perceived Noise level descriptor, L_{PNSmx}, the maximum A-weighted sound level descriptor, L_{ASmx}, and the maximum D-weighted sound level descriptor, L_{DSmx}. Figures 24b through 27b presents comparisons of spectral data for selected one-third octave-bands from 125 to 10,000 Hz.

Comparison of the L_{PNSmx}, L_{ASmx}, and L_{DSmx} noise descriptor data presented in Figures 24a through 27a (with pressure lapse) with the noise descriptor data presented in Figures 17a, 19a, 21a, and 23a (with constant sea level pressure) shows that the noise descriptor data is virtually unaffected by the introduction of pressure into the equation through 7620 meters.

Inspection of the spectral data of Figures 24b, 25b, 26b, and 27b (with pressure lapse) and the spectral data of Figures 17b, 19b, 21b, and 23b (with constant sea level pressure) shows that through the 1000 Hz band the spectral data up to and including 7620 meters is also virtually unaffected. For the four reference points tested except for the 18°C and 43 %RH point (Figure 26b), the difference data in bands greater than 1000 Hz can be seen to increase (more than 30 dB in the 10 kHz band at 7620 meters) with the introduction of pressure (that is, the attenuation, due to absorption, decreases with the introduction of pressure). The 18°C and 43 %RH difference data decreases (more than 15 dB in the 10 kHz band at 7620 meters) with the introduction of pressure (that is, the attenuation, due to absorption, increases with the introduction of pressure).

4. CONCLUSIONS

Section 4 presents the conclusions of the current study. These conclusions focus on the two questions previously identified in Section 1.2.

What is the expected difference in the certified noise levels of typical aircraft corrected using one of five methods, as compared with certified levels corrected using SAE ARP 866A?

Time-Averaged Noise Descriptors: As shown for the Case 3 comparisons in Section 3.1 through Section 3.4, in terms of time-averaged noise descriptors such as L_{AE} and L_{EPN} (represented herein by L_{PNSmx} and L_{ASmx}), the differences in certified noise levels computed with any one of the five adaptations of the new ANSI/ISO absorption algorithms as compared with those computed using the SAE Method are dependent upon many variables, including the spectral shape of the source and the test-day temperature and humidity. However, some general statements regarding the expected differences can be made. For time-averaged descriptors, adoption of any one of the five adaptations would lead to very small changes in certified noise levels. Based on the aircraft and distances analyzed herein, the average expected changes over the entire FAR 36-allowable temperature/humidity window would be less than 0.2 dB for L_{AE} and less than 0.5 dB for L_{EPN} (maximum differences of 0.8 dB and 1.5 dB, respectively). The differences tend to be larger in the low temperature/low humidity region of the FAR 36 window, and as expected tend to decrease for test-day conditions close to FAR 36 reference-day conditions. The differences were slightly larger for the MD-80 jet aircraft, as compared with the Schweizer 300 helicopter. The data presented herein indicates that noise certified levels corrected with the ANSI/ISO algorithms may be either larger or smaller than those corrected using the SAE Method, although more often than not the levels corrected with the new method were slightly larger.

Noise-Distance Data: In addition to direct application for time-averaged noise-certified levels, the five adaptations of the new ANSI/ISO absorption algorithms were examined in terms of expected differences in individual one-third-octave frequency bands and for computation of Noise-Distance relationships (Case 1 comparisons -- Section 3.5). Using MD-80 test spectra at a reference temperature/humidity of 25°C and 70 %RH and up to a distance of 7620 meters no one method stands out as significantly different from the others for the L_{PNSmx}, L_{ASmx}, and L_{DSmx} noise descriptor data. More specifically, up to 1920 meters the L_{ASmx} descriptor compares closely with the SAE Method (within +0.2 dB) regardless of the method used to generate the noise-distance curves; while the L_{PNSmx} and L_{DSmx} descriptor compares within +0.5 dB. All three noise descriptors track the SAE Method to within +1 dB to 3048 meters, +2 dB to **4876** meters, and +3.5 dB to 7620 meters regardless of the method used. A positive difference represents an increase in level over the SAE Method.

One-Third Octave-Band Data: All methods closely track one another, versus the SAE Method, in all bands up to and including the 1000 Hz band through 7620 meters with differences increasing to less than approximately ±5 dB at 7620 meters. Method 5, the pure-tone method with empirically-derived "edge-frequencies", displays the closest Case 1 agreement in all bands when compared with the SAE Method. The maximum difference was observed to be +25 dB in the 10 kHz band at 7620 meters. This is not surprising, since the "edge-frequencies" for Method 5 were developed with the

idea of minimizing the differences as compared with the SAE Method. The differences using the other methods in the 10 kHz band were found to be well in excess of ±100 dB at distances up to 7620 meters.

Atmospheric Pressure Effects: Case 1 comparisons of Method 5 versus the SAE Method, show the L_{PNSmx}, L_{ASmx}, and L_{DSmx} noise descriptor data are virtually unaffected by the introduction of atmospheric pressure through a distance of 7620 meters. It was further shown that the spectral data through the 1000 Hz band and up to a distance of 7620 meters is also virtually unaffected. However, for the four reference points tested except the 18°C and 43 %RH point (Figure 26b), the difference data in bands greater than 1000 Hz can be seen to increase with the introduction of pressure (that is, the attenuation, due to absorption, decreases with the introduction of pressure). The 18°C and 43 %RH difference data decreases with the introduction of pressure (that is, the attenuation, due to absorption, increases with the introduction of pressure).

What potential complications exists for noise certification applicants should they have to implement a new method?

Although more accurate than the other methods, Method 1, the Spectrum Integration Method, is not considered herein as a viable option for regulatory adoption. It requires applicants to maintain an in-depth knowledge of their one-third octave-band filter characteristics, as well as establish a standardized means of obtaining narrow-band data, either through measurement or derivation. Also, it may be subject to large filter "leakage" errors (See Section 3.5). Such requirements would likely be far too costly, too time-consuming, and too burdensome for most applicants.

Implementation of Method 2, the Approximate Method of ANSI S1.26 or one of the pure-tone methods, Methods 3, 4, and 5, evaluated herein is relatively trivial, and generally no more complicated than the current method of SAE ARP 866A*. The primary difference is that the

---

*One requirement of the user that is unique to Method 2, the Approximate Method, as compared with the other methods, as well as the SAE Method, is that the applicant must determine if the filter set in their analyzer was designed as a base-10 or base-2 system. Both systems are widely used by the major analyzer manufacturers, e.g., Brüel and Kær Instruments, Inc. and Larson Davis Laboratories (LDL) use base-2 design filters in their analyzers, while the Hewlett Packard Company use base-10 design filters. If filter design information is not provided in the user's manual for the analyzer, it is readily available information from the manufacturer. While ANSI S1.26 is directly applicable for base-10 systems only, Section 2 of this report presents the appropriate constants and equations for both systems.

Also, it must be kept in mind that Equation [9] for computing band-level attenuation for Method 2, the Approximate Method, were based upon the response characteristics of a third-order Butterworth filter shape. Use of this method with one-third octave-band analysis systems containing different filter shapes may not be appropriate. Although the third-order Butterworth is by far the most common filter shape used by certification applicants today, FAR 36 does currently allow for the use of other shapes as long as they meet the requirements of the International Electrotechnical Commission (IEC) Standard, "Octave, half-octave and third-octave band filters intended for the analysis of sounds and vibrations", IEC Publication 225.[12]

The only exception to the Butterworth filter currently known to the authors is the so-called "long" filter capability offered in analyzers available from LDL. It should be kept in mind that all analyzers available from LDL also have a "short" filter capability. The short filter is generally consistent with the third-order Butterworth response characteristics. As such, use of LDL analyzers would not be precluded, but rather limited to use with the "short" filter option only.

Approximate Method requires that the pure-tone sound absorption be corrected using a filter bandwidth adjustment function while the SAE Method and the other pure-tone methods tested utilize

a single mid-band or edge-frequency to account for the effects of fractional-octave-band analysis for bands above 4000 Hz. Because of the uniqueness of the bandwidth adjustment factor, and more importantly the fact that the equation used to compute this factor tends to breakdown for total absorption over the path length of greater than 50 dB, the approximate method is also not a viable option for regulatory adoption. Any of the remaining three option herein would be viable options from the standpoint of regulatory adoption and ease of applicant implementation.

The primary source of complication in adopting the new method is not necessarily tied to the implementation itself, but rather to the validation required to ensure that the procedure was implemented properly. This would likely require revalidation of all previously-approved applicants. It is anticipated that revalidation could be performed relatively easily using a method similar to the current revalidation process. Specifically, previously-approved applicants would be required to resubmit data from one of their previously submitted events, but with a different set of arbitrarily-chosen temperature/humidity data plus atmospheric pressure data.

5. RECOMMENDATIONS

The new ANSI/ISO absorption methodology offers the added benefit of taking into account the effects of atmospheric pressure. Because it is based upon the most current theoretical work and empirical validation, it should be more accurate than the SAE Method. However, a controlled field measurement which focuses in on the highly sensitive frequency region above 4 kHz is needed to confirm its accuracy. The authors understand that a European contingent is performing such a test and will report the results at an upcoming meeting of SAE A-21. If the results conclude that the new method is more accurate, then the method should be adopted. Volpe is also currently pursuing other methods of addressing the accuracy issue.

This letter report makes no such recommendations in favor of, or against the new ANSI/ISO absorption methodology. What is addressed in this section are recommendations should the FAA decide to adopt the new method. These recommendations are as follows:

- Method 1, the Spectral Integration Method, is too complex and burdensome, and subject to large filter "leakage" errors (See Section 3.5), to be used for certification.

- Method 2, the ANSI Approximate Method, also should not be used for certification since it is filter-shape dependant, and breaks down when the recommended ANSI limit of 50 dB total absorption over the propagation path is exceeded. The 50 dB limit would be exceeded regularly in processing typical noise certification data.

- Ensure strict enforcement of the current test "window" allowed by FAR 36, or possibly consider making it more stringent, since this study brings to light the inherent differences associated with the methods, especially at the extreme limits of the current FAR 36 test "window".

- A potentially important, non-technical concern affecting the decision on whether or not to replace the current method, is the applicability of relative comparisons between currently-published, certified levels, and future certified levels computed using a new absorption methodology. The adoption of an empirical correction to older certified noise level data may need to be considered to facilitate a more appropriate comparison with data processed using the new ANSI/ISO methodology.

- Require a software revalidation of all previously-validated applicants.

6. REFERENCES

[1] Federal Aviation Regulations, Part 36, Noise Standards: Aircraft Type and Airworthiness Certification, Washington, D.C.: Federal Aviation Administration, September, 1992.

[2] Society of Automotive Engineers, Committee A-21, Aircraft Noise, Standard Values of Atmospheric Absorption as a Function of Temperature and Humidity, Aerospace Recommended Practice No. 866A, Warrendale, PA: Society of Automotive Engineers, Inc., March, 1975.

[3] American National Standards Institute, Committee S1, Acoustics, Method for Calculation of the Absorption of Sound by the Atmosphere, ANSI S1.26-1995, New York, NY: American National Standards Institute, September, 1995.

[4] International Organization for Standardization, Committee ISO/TC 43, Acoustics, Sub-Committee SC 1, Noise, Acoustics - Attenuation of sound during propagation outdoors - Part 1: Calculation of the absorption of sound by the atmosphere, ISO 9613-1, Geneva, Switzerland: International Organization for Standardization, 1993.

[5] American National Standards Institute, Committee S1, Acoustics, Specification for Octave-Band and Fractional-Octave-Band Analog and Digital Filters, ANSI S1.11-1986 (R1993), New York, NY: American National Standards Institute, 1993.

[6] Anton, H., Calculus, New York, NY: John Wiley and Sons, 1980.

[7] Joppa, P.D., Sutherland, L.C., Zuckerwar, A.J., Filter Effects in Analysis of Noise Bands, Paper 2aNS5 before 128th Meeting of Acoustical Society of America, Austin, TX, December, 1994.

[8] Joppa, P.D., Sutherland, L.C., Zuckerwar, A.J., Representative Frequency Approach to the Effect of Bandpass Filters on the Evaluation of Sound Absorptions, Noise Control Engineering Journal, Publication Pending.

[9] Payne, R.C., The Effect of Atmospheric Pressure on Measured Aircraft Noise Levels, Report Number RSA(EXT) 0048, Teddington, Middlesex, United Kingdom: National Physical Laboratory, 1994.

[10] Connor, T., Ehnbom, L., Fleming, G., Haight, N., May, D., Montuori, P., Svane, C., Payne, R.C., Accuracy of the Integrated Noise Model (INM): MD-80 Operational Noise Levels, A Joint Report of Luftfartsverket, Swedish Aviation Administration, and U.S. Department of Transportation, Federal Aviation Administration, May 1995.

[11] Rickley, E.J., Jones, K.E., Keller, A.S. Fleming, G.G., Noise Measurement Flight Test of Five Light Helicopters, Report Number DOT/FAA/EE/93/01, Cambridge, MA: John A. Volpe National Transportation Systems Center, July 1993.

[12] International Electrotechnical Commission, Octave, half-octave and third-octave band filters

intended for the analysis of sounds and vibrations, IEC Publication 225, Geneva, Switzerland: International Electrotechnical Commission, 1966

[13] Kryter, K.D., The Effects of Noise on Man, Academic Press, Inc., New York, Chapter II and Part III, 1970.

Figure 3a Comparison Calculation of Attenuation by Atmospheric Absorption
ISO Pure-Tone 10000Hz Attenuation minus SAE 9000Hz Attenuation

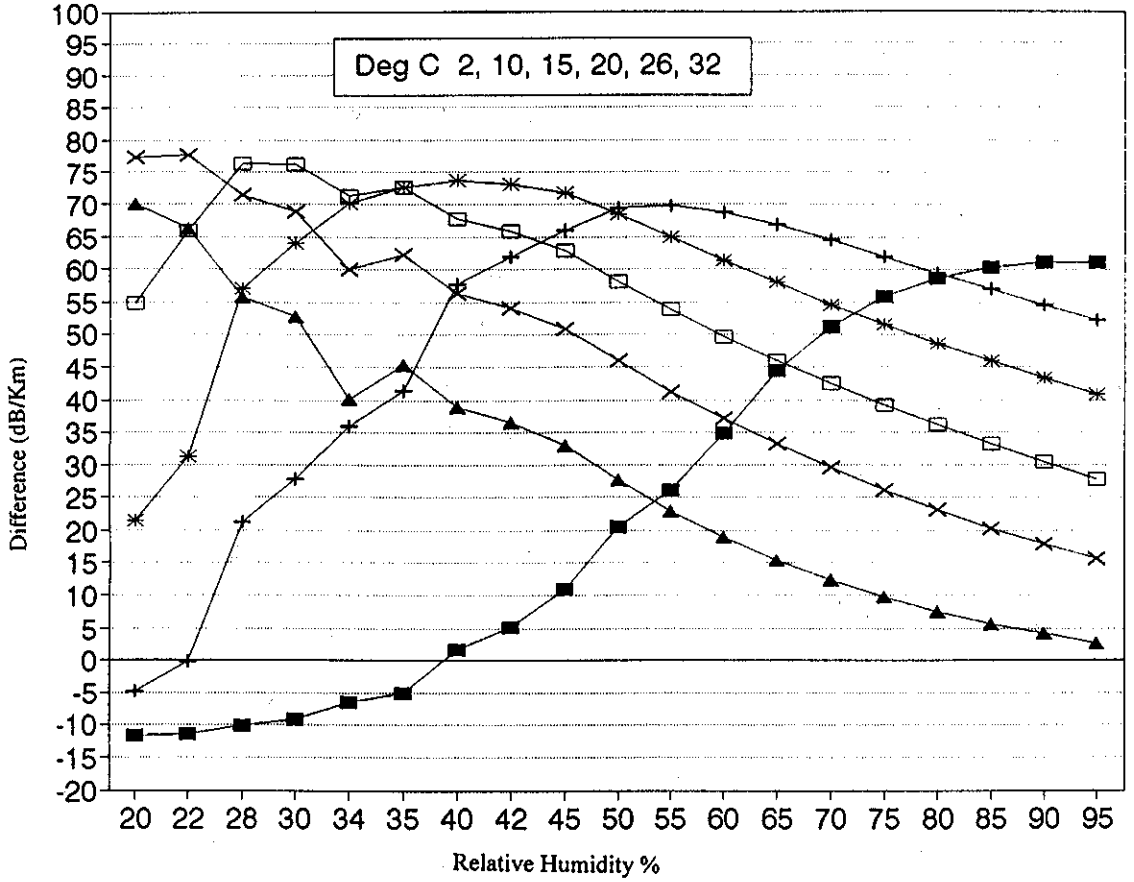

Figure 3b Comparison Calculation of Attenuation by Atmospheric Absorption
ISO Pure-Tone 8286Hz Attenuation minus SAE 9000Hz Attenuation

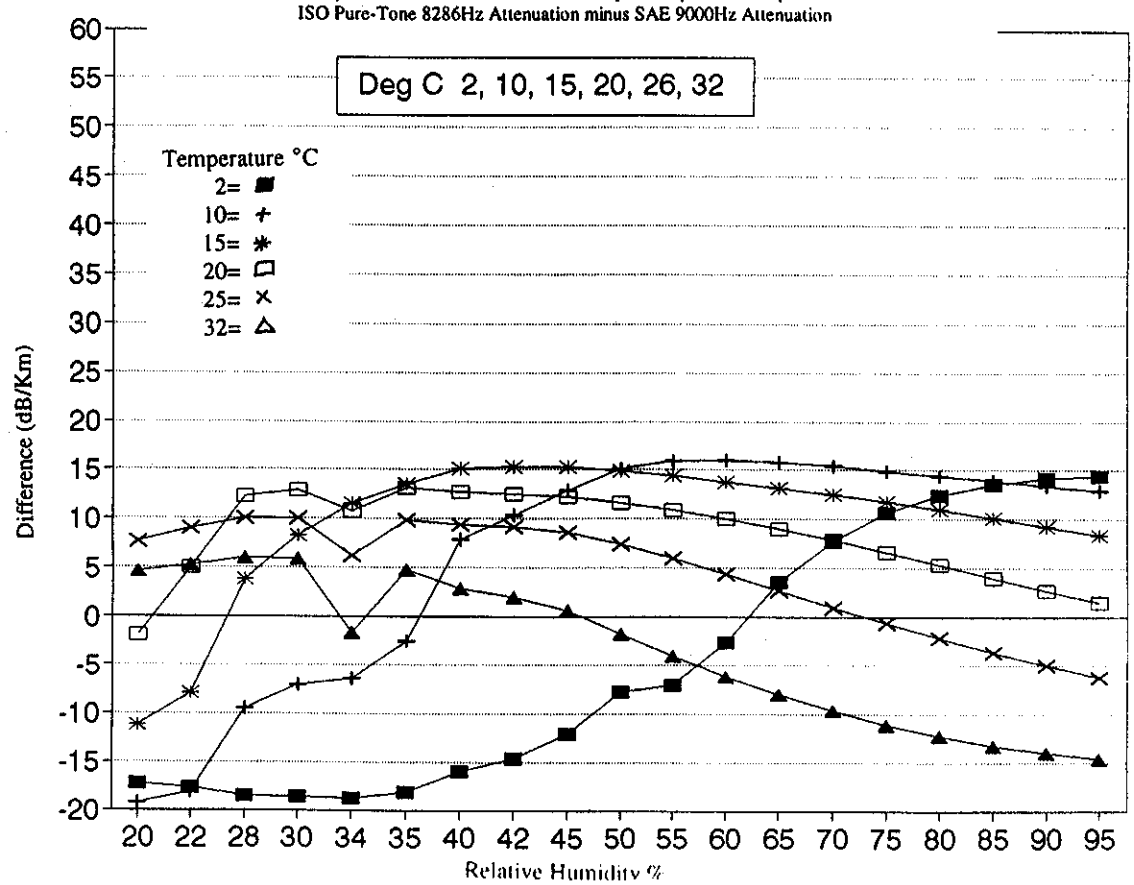

Figure 4a As-Measured Levels -- Modern Jet Aircraft
Takeoff, Propagation Distance 450 meters, Speed 166.7 feet/second
Temperature 18° C, Relative Humidity 43%

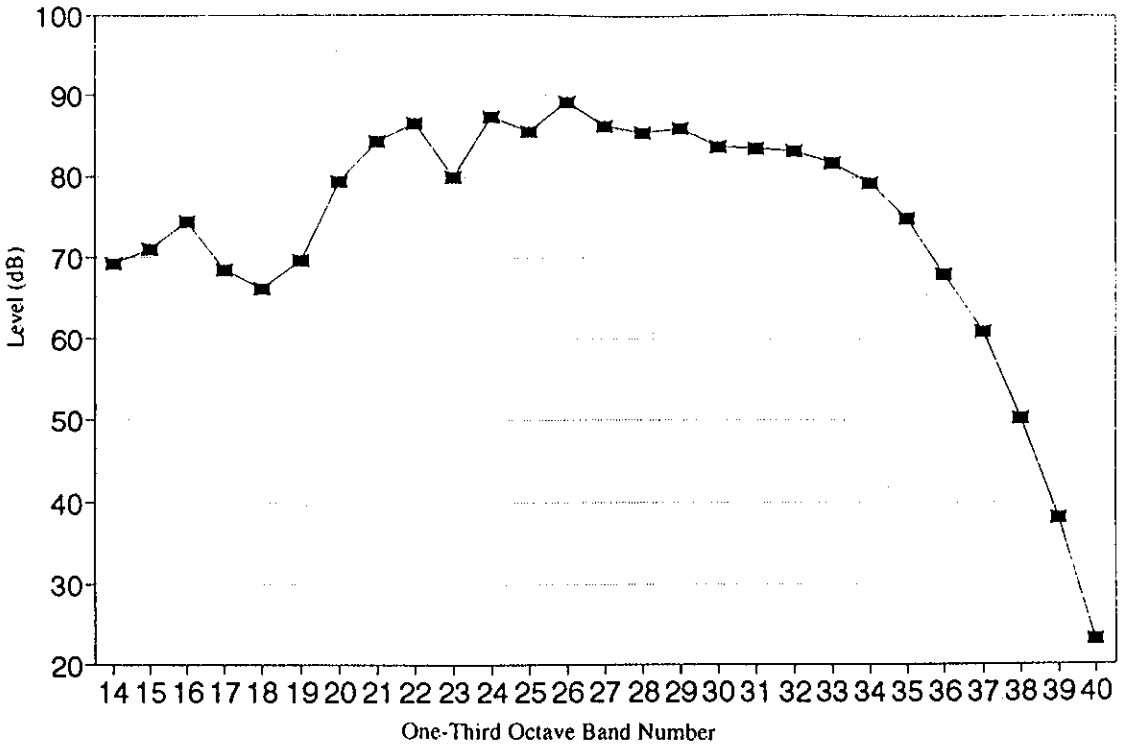

Figure 4b As-Measured Levels -- Modern Helicopter
Level Flyover, Propagation Distance 265.7 meters, Speed 58 feet/second
Temperature 33° C, Relative Humidity 50%

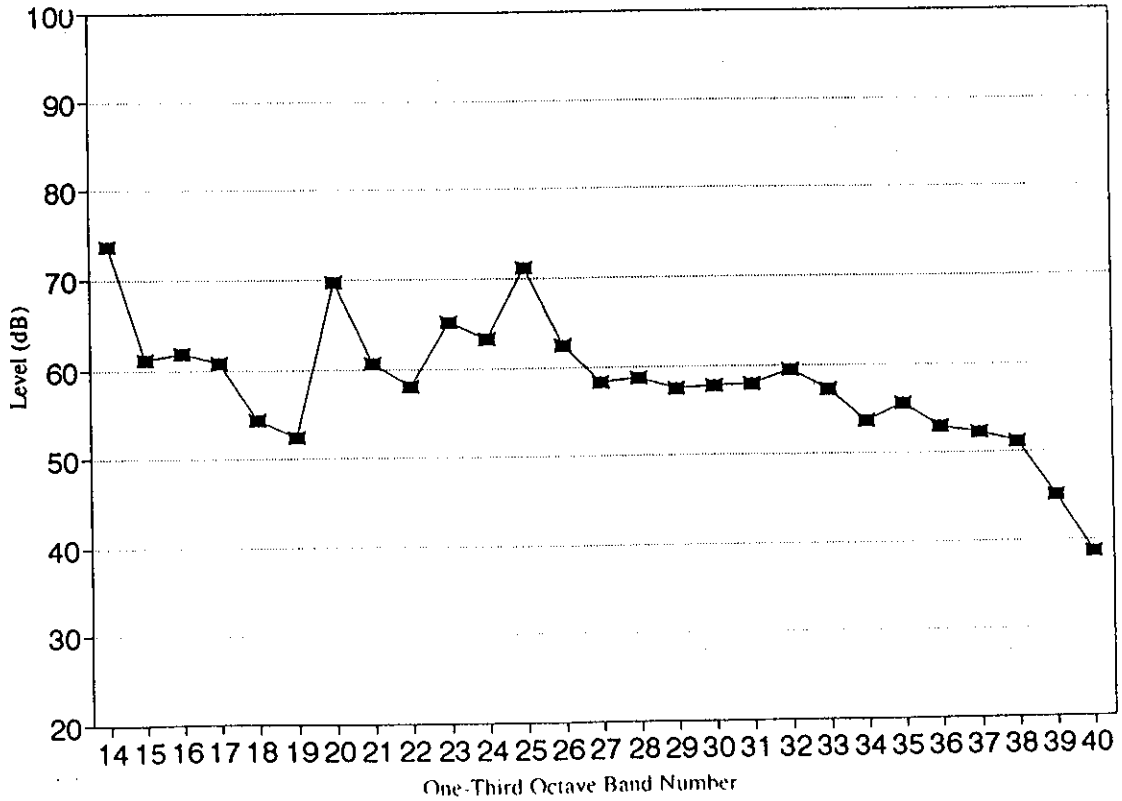

Figure 5a Modem Jet Aircraft

L_{ASmax} Difference Levels -- Reference Distance 300 meters -- (Δ1,Δ2)

Δ1 = Spectrum Integrated - SAE, Δ2 = Approximate - SAE

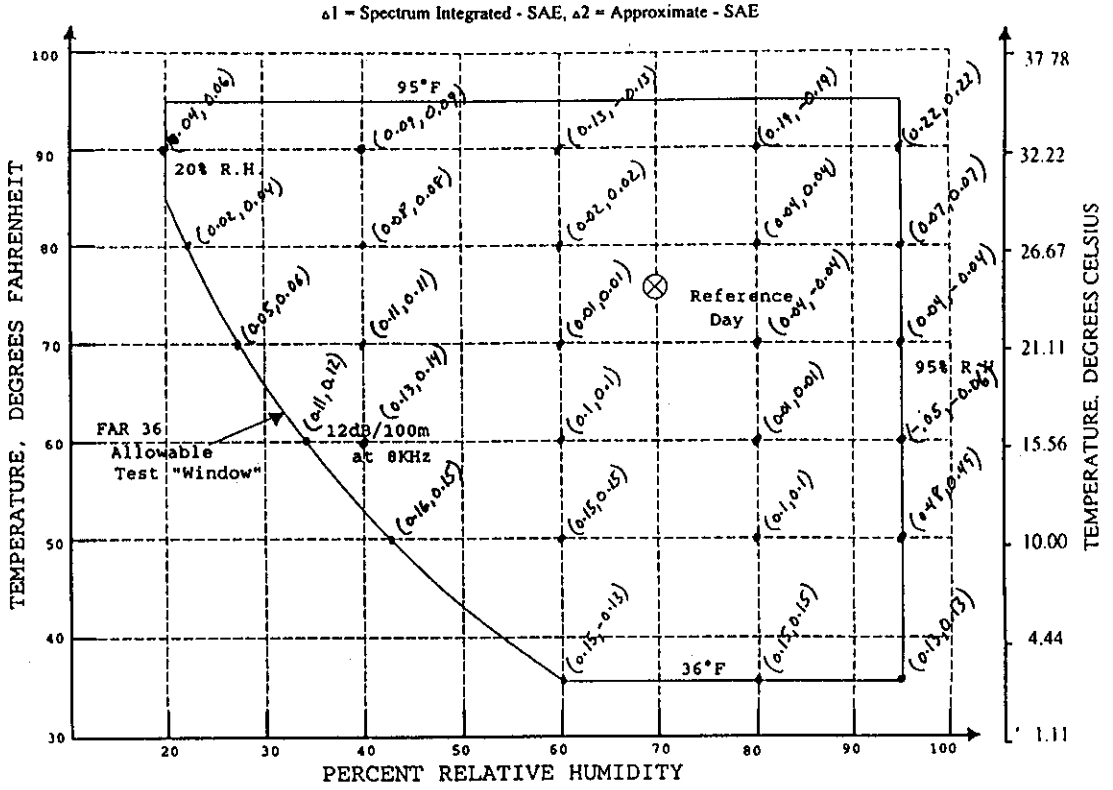

Figure 5b Modem Jet Aircraft

L_{ASmax} Difference Levels -- Reference Distance 300 meters -- (Δ3,Δ4,Δ5)

Δ3 = Pure-tone mid-band frequencies - SAE, Δ4 = Pure-tone SAE edge frequencies - SAE,

Δ5 = Pure-tone empirical edge frequencies - SAE

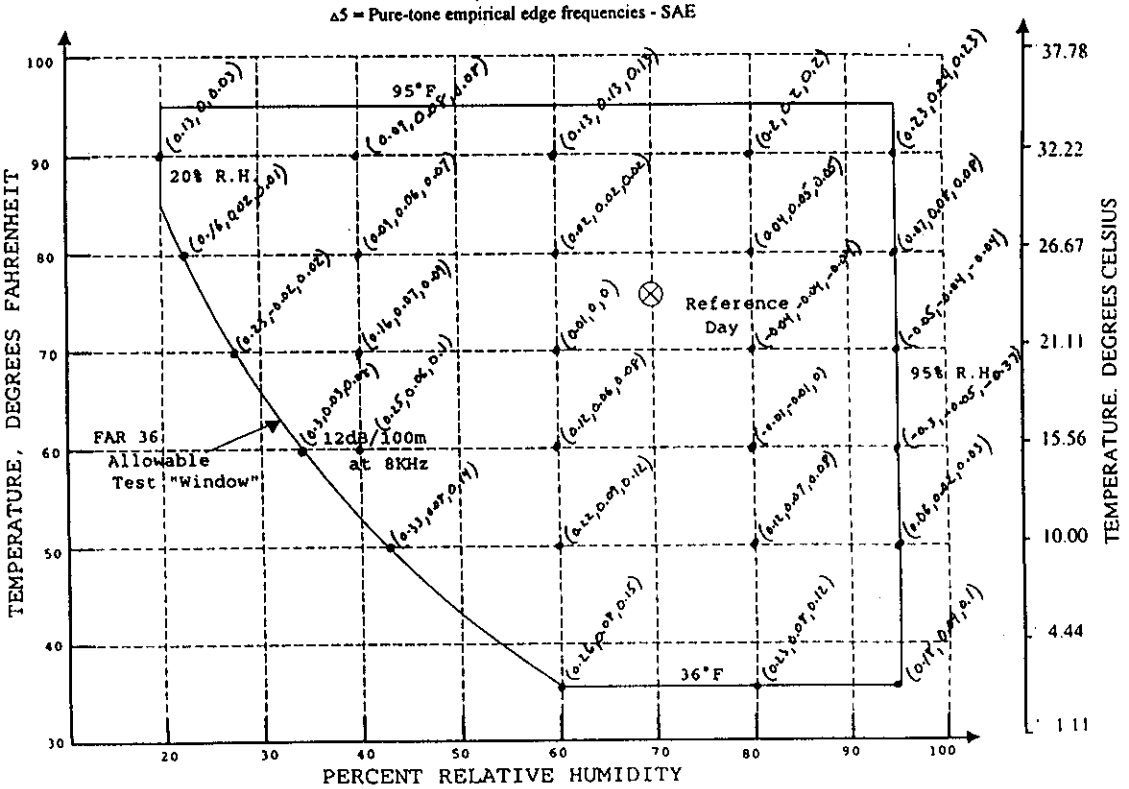

Figure 6a Modern Jet Aircraft

L_{ASmax} Difference Levels -- Reference Distance 1000 meters -- (Δ1,Δ2)

Δ1 = Spectrum Integrated - SAE, Δ2 = Approximate - SAE

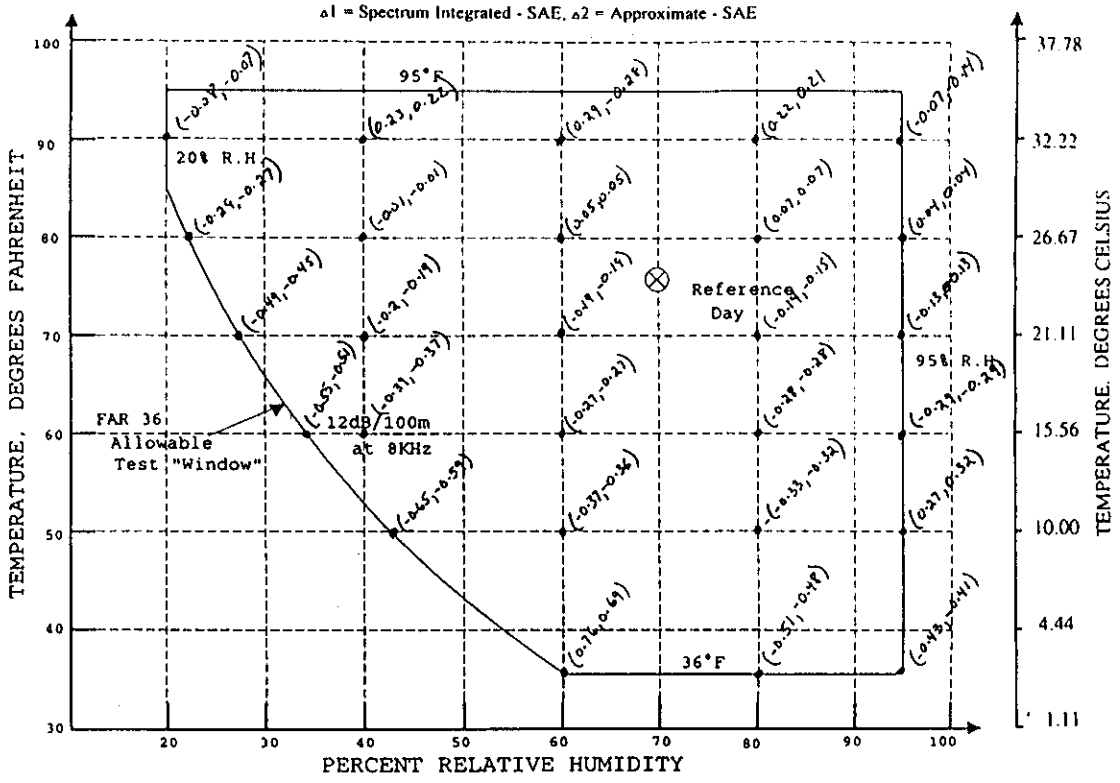

Figure 6b Modern Jet Aircraft

L_{ASmax} Difference Levels -- Reference Distance 1000 meters -- (Δ3,Δ4,Δ5)

Δ3 = Pure-tone mid-band frequencies - SAE, Δ4 = Pure-tone SAE edge frequencies - SAE,

Δ5 = Pure-tone empirical edge frequencies - SAE

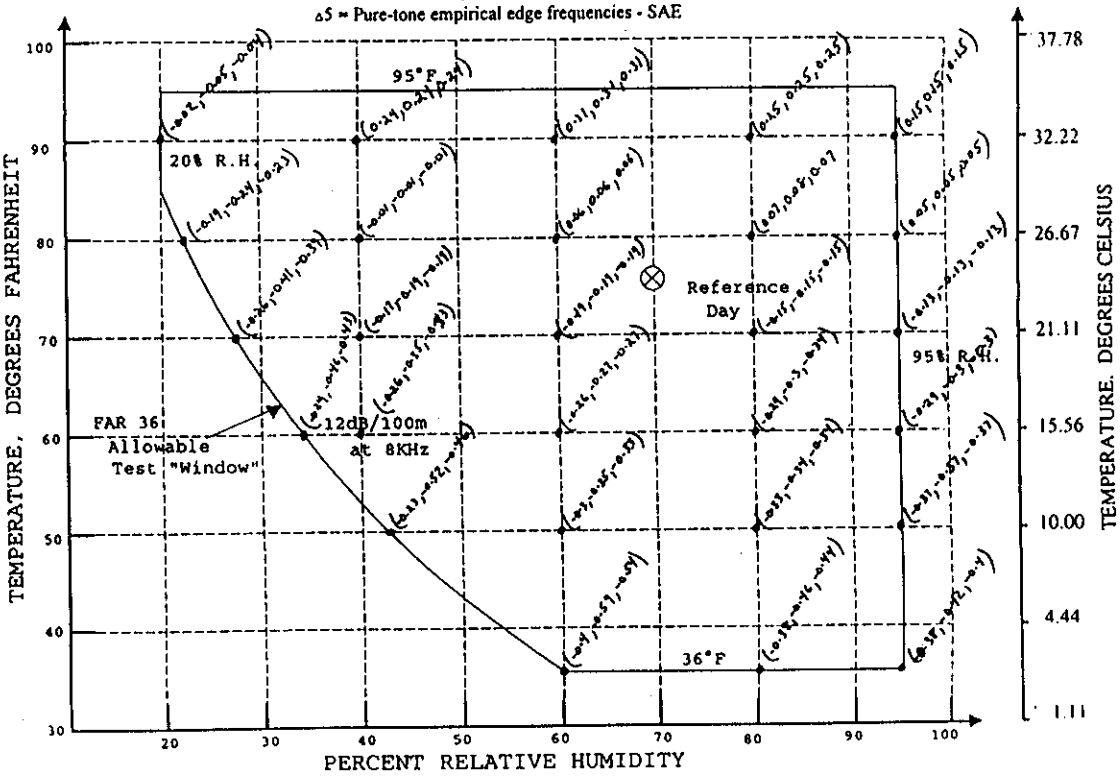

Figure 7a Modem Jet Aircraft

L_{PNSmax} Difference Levels -- Reference Distance 300 meters -- (Δ1,Δ2)

Δ1 = Spectrum Integrated - SAE, Δ2 = Approximate - SAE

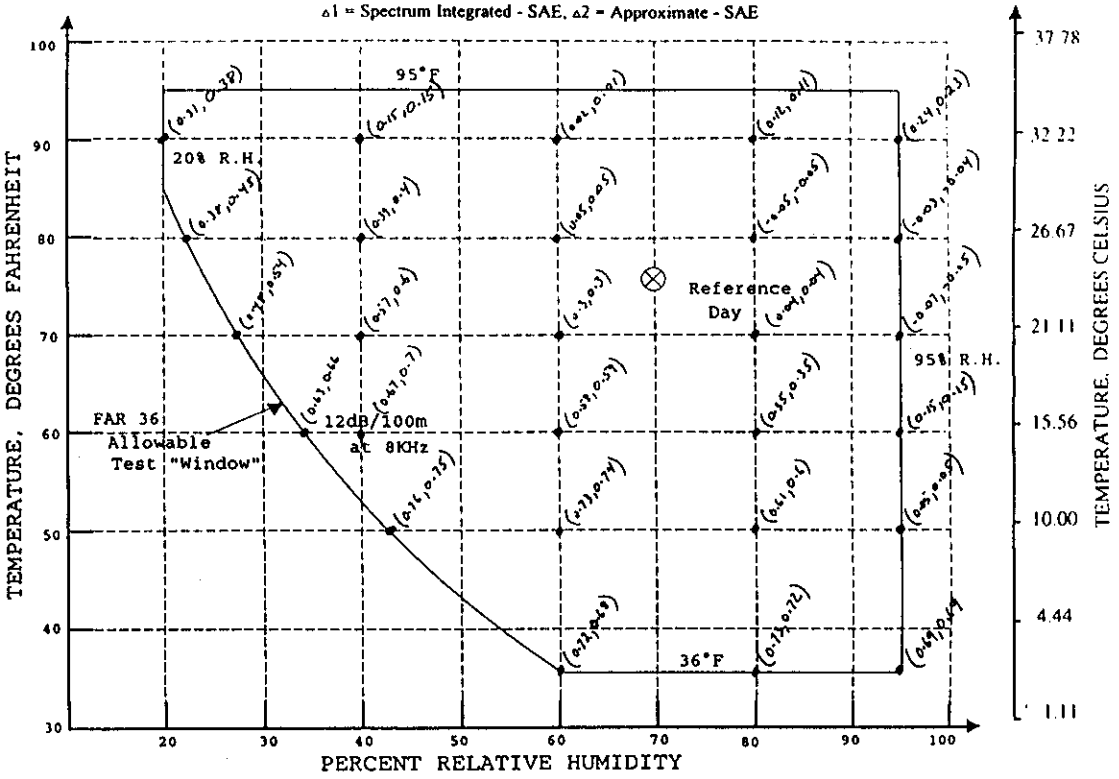

Figure 7b Modem Jet Aircraft

L_{PNSmax} Difference Levels -- Reference Distance 300 meters -- (Δ3,Δ4,Δ5)

Δ3 = Pure-tone mid-band frequencies - SAE, Δ4 = Pure-tone SAE edge frequencies - SAE,

Δ5 = Pure-tone empirical edge frequencies - SAE

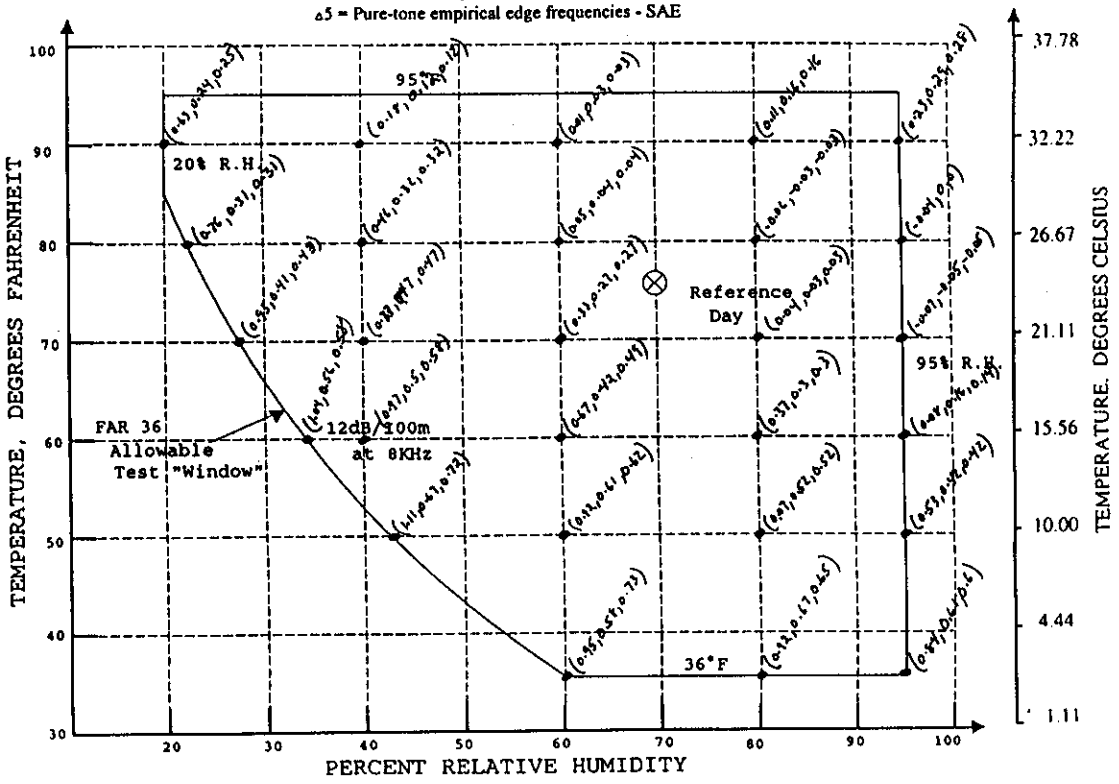

Figure 8a Modern Jet Aircraft

L_{PNSmax} Difference Levels -- Reference Distance 1000 meters -- (Δ1,Δ2)

Δ1 = Spectrum Integrated - SAE, Δ2 = Approximate - SAE

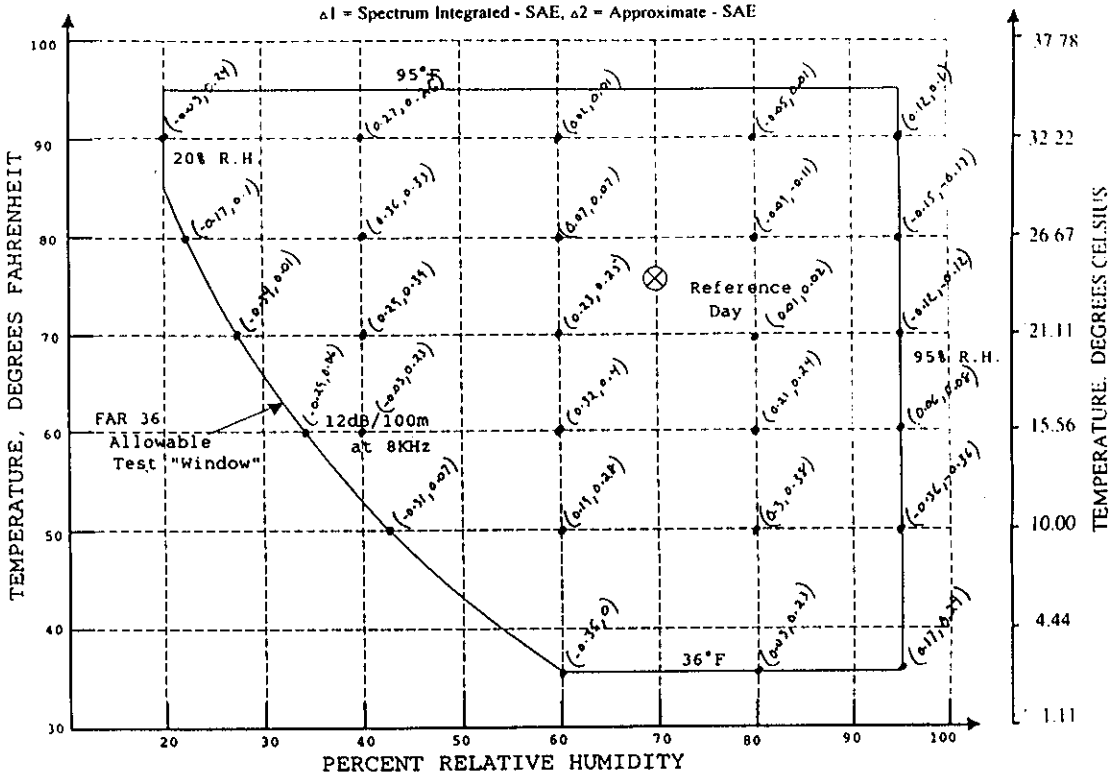

Figure 8b Modern Jet Aircraft

L_{PNSmax} Difference Levels -- Reference Distance 1000 meters -- (Δ3,Δ4,Δ5)

Δ3 = Pure-tone mid-band frequencies - SAE, Δ4 = Pure-tone SAE edge frequencies - SAE,

Δ5 = Pure-tone empirical edge frequencies - SAE

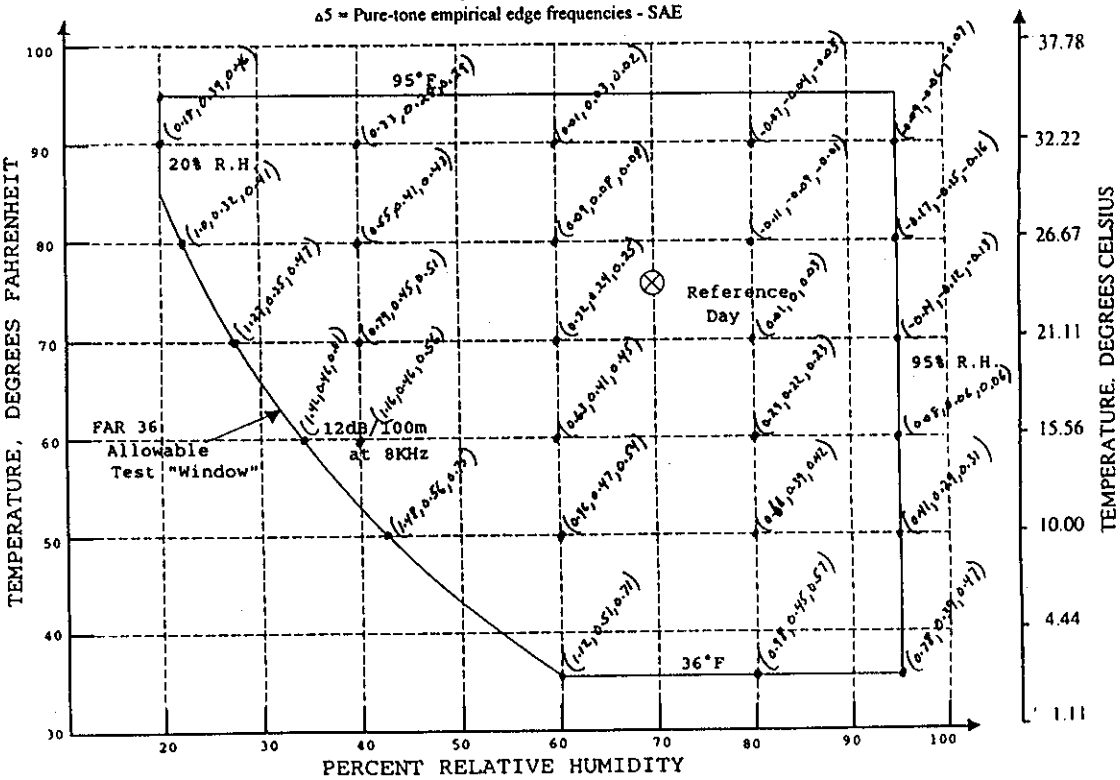

Figure 9a Modern Helicopter

L_{ASmax} Difference Levels -- Reference Distance 300 meters -- (Δ1,Δ2)

Δ1 = Spectrum Integrated - SAE, Δ2 = Approximate - SAE

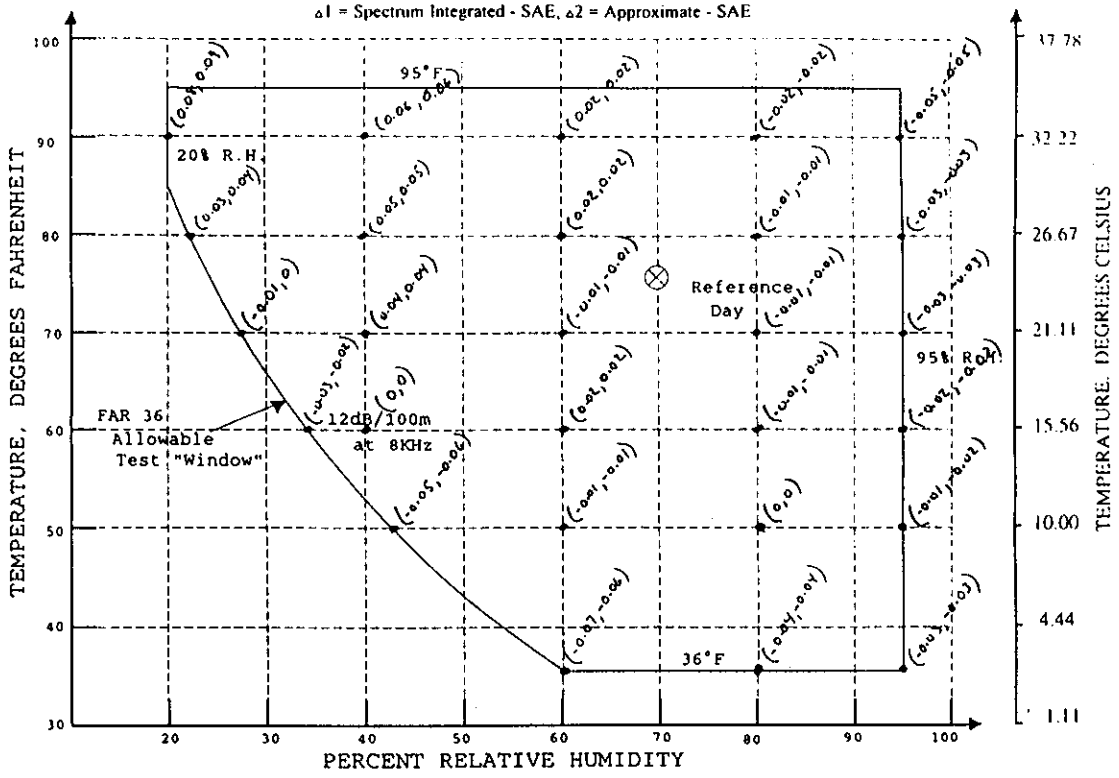

Figure 9b Modern Helicopter

L_{ASmax} Difference Levels -- Reference Distance 300 meters -- (Δ3,Δ4,Δ5)

Δ3 = Pure-tone mid-band frequencies - SAE, Δ4 = Pure-tone SAE edge frequencies - SAE,

Δ5 = Pure-tone empirical edge frequencies - SAE

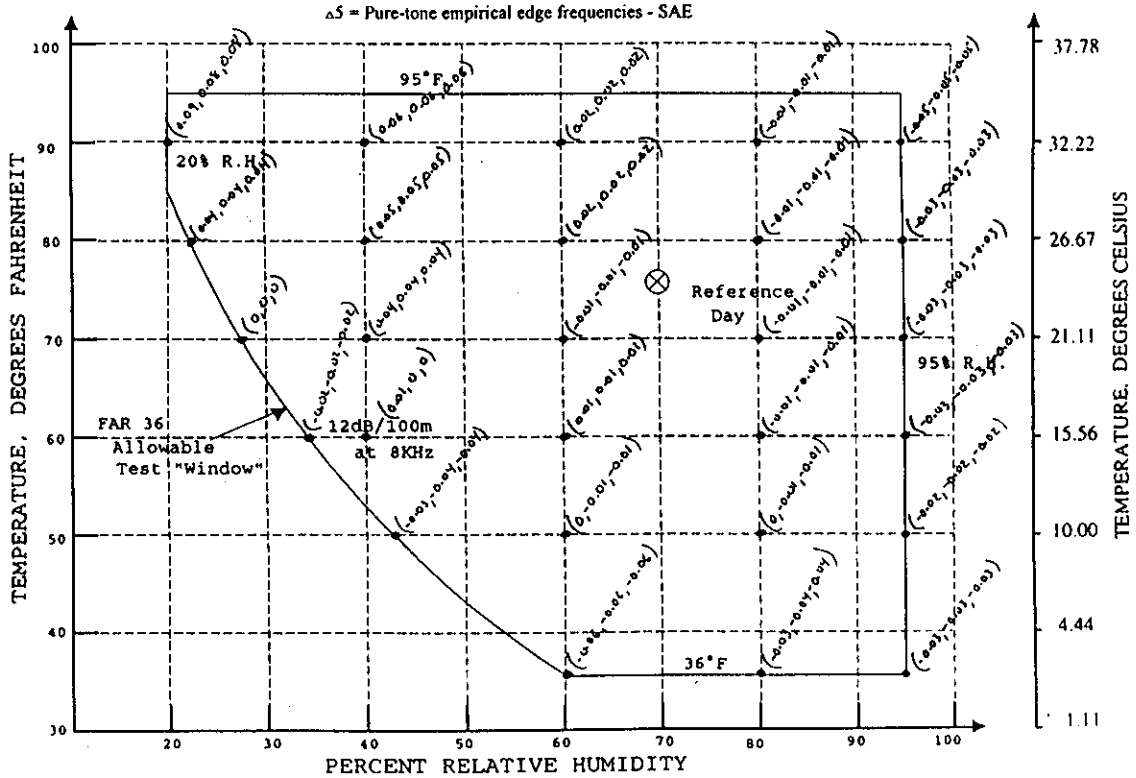

Figure 10a Modern Helicopter

L_{ASmax} Difference Levels -- Reference Distance 1000 meters -- (Δ1,Δ2)

Δ1 = Spectrum Integrated - SAE, Δ2 = Approximate - SAE

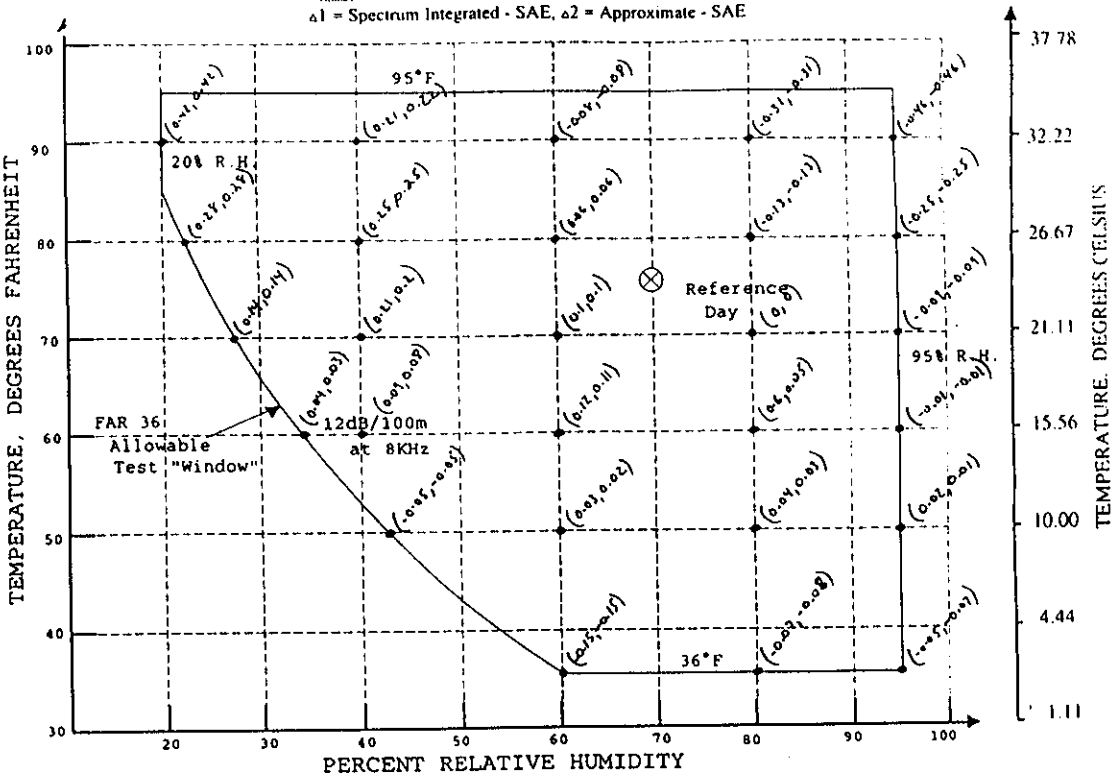

Figure 10b Modern Helicopter

L_{ASmax} Difference Levels -- Reference Distance 1000 meters -- (Δ3,Δ4,Δ5)

Δ3 = Pure-tone mid-band frequencies - SAE, Δ4 = Pure-tone SAE edge frequencies - SAE,

Δ5 = Pure-tone empirical edge frequencies - SAE

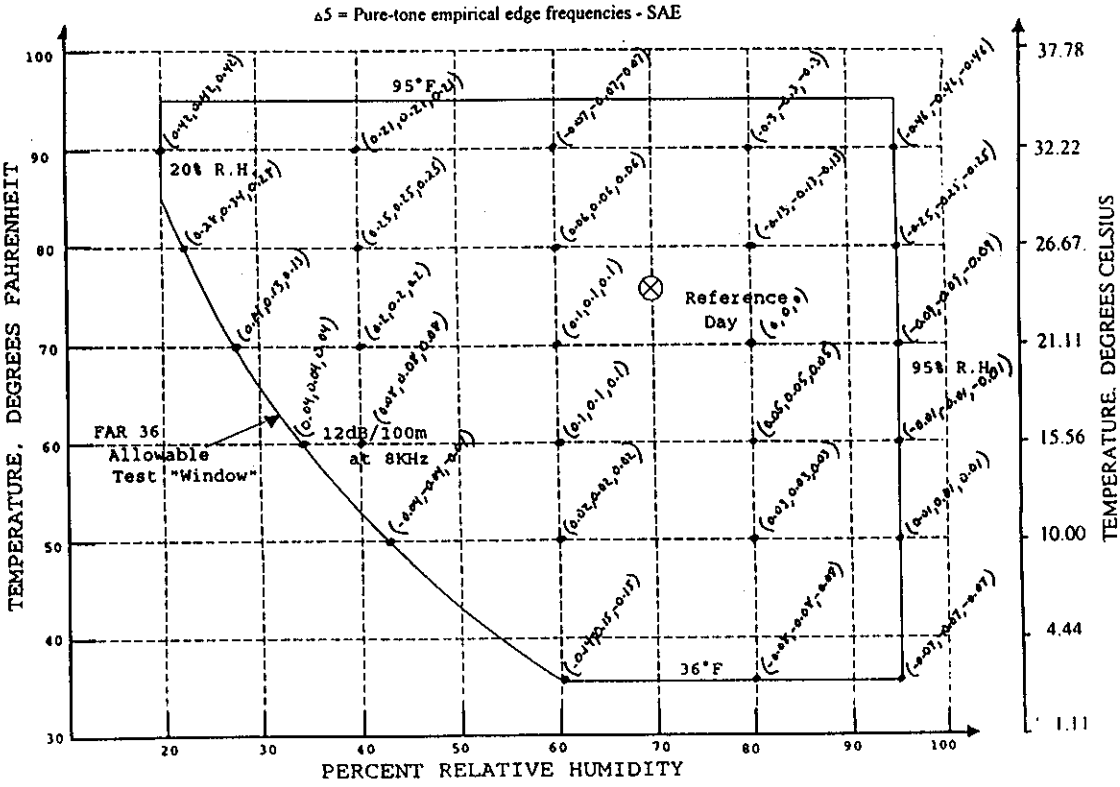

Figure 11a Modern Helicopter

L_{PNSmax} Difference Levels -- Reference Distance 300 meters -- (Δ1,Δ2)

Δ1 = Spectrum Integrated - SAE, Δ2 = Approximate - SAE

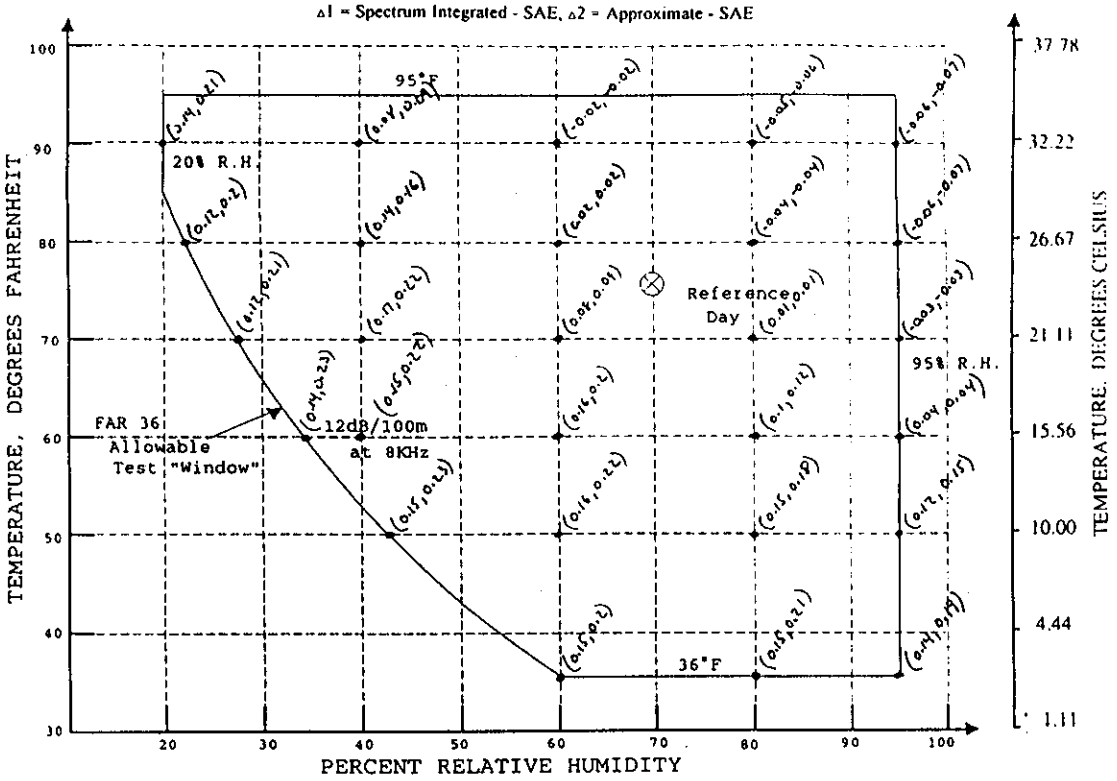

Figure 11b Modern Helicopter

L_{PNSmax} Difference Levels -- Reference Distance 300 meters -- (Δ3,Δ4,Δ5)

Δ3 = Pure-tone mid-band frequencies - SAE, Δ4 = Pure-tone SAE edge frequencies - SAE,

Δ5 = Pure-tone empirical edge frequencies - SAE

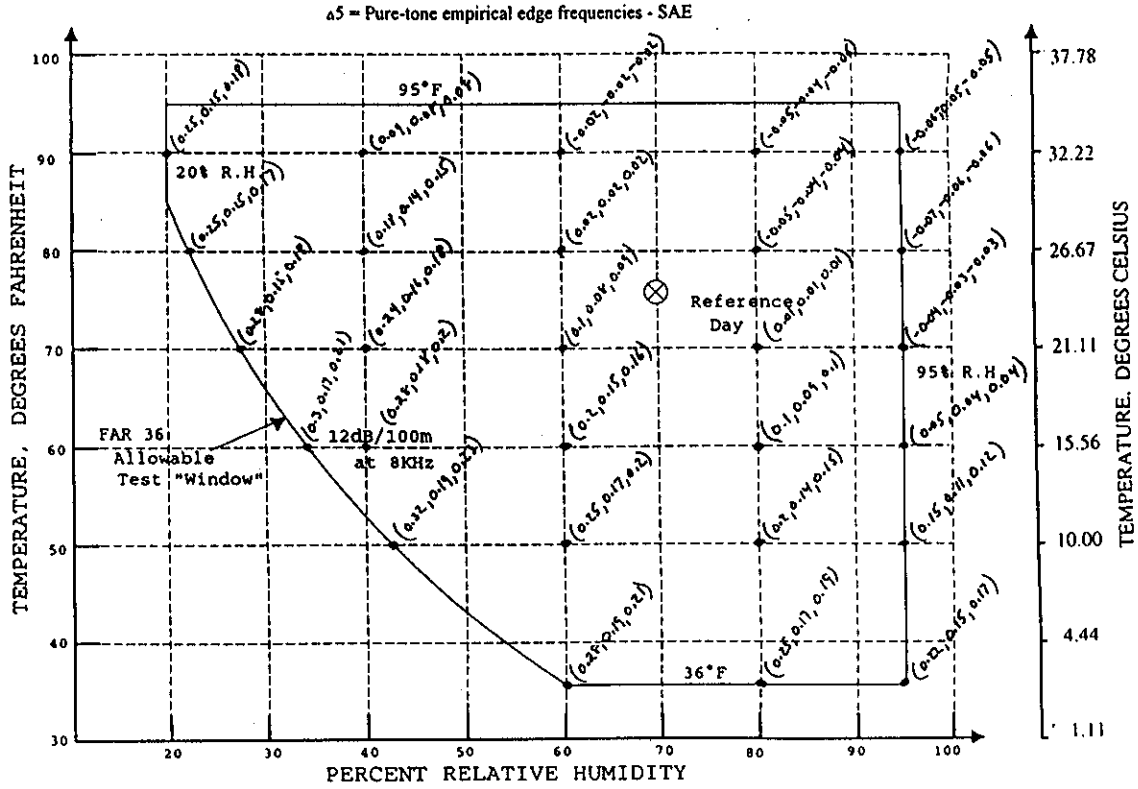

Figure 12a Modern Helicopter

L_{PNSmax} Difference Levels -- Reference Distance 1000 meters -- (Δ1,Δ2)

Δ1 = Spectrum Integrated - SAE, Δ2 = Approximate - SAE

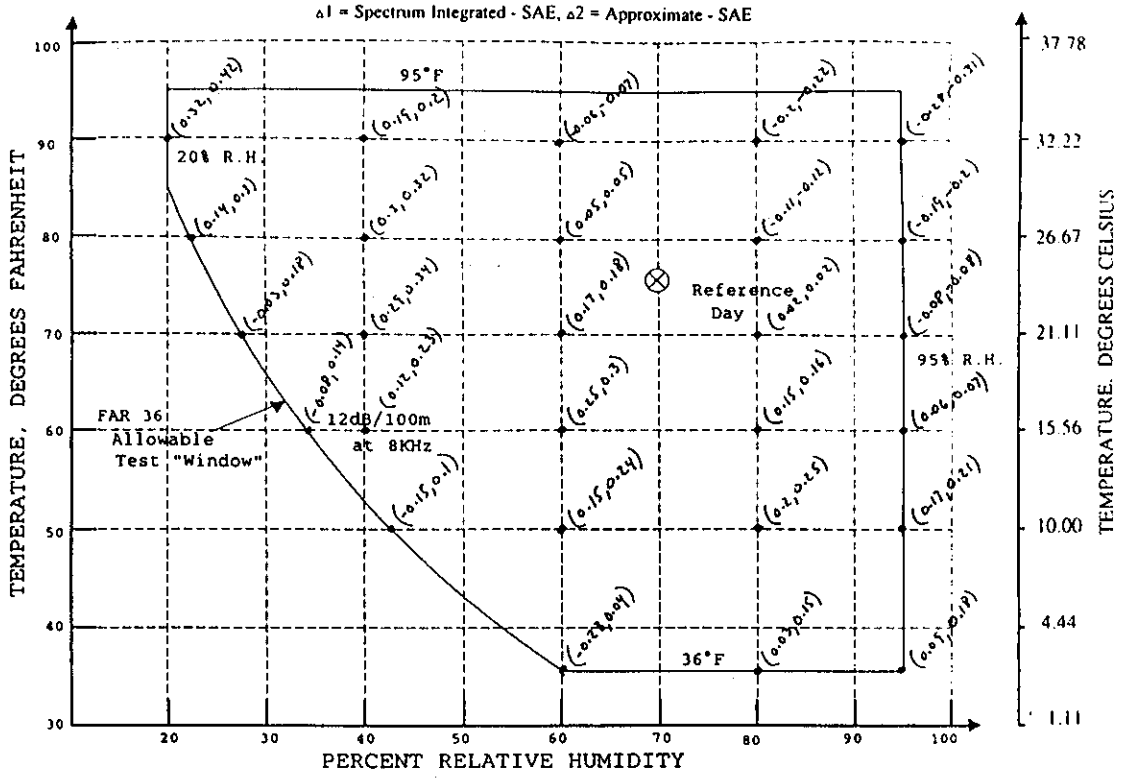

Figure 12b Modern Helicopter

L_{PNSmax} Difference Levels -- Reference Distance 1000 meters -- (Δ3,Δ4,Δ5)

Δ3 = Pure-tone mid-band frequencies - SAE, Δ4 = Pure-tone SAE edge frequencies - SAE,

Δ5 = Pure-tone empirical edge frequencies - SAE

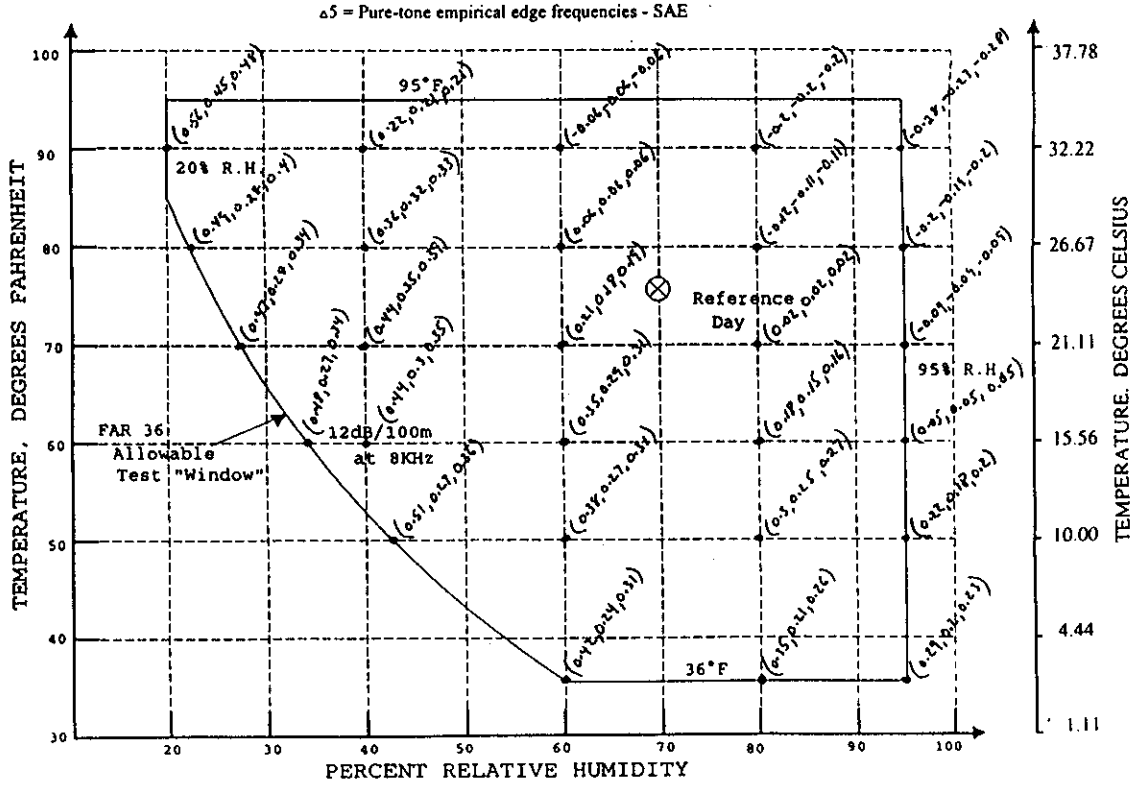

Figure 13 Comparison of Noise-Distance Curves
Spectral Integration Method minus SAE Method
Reference 25 C, 70% Relative Humidity

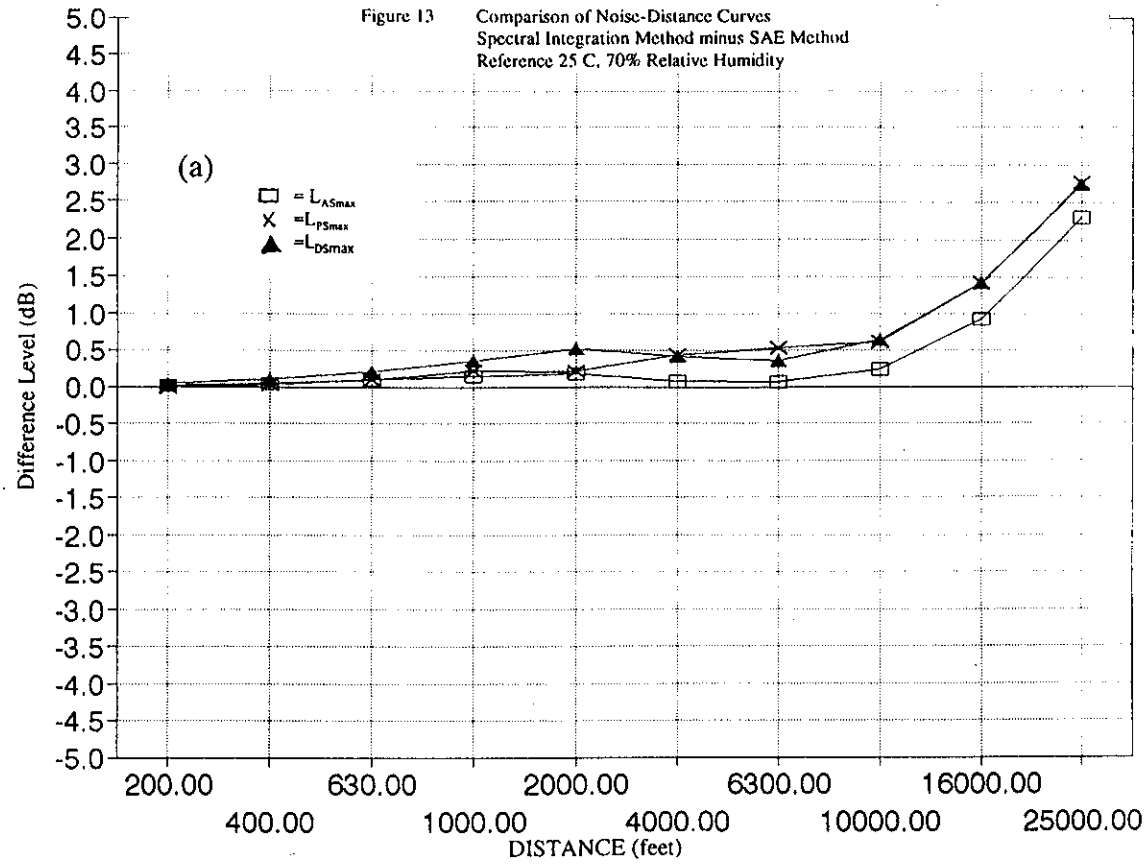

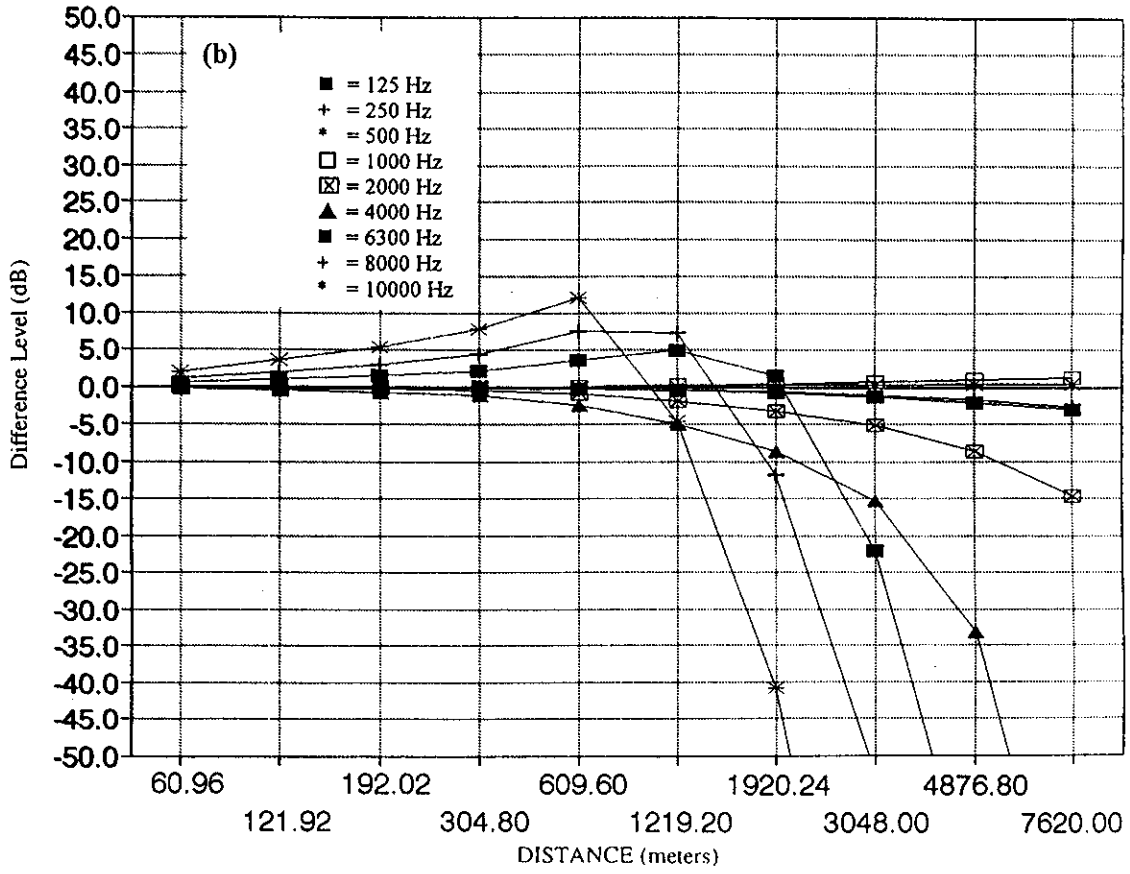

Figure 14 Comparison of Noise-Distance Curves
Approximate Method minus SAE Method
Reference 25 C, 70% Relative Humidity

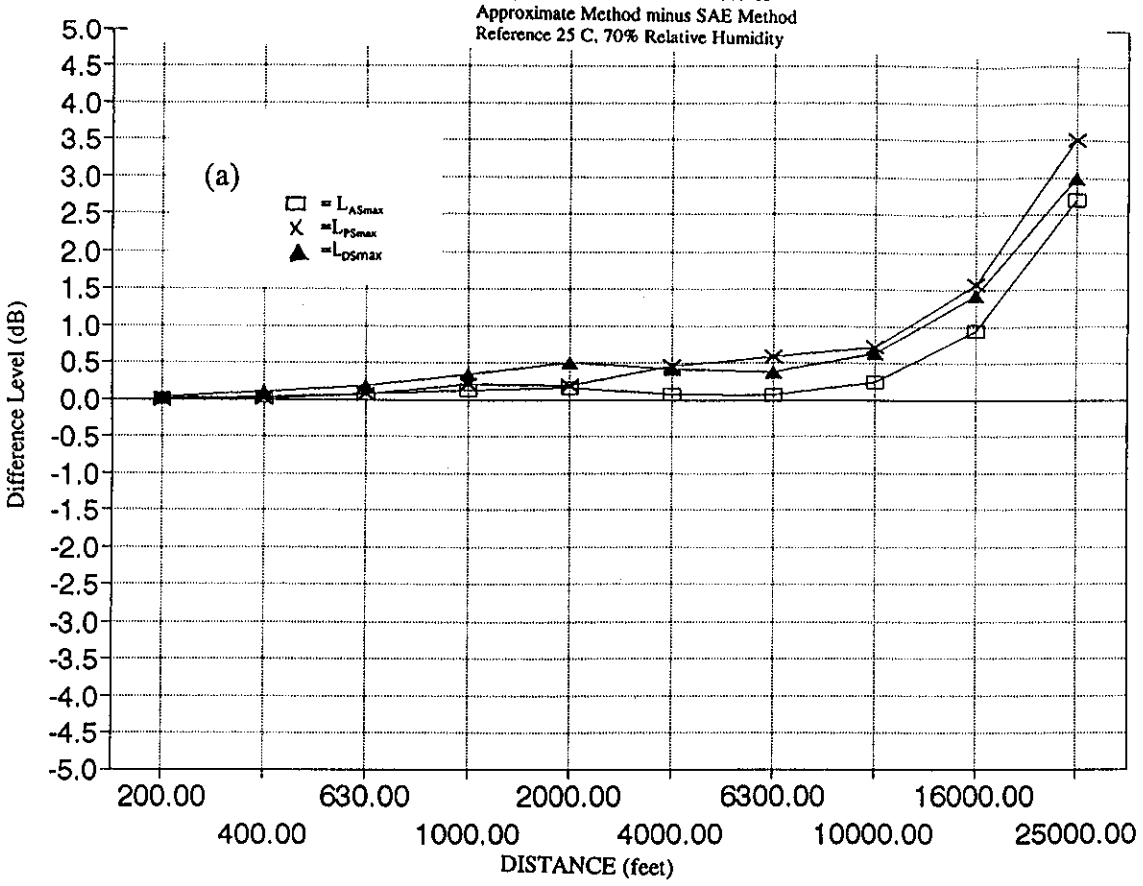

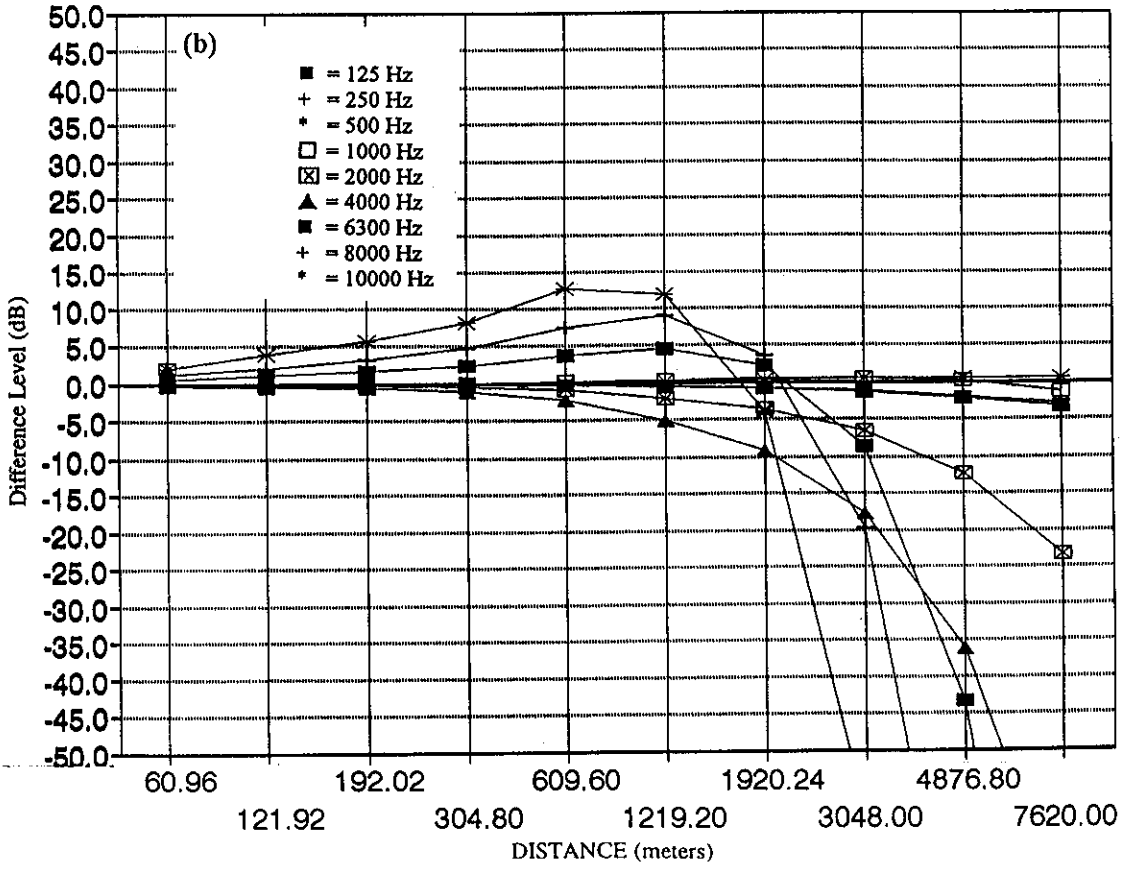

Figure 15 Comparison of Noise-Distance Curves
Pure-Tone Mid-Band Frequency Method minus SAE Method
Reference 25 C, 70% Relative Humidity

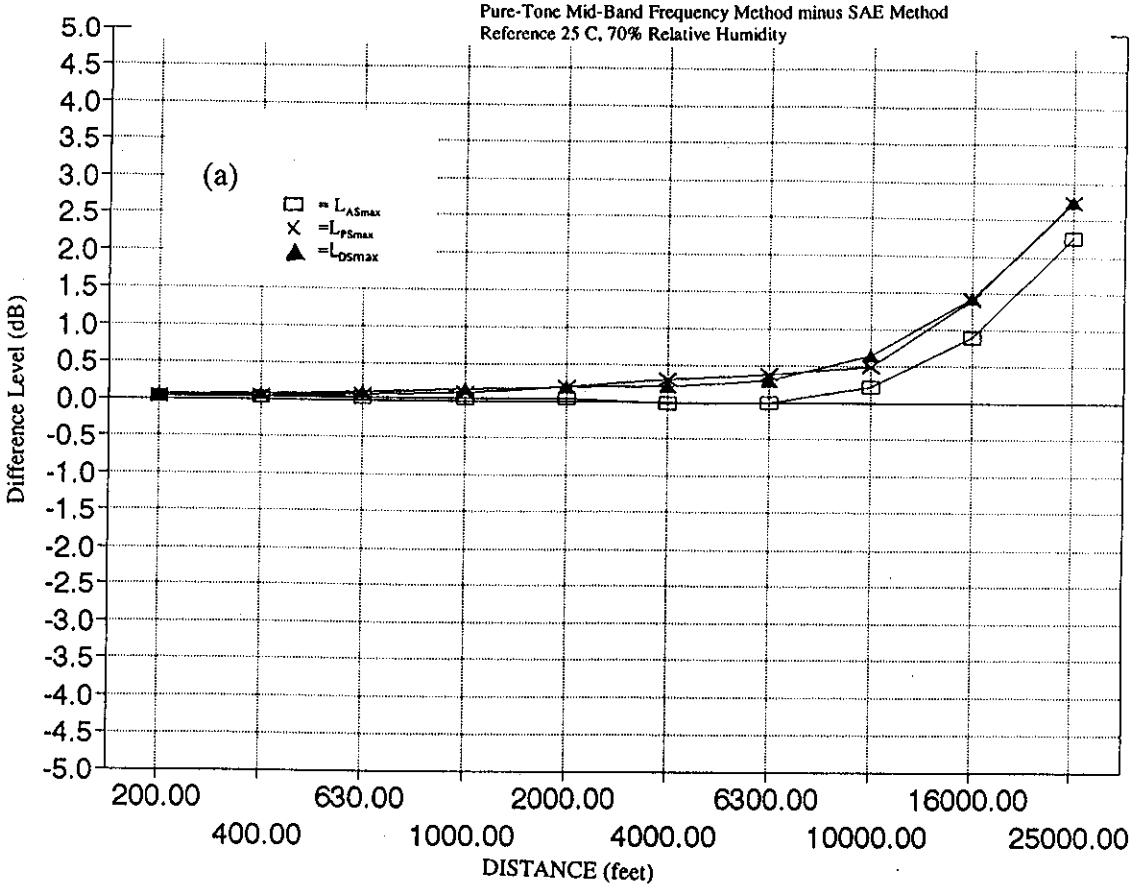

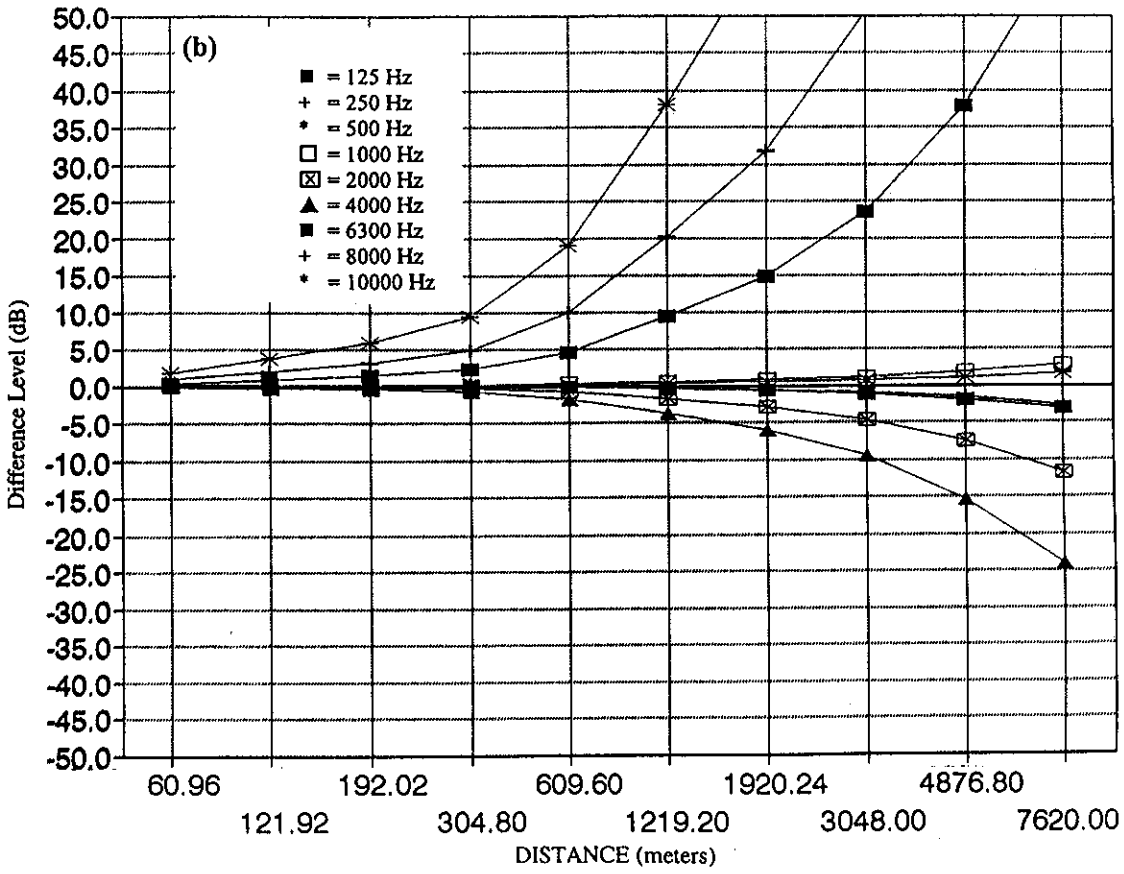

Figure 16 Comparison of Noise-Distance Curves
Pure-Tone SAE Edge Frequency Method minus SAE Method
Reference 25 C, 70% Relative Humidity

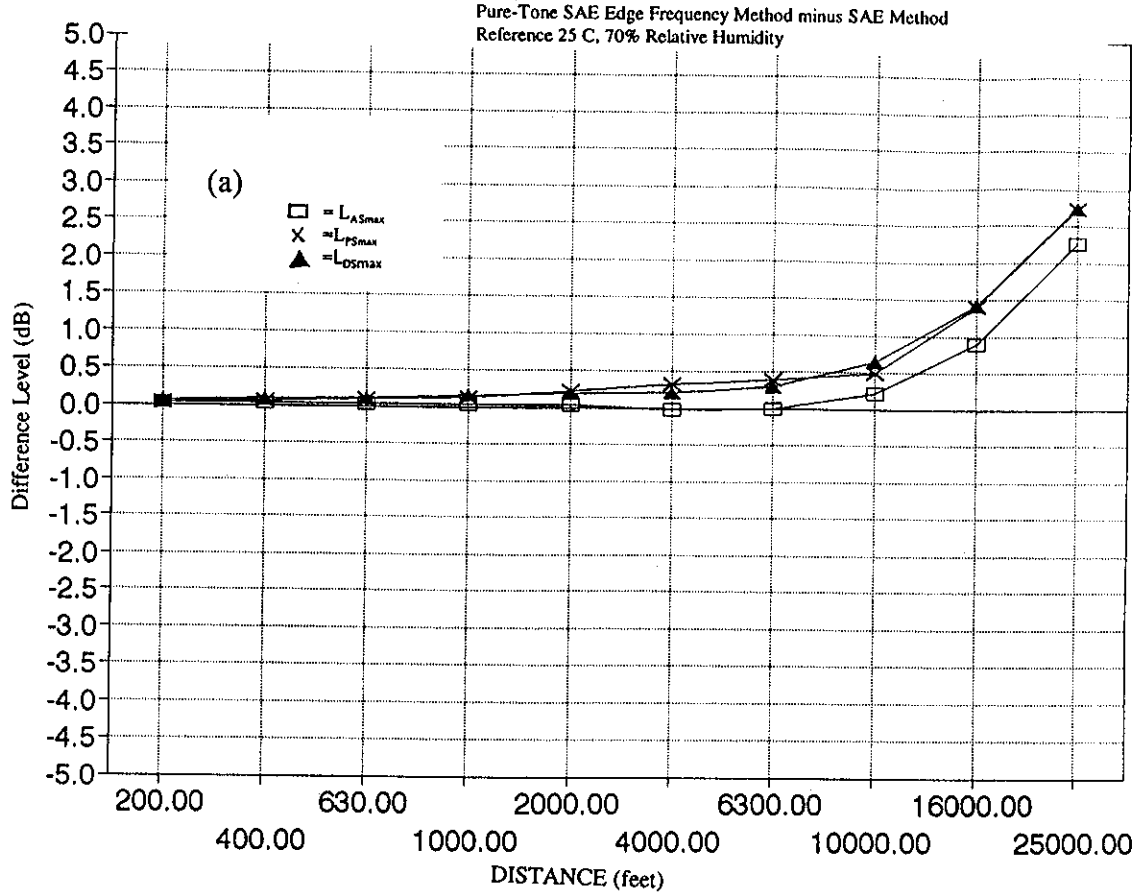

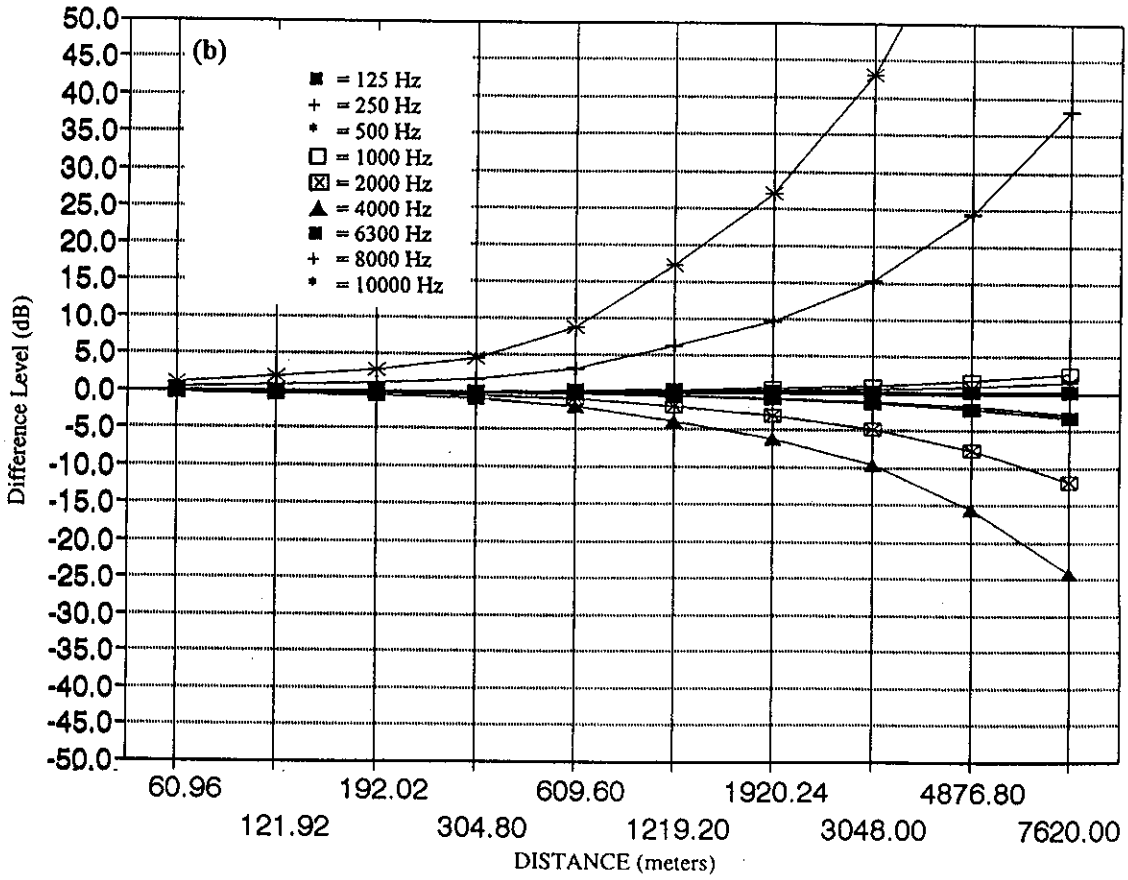

Figure 17 Comparison of Noise-Distance Curves
Pure-Tone Empirical Edge Frequency Method minus SAE Method
Reference 25 C, 70% Relative Humidity

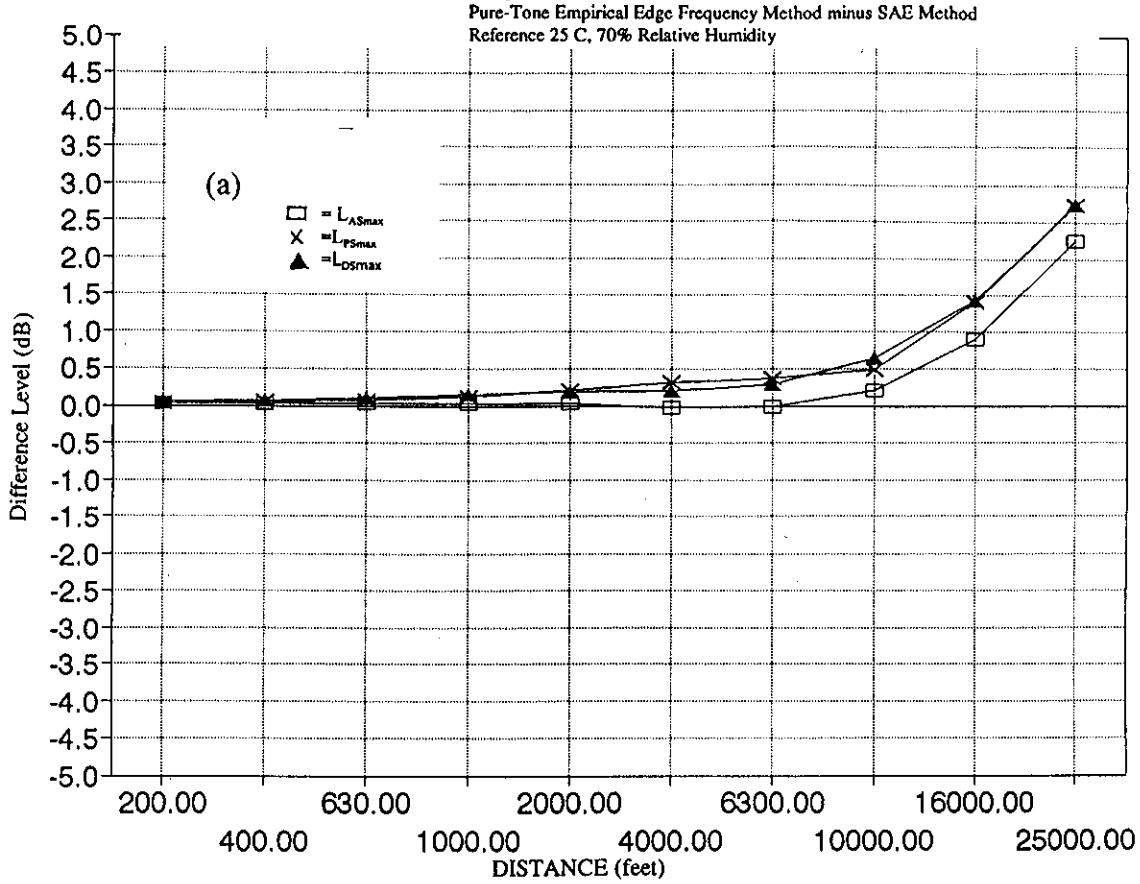

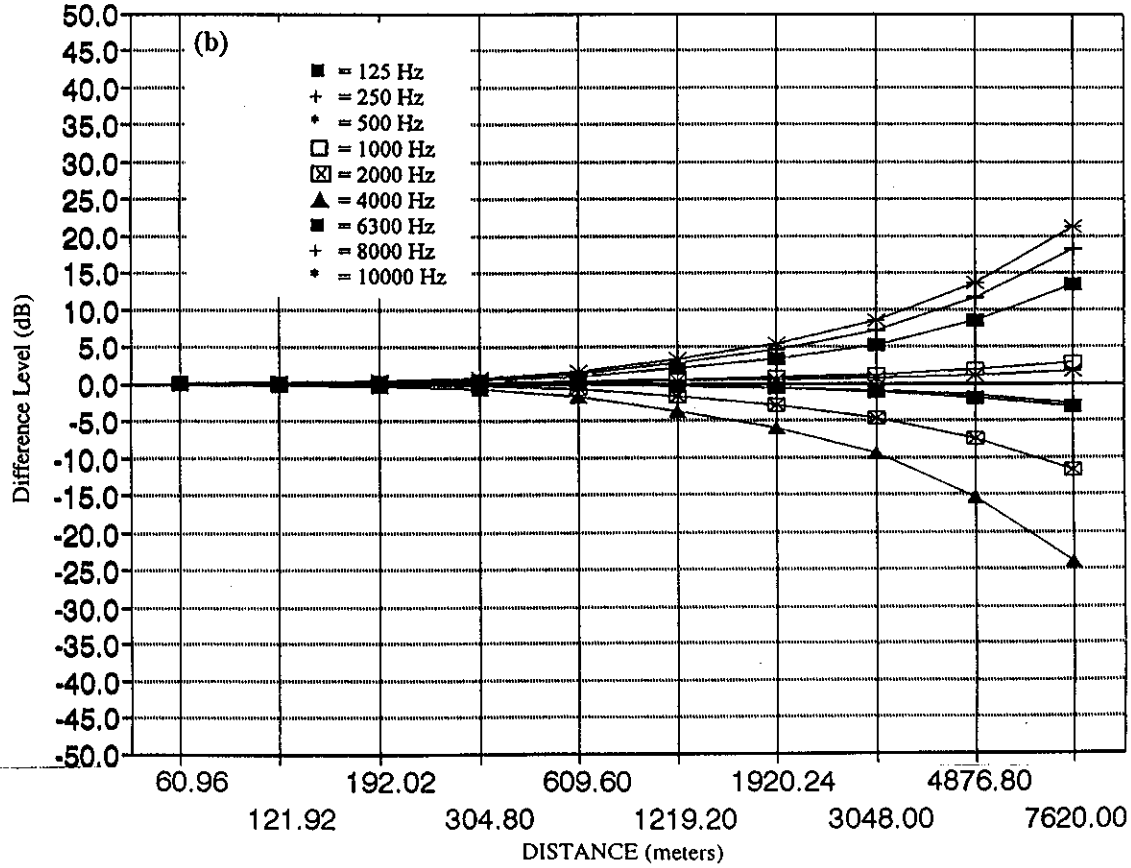

Figure 18 Comparison of Noise-Distance Curves
Spectral Integration Method minus SAE Method
Reference 4°C, 70% Relative Humidity

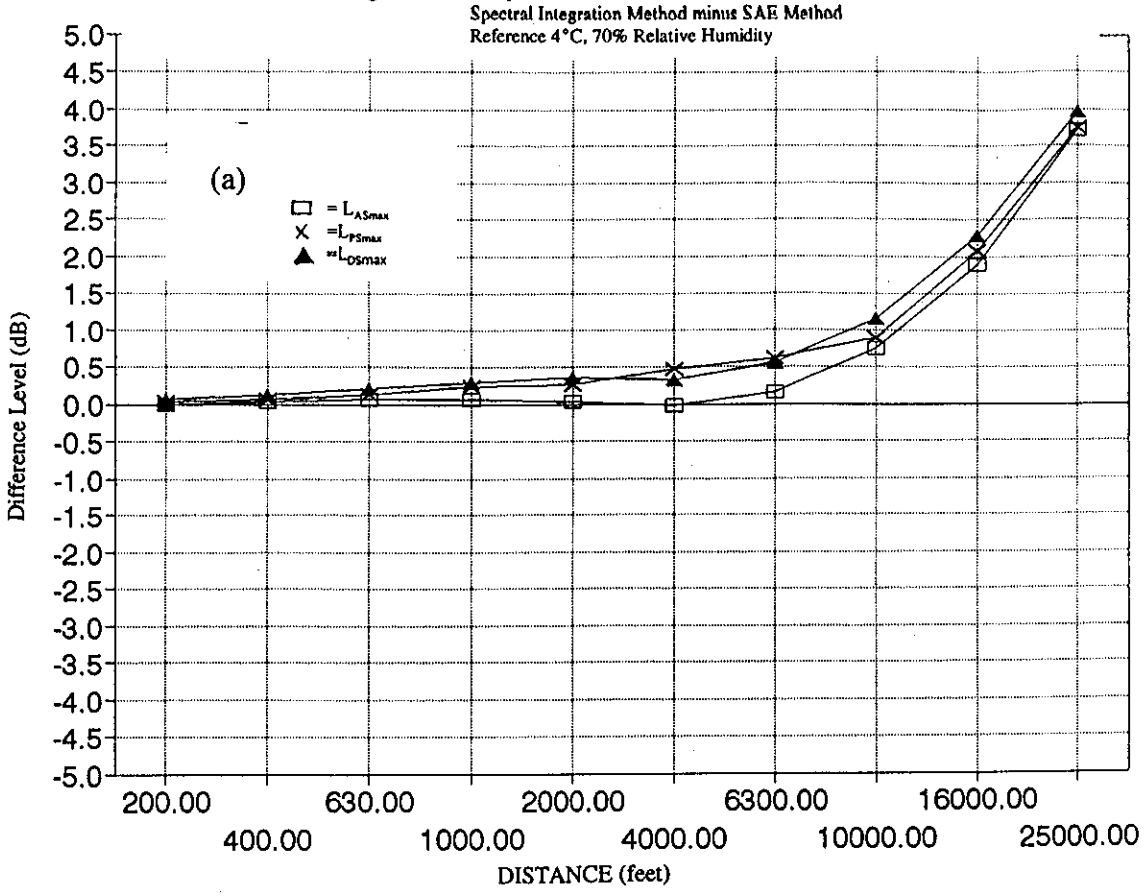

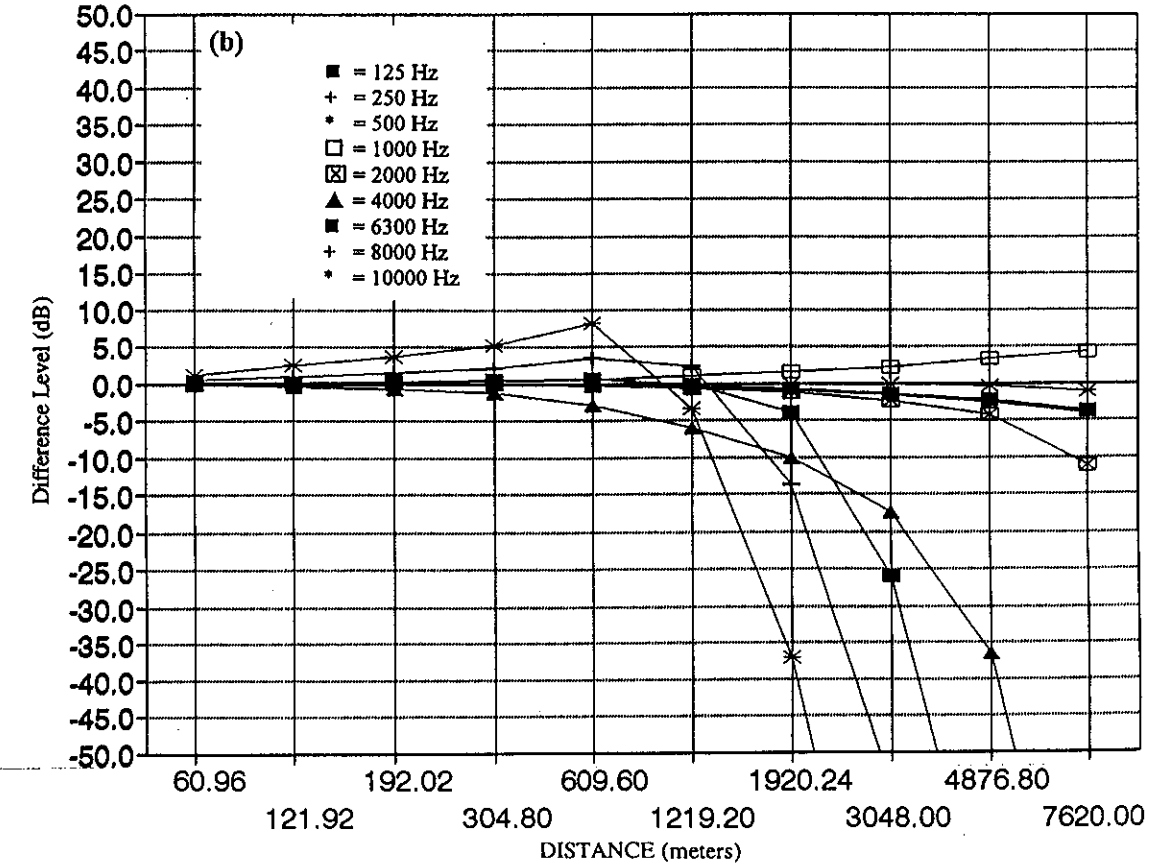

Figure 19 Comparison of Noise-Distance Curves
Pure-Tone Empirical Edge Frequency Method minus SAE Method
Reference 4°C, 70% Relative Humidity

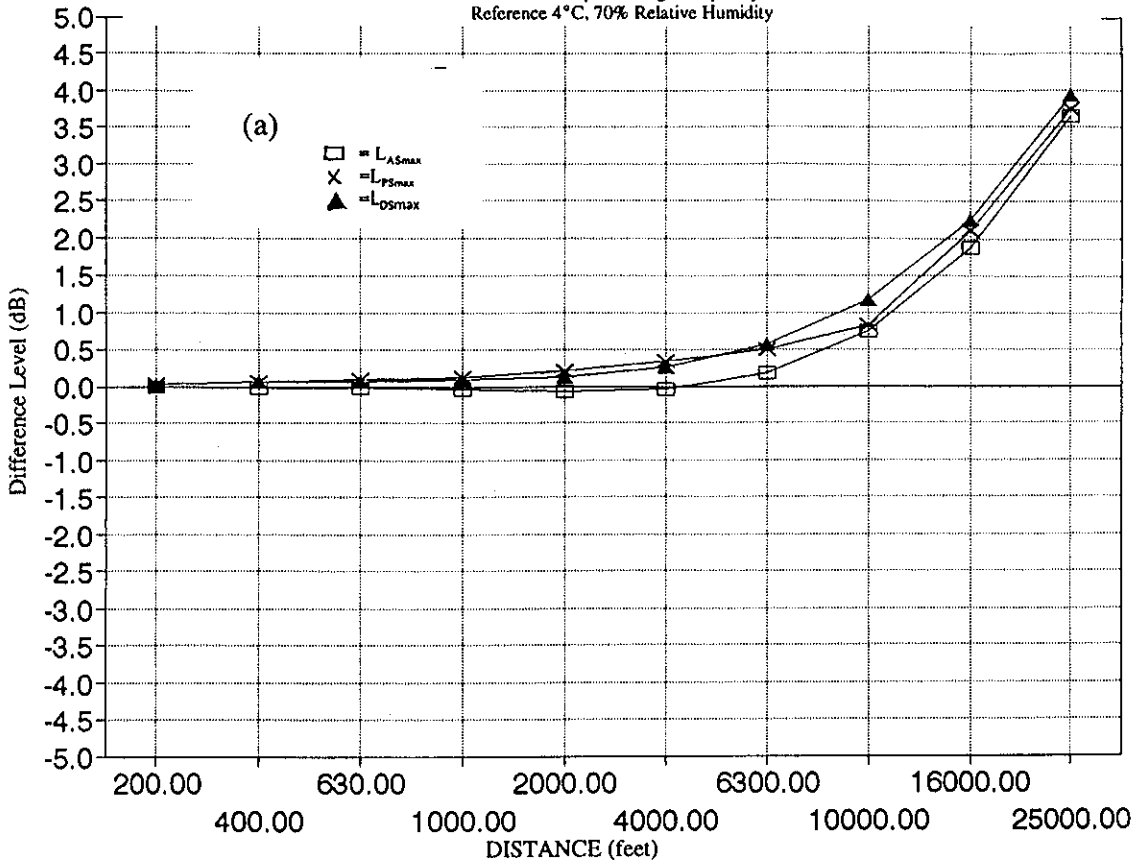

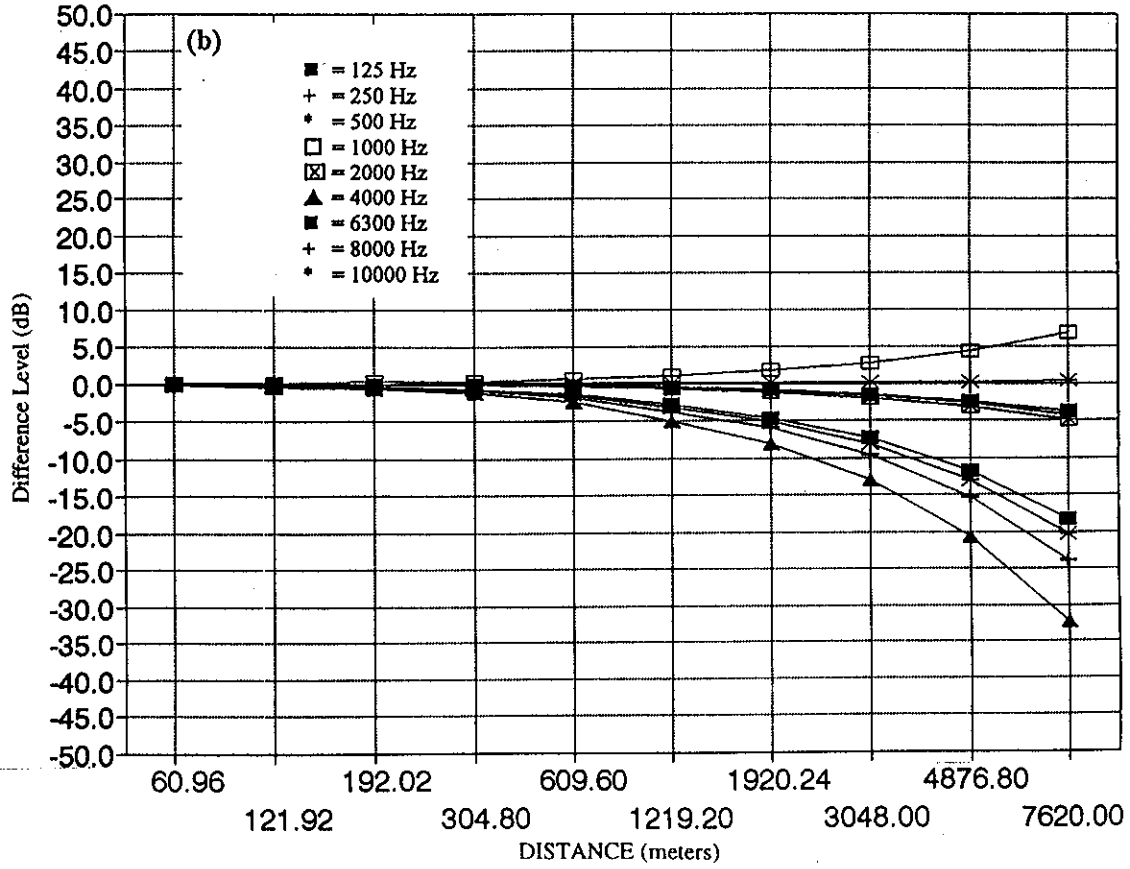

Figure 20 Comparison of Noise-Distance Curves
Spectral Integration Method minus SAE Method
Reference 18°C, 43% Relative Humidity

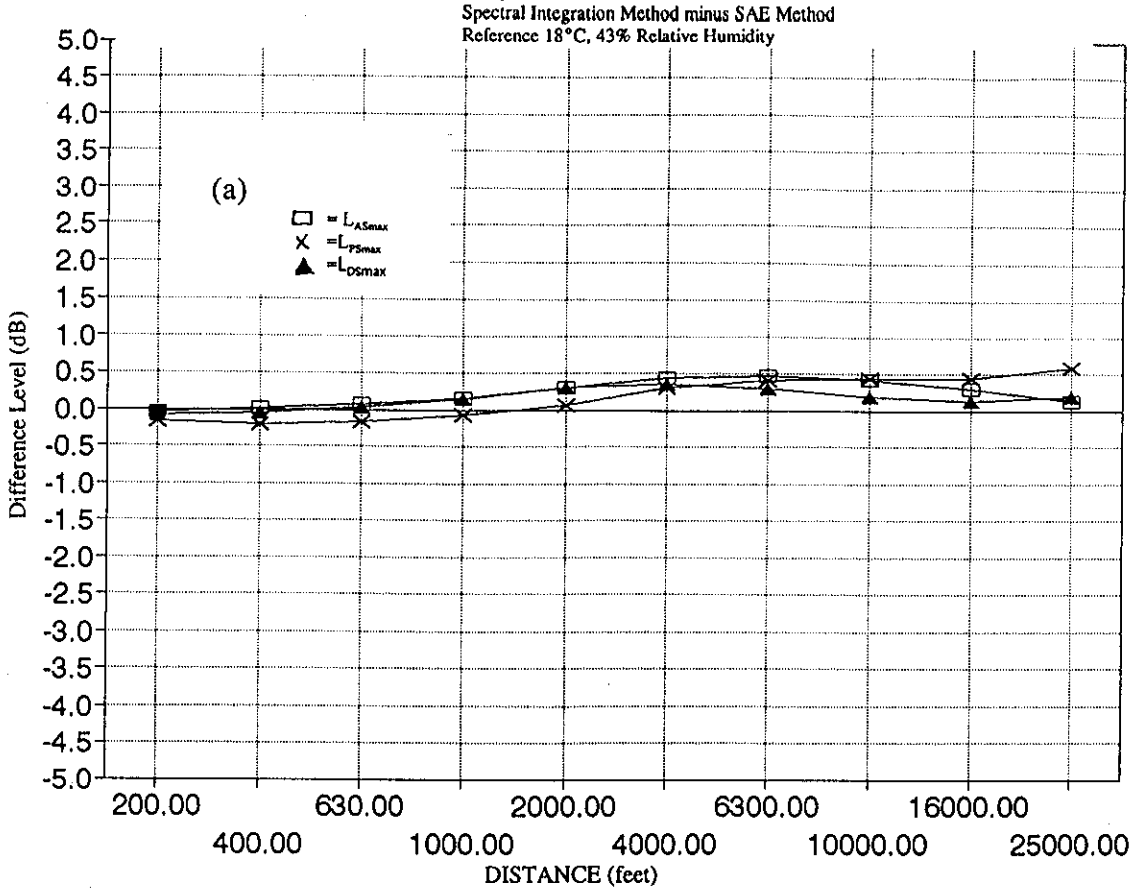

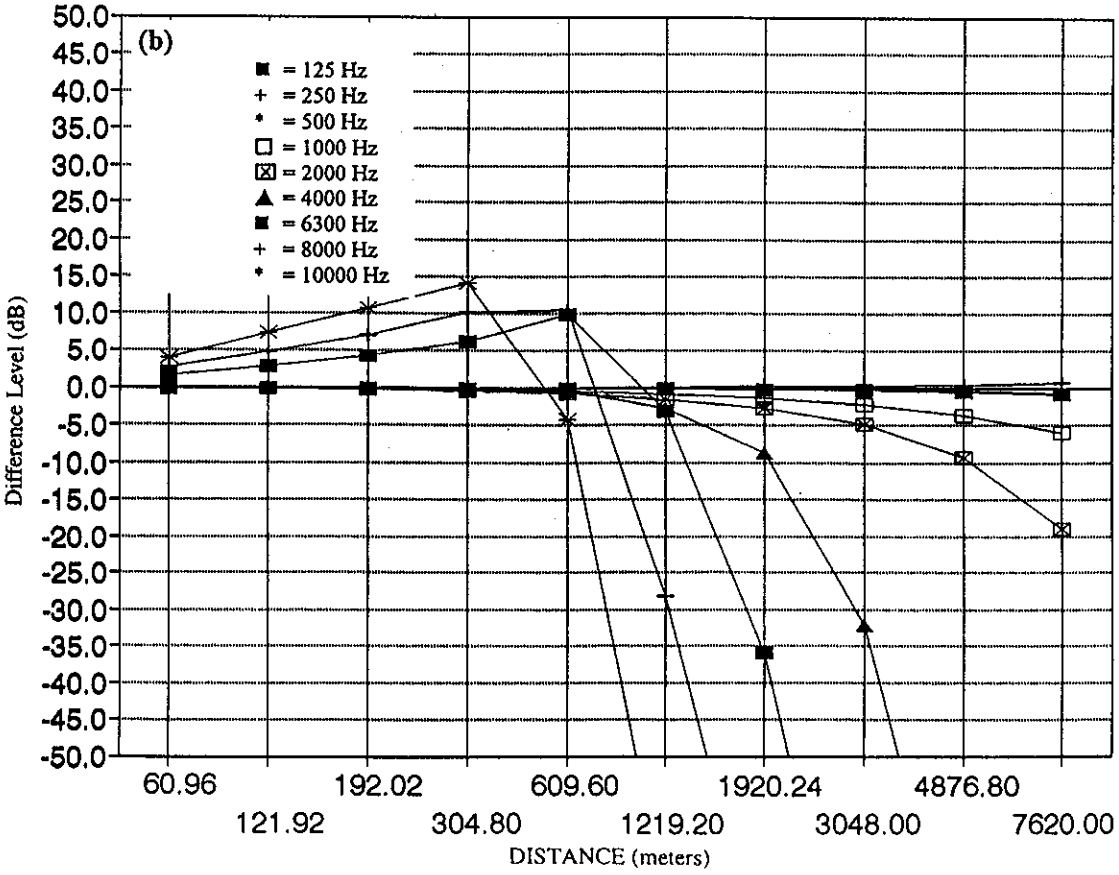

Figure 21 Comparison of Noise-Distance Curves
Pure-Tone Empirical Edge Frequency Method minus SAE Method
Reference 18°C, 43% Relative Humidity

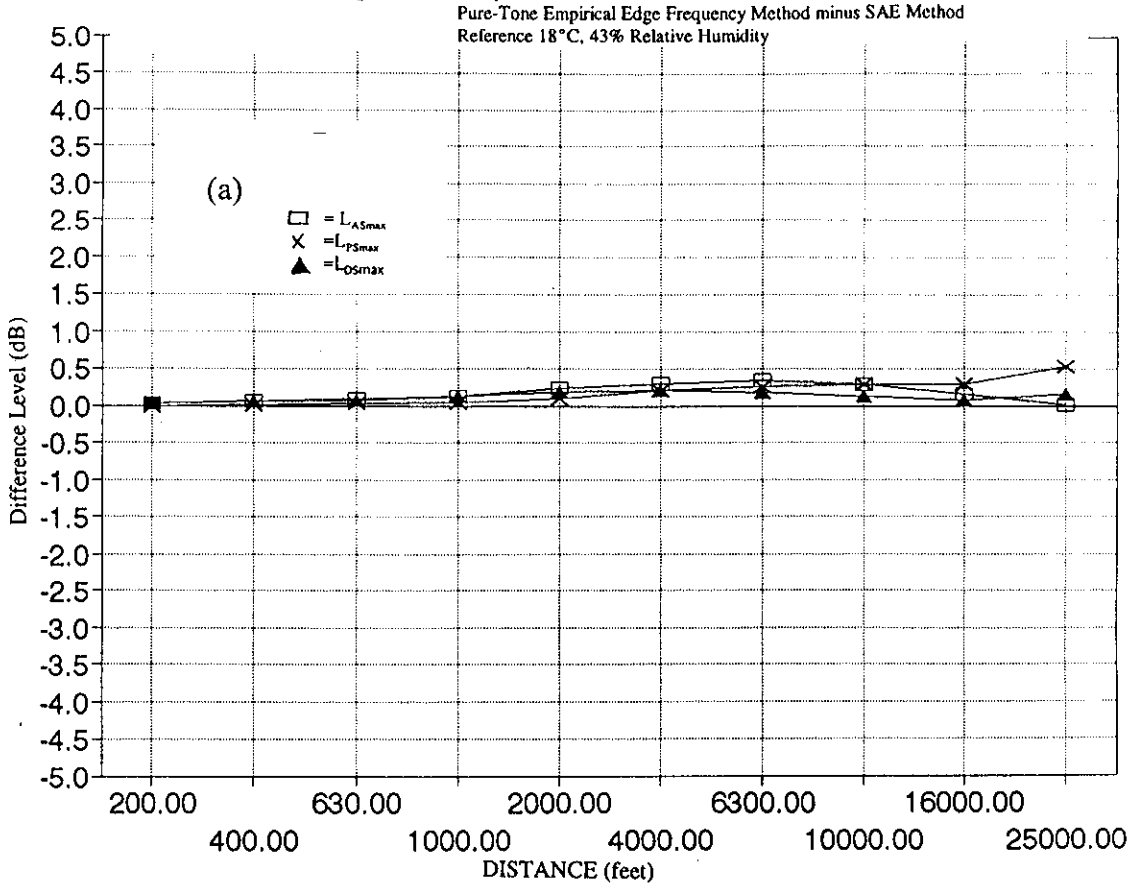

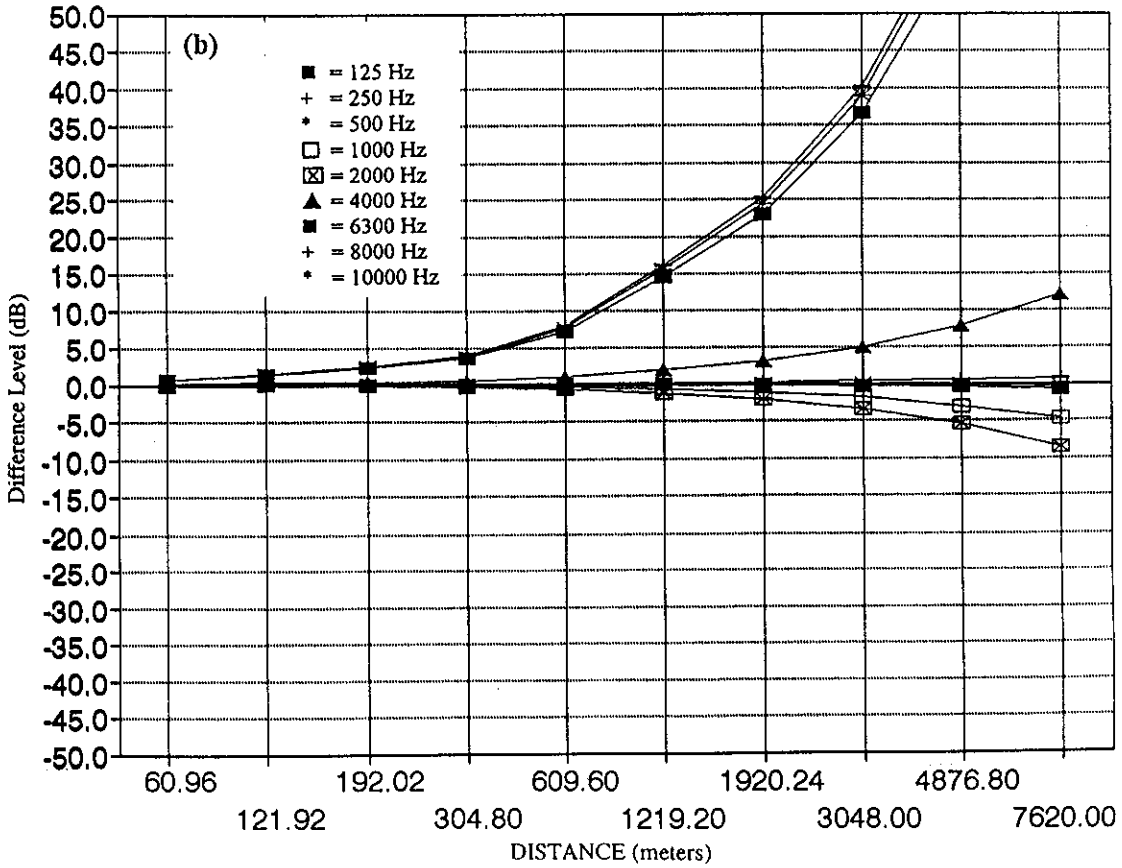

Figure 22 Comparison of Noise-Distance Curves
Spectral Integration Method minus SAE Method
Reference 33°C, 50% Relative Humidity

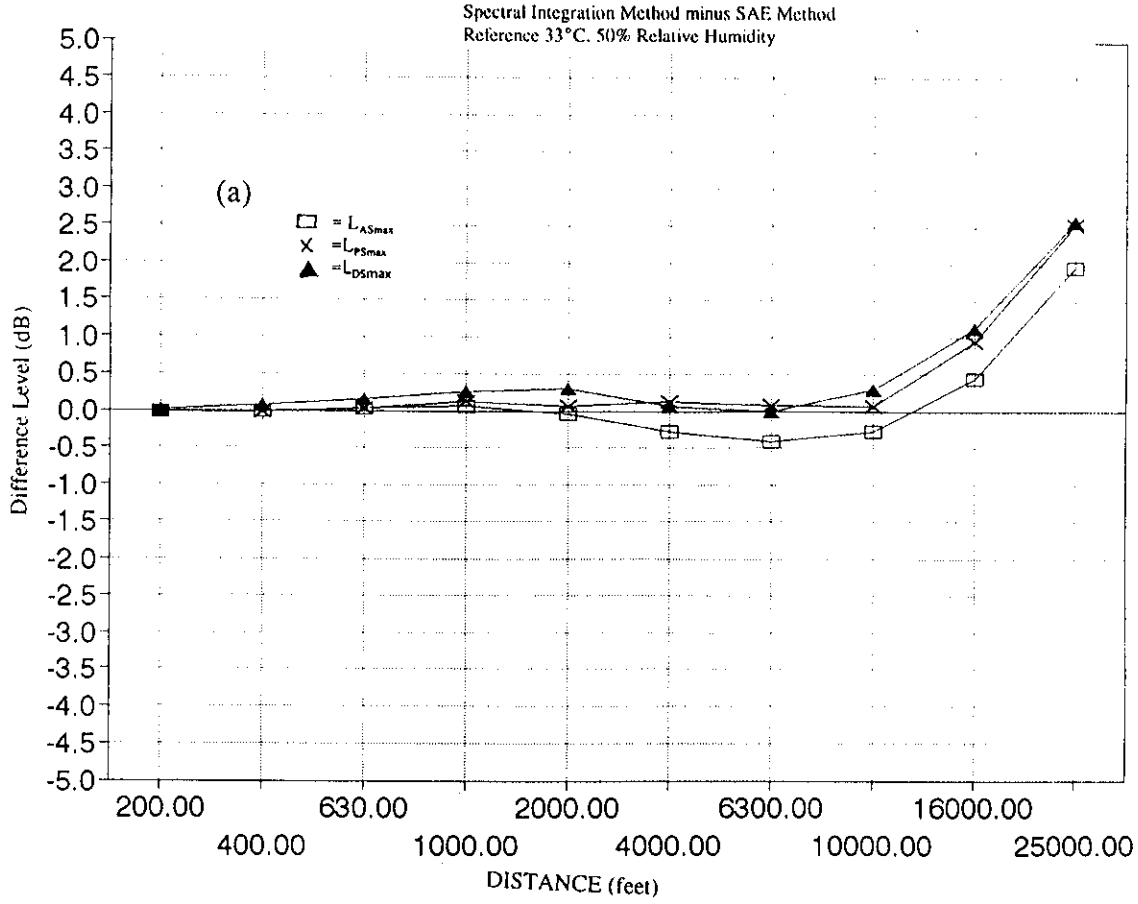

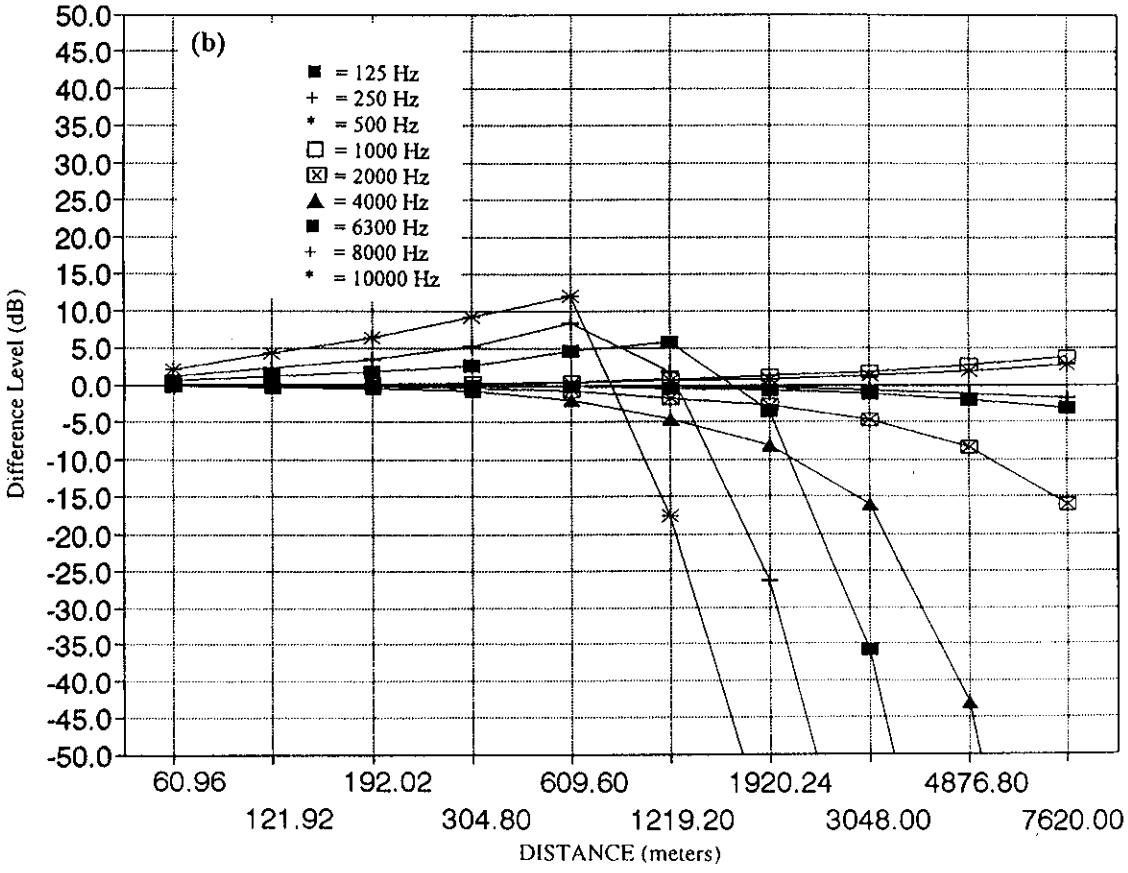

Figure 23 Comparison of Noise-Distance Curves
Pure-Tone Empirical Edge Frequency Method minus SAE Method
Reference 33°C, 50% Relative Humidity

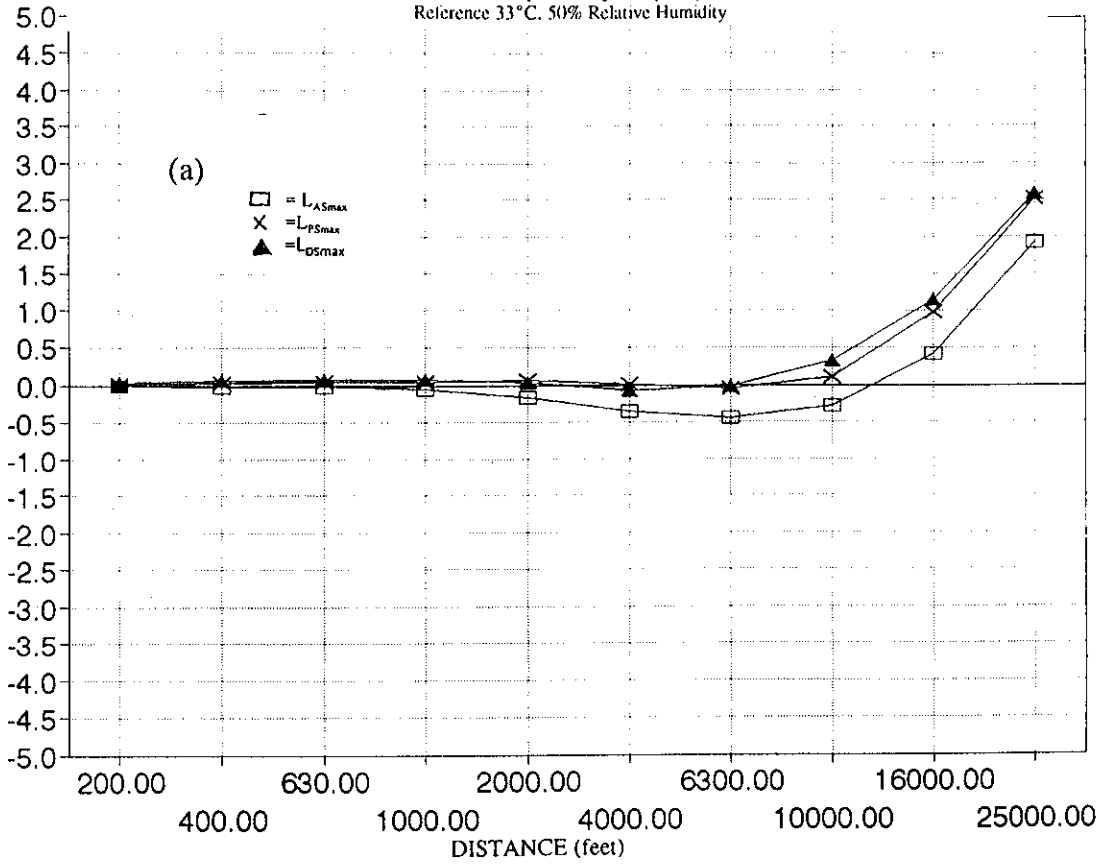

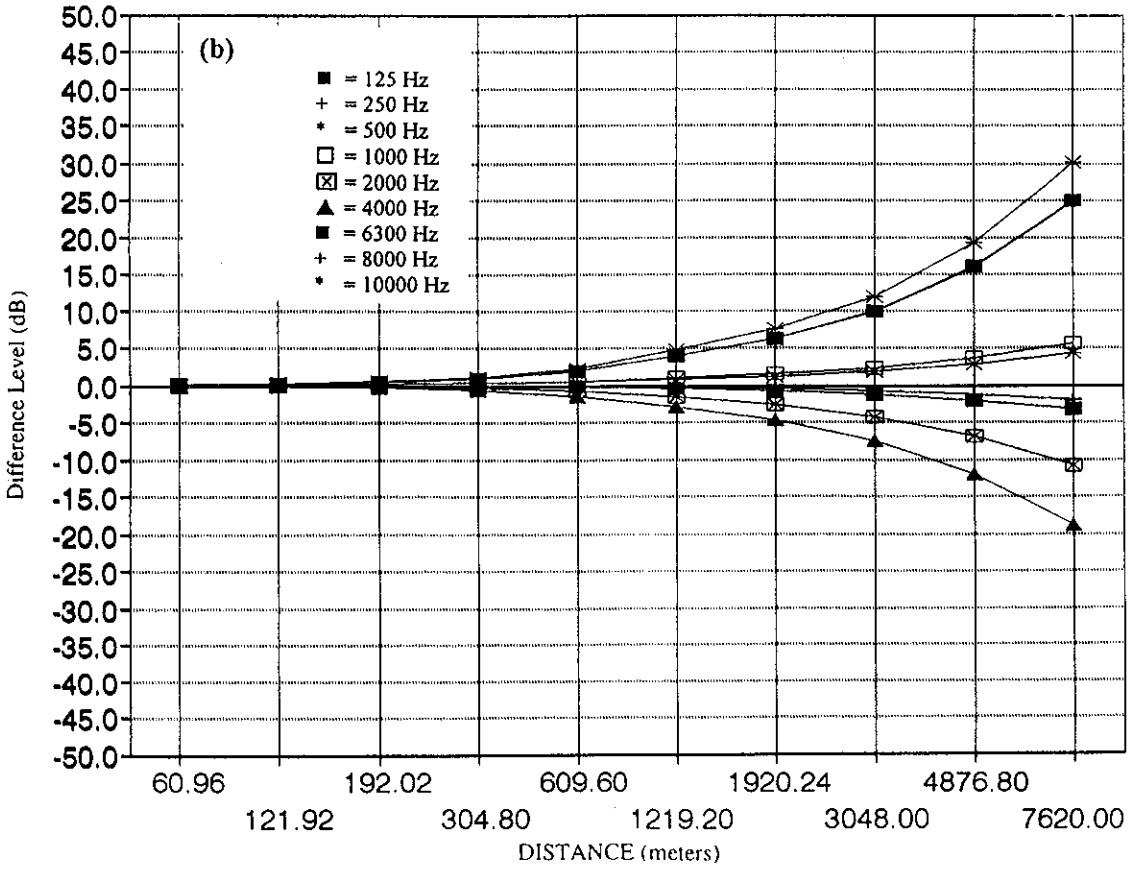

Figure 24 Comparison of Noise-Distance Curves
Pure-Tone Empirical Edge Frequency Method minus SAE Method
Reference 25°C, 70% Relative Humidity, ISO Pressure Lapse

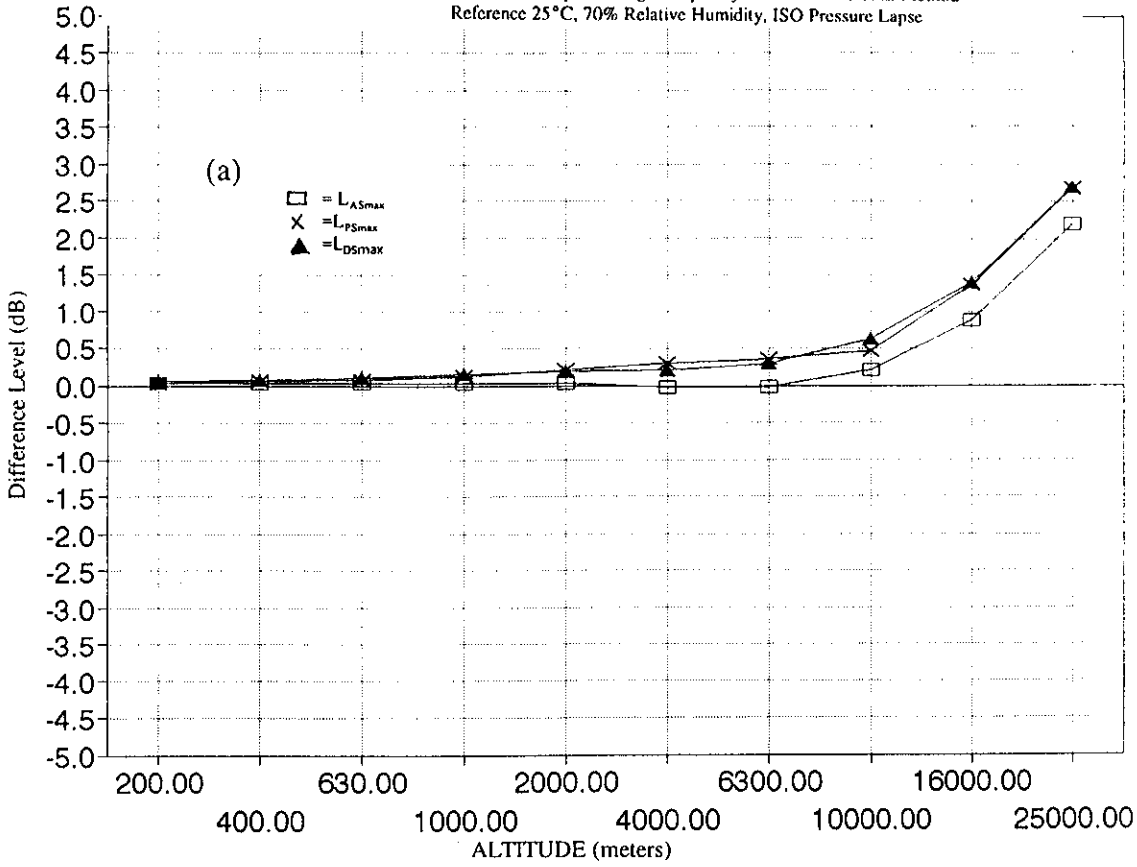

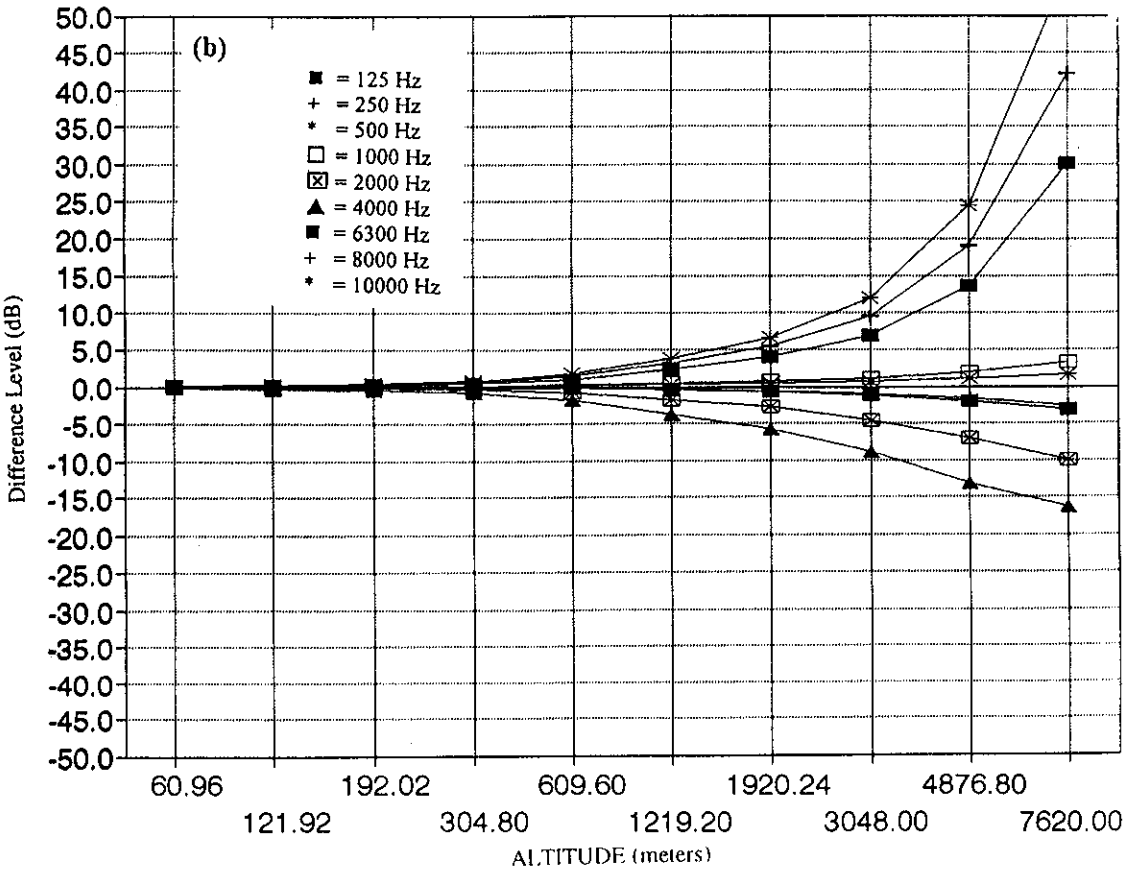

Figure 25 Comparison of Noise-Distance Curves
Pure-Tone Empirical Edge Frequency Method minus SAE Method
Reference 4°C, 70% Relative Humidity, ISO Pressure Lapse

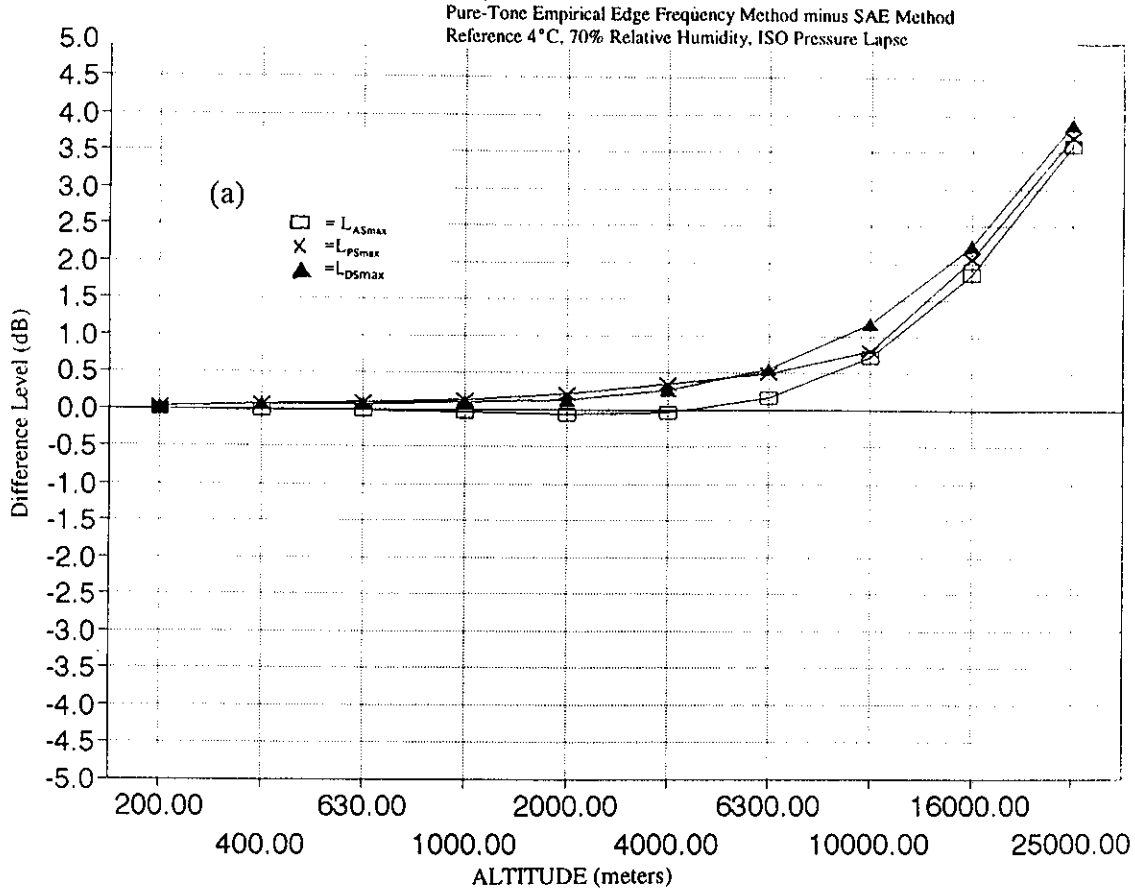

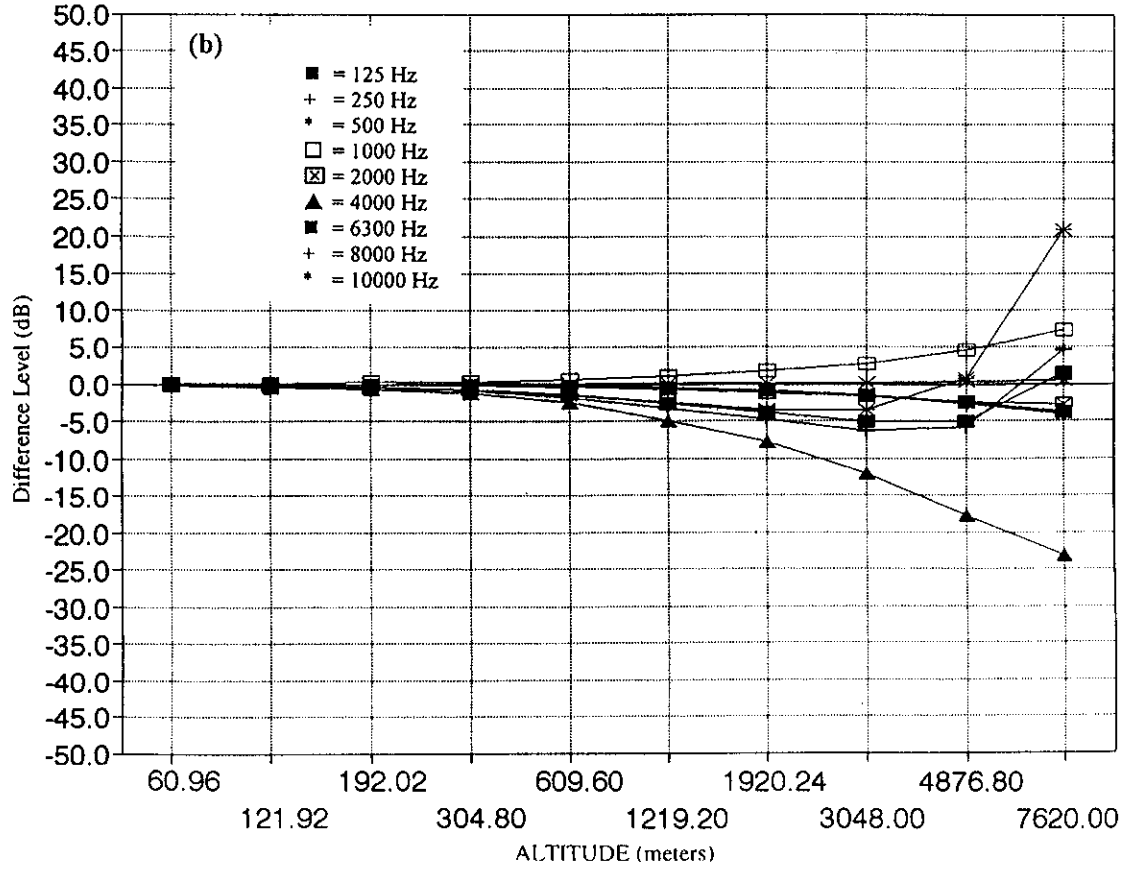

Figure 26 Comparison of Noise-Distance Curves
Pure-Tone Empirical Edge Frequency Method minus SAE Method
Reference 18°C, 43% Relative Humidity, ISO Pressure Lapse

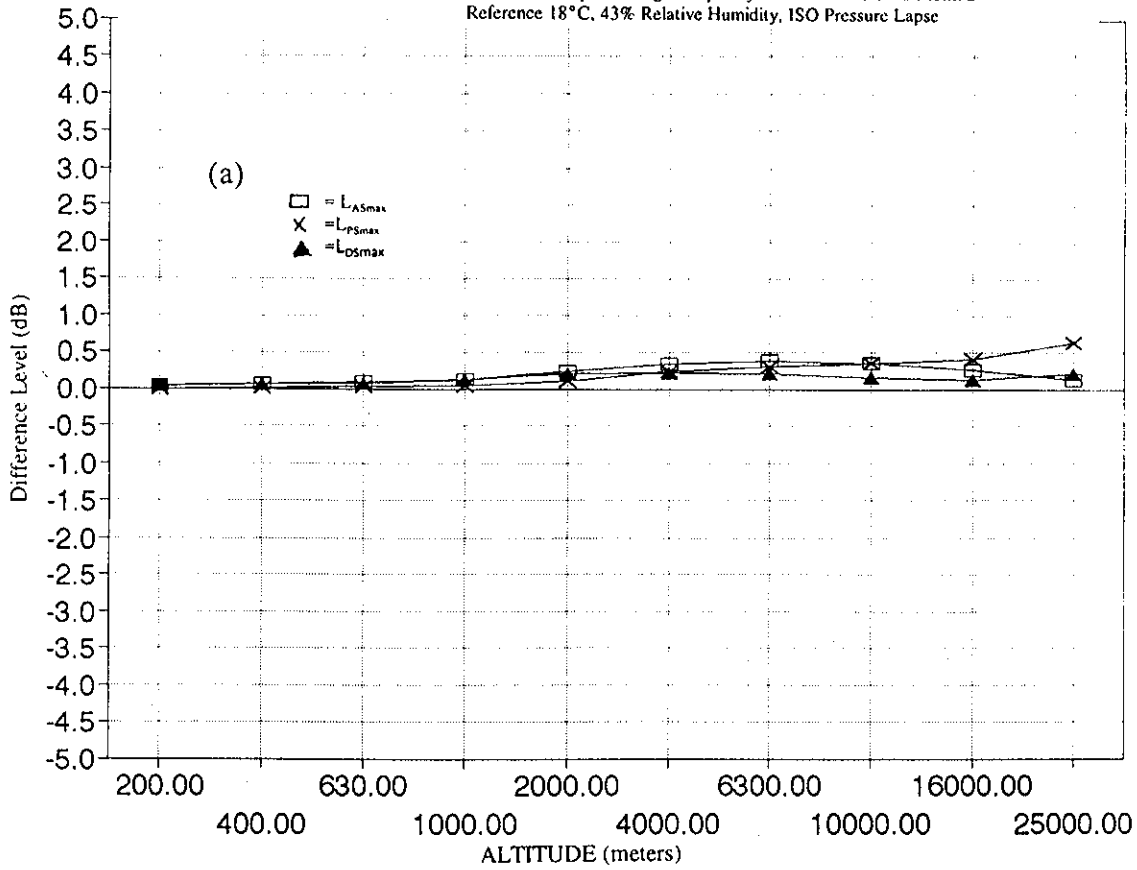

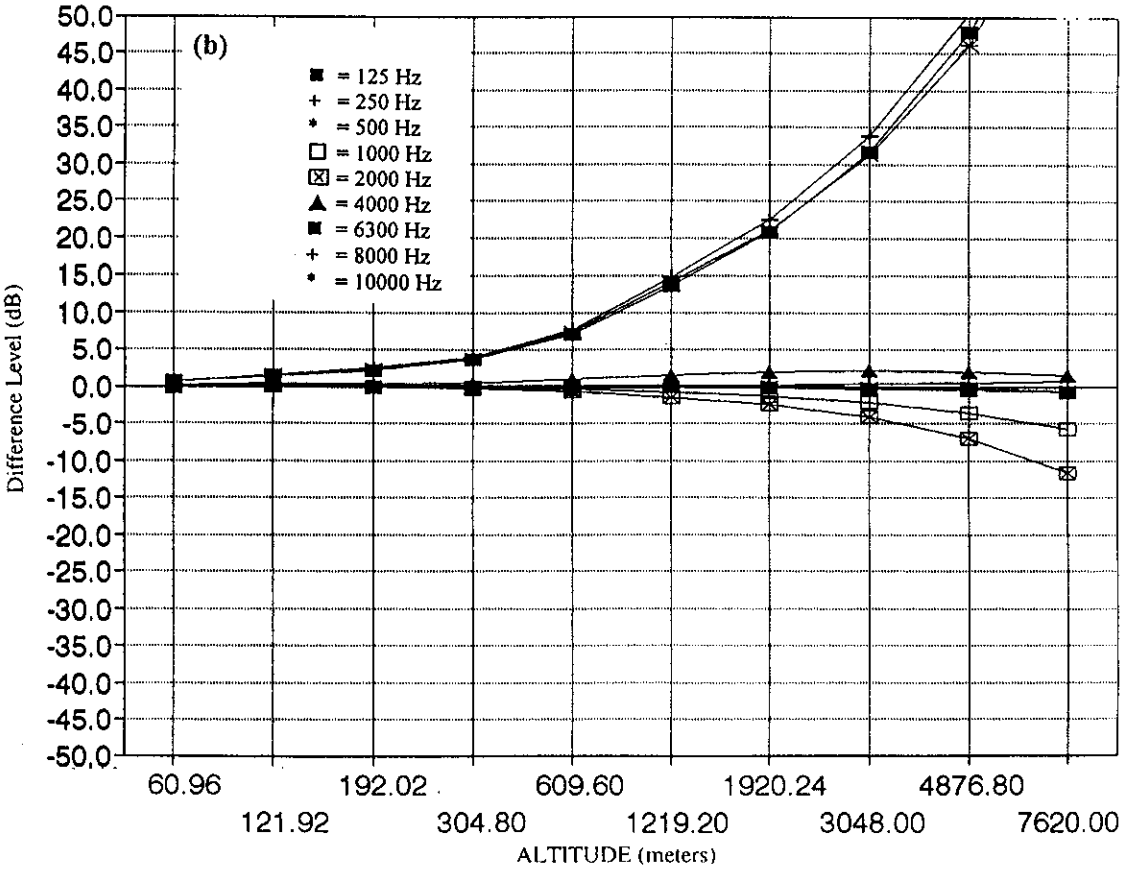

Figure 27 Comparison of Noise-Distance Curves
Pure-Tone Empirical Edge Frequency Method minus SAE Method
Reference 33°C, 50% Relative Humidity, ISO Pressure Lapse

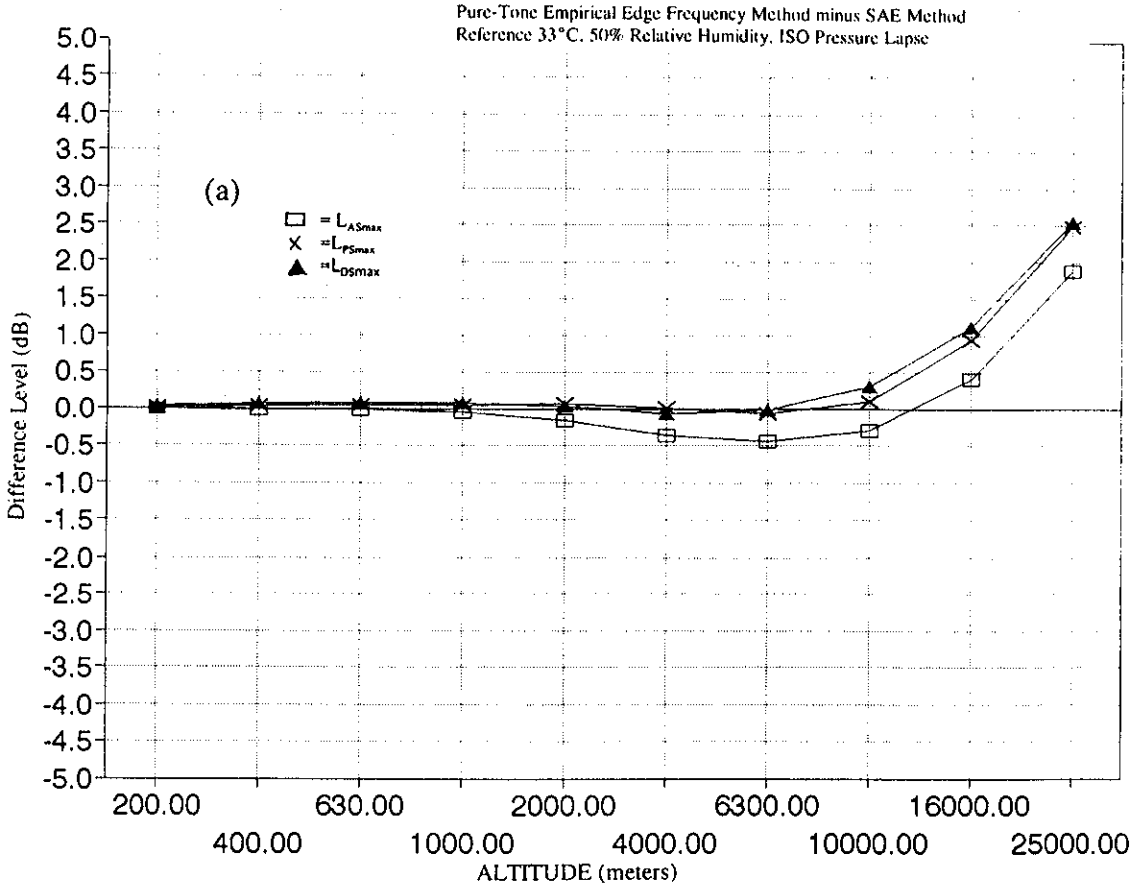

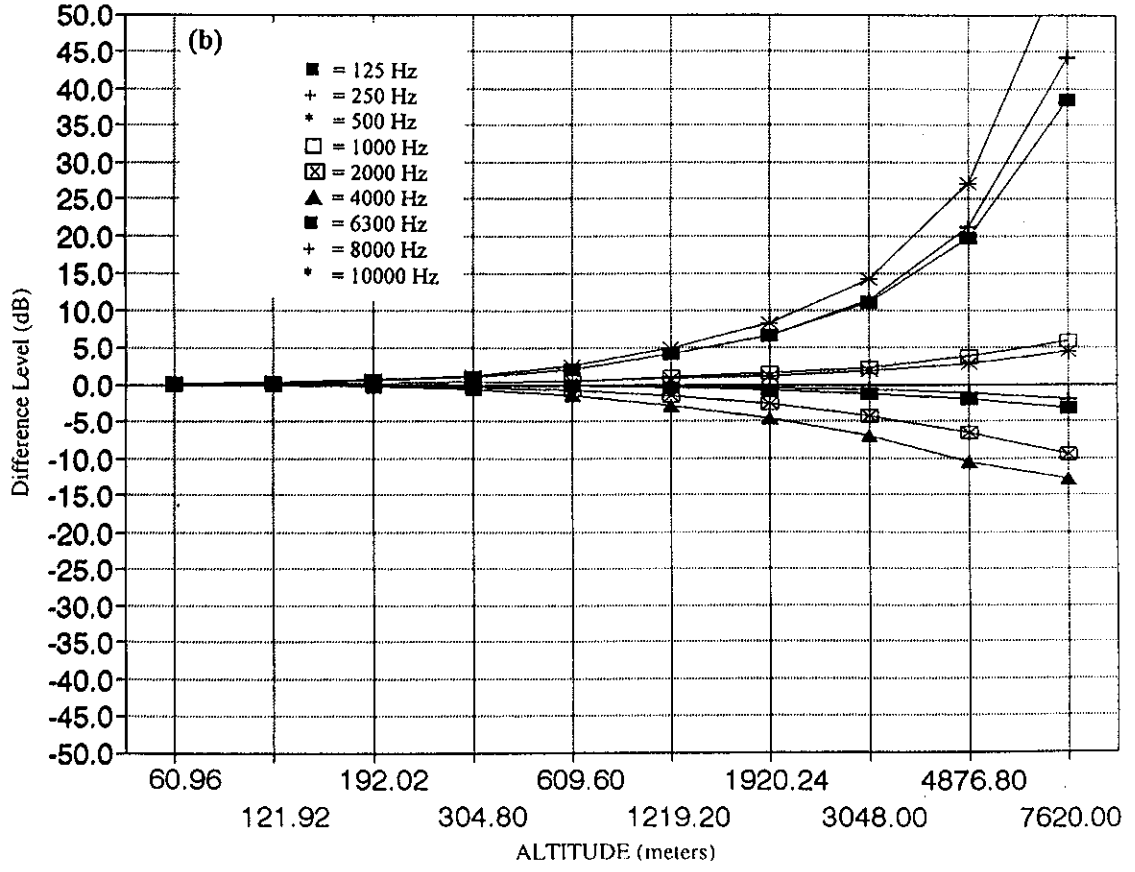

Figure 28 Comparison of Noise-Distance Curves
Spectral Integration Method (IDEAL FILTER)minus SAE Method
Reference 25 C. 70% Relative Humidity